

THE UNIVERSITY OF MICHIGAN
INDUSTRY PROGRAM OF THE COLLEGE OF ENGINEERING

FINITE DIFFERENCE COMPUTATION
OF
NATURAL CONVECTION HEAT TRANSFER

Jesse David Hollams

A dissertation submitted in partial fulfillment
of the requirements for the degree of
Doctor of Philosophy in the
University of Michigan
1960

August, 1960

IP-461

Doctoral Committee:

Professor Stuart W. Churchill, Chairman
Professor John A. Clark
Assistant Professor Bernard A. Galler
Professor Joseph J. Martin
Professor Edwin H. Young

ACKNOWLEDGMENTS

The author wishes to express his appreciation for the assistance and guidance provided by the members of the Doctoral Committee during this work; especially that of Professor Stuart W. Churchill, the committee chairman. The aid and cooperation of the staff of the University of Michigan Computing Center is also greatly appreciated.

The author extends his gratitude to the Bendix Aviation Corporation for financial support during the academic year 1959-1960

Finally, the work in preparing the manuscript by the Industry Program of the College of Engineering is appreciated.

FINITE DIFFERENCE COMPUTATION OF NATURAL
CONVECTION HEAT TRANSFER

Jesse David Hellums

ABSTRACT

The use of finite difference methods for the solution of the partial differential equations describing the conservation of mass, energy and momentum in natural convection was investigated. The great advantage of the finite difference approach is that the idealizations required to obtain analytical solutions are not necessary. The main problems associated with the method are the stability and convergence of the difference equations and the amount of computation required. These problems have retarded the widespread use of difference methods in convection problems which would seem to be warranted by the great advances in computer technology of the last few years.

Explicit difference equations were devised that are stable and that require only moderate amounts of computer time and storage by modern standards. The equations are written in time dependent form and treated as an initial value problem. Starting from a motionless, isothermal initial condition, the velocity and temperature distributions are computed as functions of space and time. The complete transient solution, including the steady state as a limiting condition, is obtained. This time-dependent approach is indicated to be preferable to methods in which steady state is assumed at the outset even if the steady state solution is of primary interest.

The infinite, isothermal, flat plate; and the region inside an infinite, horizontal cylinder with the vertical halves of the wall maintained at different uniform temperatures were chosen for illustrative calculations on an IBM-704 because of the availability of experimental data and analytical solutions as a reference and test for convergence.

The flat plate solution was obtained for a Prandtl number of 0.733. The solution is compared with the short time solution for conduction alone, and with Ostrach's solution for the steady state. The results are in good agreement in both cases. In the intermediate time range the problem has not been solved before so the results represent new information.

The cylinder problem was solved for a Prandtl number of 0.7 and three different values of the Grashof number. An additional solution was obtained for a Prandtl number of 10. The results are brought together by dimensional analysis so that the four solutions permit prediction of heat transfer rates in the cylinder over wide ranges of both parameters. The results are shown to be in good agreement with the experimental measurements of Martini and Churchill.

A discussion is given on the application of finite difference methods to other problems. The method used in this work applies practically without change to any problem in fluid motion in which the pressure distribution is specified or can be calculated from perfect fluid theory. Eventually the most difficult problems in fluid mechanics and heat transfer will almost certainly be solved by the finite difference approach. This work constitutes a significant step in that direction.

TABLE OF CONTENTS

	Page
ACKNOWLEDGMENTS	ii
ABSTRACT	iii
LIST OF TABLES	vii
LIST OF FIGURES	viii
NOMENCLATURE	x
I. INTRODUCTION	1
II. REVIEW OF PRIOR WORK AND THEORETICAL BACKGROUND	4
A. The Mathematical Model	4
B. The Flat Plate	7
1. A General Model	8
2. The Schmidt-Beckmann Model	10
3. A Highly Simplified Model	14
4. Comparison of Models	15
C. Confined Fluids - The Horizontal Cylinder	16
1. Previous Experimental Measurements	17
2. Analytical Solutions	18
3. A General Model	21
4. A Simplified Model	23
5. A Highly Simplified Model	25
III. FINITE DIFFERENCE METHODS	29
A. Methods of Attack	31
1. The Steady State Approach	32
2. The Unsteady State Approach	32
B. Stability and Convergence	33
C. Stability Analysis	36
1. Positive Type Difference Equations	37
2. The von Neumann Method of Stability Analysis	38
IV. THE FLAT PLATE	43
A. The Differential Problem	44
B. The Difference Problem	45
1. The Space Grid	45
2. The Difference Equations	47
3. The Stability Criterion	47
4. The Calculations	49
C. Results	51
1. The Leading Edge	51
2. Principal Results	54

TABLE OF CONTENTS (cont.)

	Page
V. THE HORIZONTAL CYLINDER	62
A. The Differential Problem	63
B. The Difference Problem	64
1. The Space Grid	65
2. The Difference Equations	70
3. The Stability Criterion	72
4. The Calculations	75
C. Results	79
1. The Transient Solution	80
2. Comparison of Two Models	84
3. Effect of Subdivision of the Grid	86
4. Direct Comparison with Experiment	94
5. Variation of Parameters and Additional Comparison with Experiment	99
VI. DISCUSSION OF APPLICATIONS TO RELATED PROBLEMS	118
VII. SUMMARY OF RESULTS	123
REFERENCES	125
APPENDIX A - ANALYSIS FOR THE CYLINDER	128
APPENDIX B - RESULTS FOR THE FLAT PLATE	131
APPENDIX C - RESULTS FOR THE CYLINDER	135
APPENDIX D - COMPUTER PROGRAM	153

LIST OF TABLES

Table		Page
I	Summary of Calculations for the Cylinder	77
II	Summary of Solutions for the Cylinder	99
III	Fluctuations in the Heat Transfer Results of Solution 4	108
IV	Parameters from the Results of Martini and Churchill	112
V	Comparison with the Results of Martini and Churchill	114
VI	Transient Results for the Flat Plate	132
VII	The Steady State Flat Plate Solution after Extension of the Y Coordinate	133
VIII	Transient Heat Transfer Group for the Flat Plate	134
IX	Transient Nusselt Numbers for the Cylinder	136
X	Results for the Cylinder	138
XI	Steady State Heat Transfer Results for the Cylinder	149
XII	Velocities from Martini and Churchill	151
XIII	Temperatures from Martini and Churchill	152

LIST OF FIGURES

Figure		Page
1	The Horizontal Cylinder	17
2	The Space Grid	46
3	Effect of Leading Edge Error on Heat Transfer Group	53
4	Effect of Leading Edge Error on Velocity Profile	53
5	Transient Velocity Profiles	55
6	Transient Temperature Profiles	56
7	Transient Velocity at Various Positions	57
8	Transient Temperature and Heat Transfer Group	58
9	The Cylindrical Space Grid	66
10	Subdivision of Outer Grid	67
11	Approximation of Boundary Temperature	69
12	Transient Velocities in the Cylinder	81
13	Transient Nusselt Numbers in the Cylinder	83
14	Velocity and Temperature Profiles from First Grid	85
15	Effect of Subdivision on Velocity and Temperature Profiles for Solution 1	88
16	Effect of Subdivision on Nusselt Number for Solution 1	90
17	Effect of Subdivision on Velocity and Temperature Profiles for Solution 3	92
18	Effect of Subdivision on Nusselt Number for Solution 3	93
19	Comparison of Velocities with Measurements	95
20	Comparison of Temperatures with Measurements	97
21	Comparison of Nusselt Numbers with Measurements	98
22	Collected Profiles Near the Discontinuity	101
23	Collected Profiles on the Hot Side of the Cylinder	102

LIST OF FIGURES (cont.)

Figure		Page
24	Collected Heat Transfer Results	104
25	Profiles from Solution 4 Showing Fluctuations	106
26	Velocity Fluctuations in Solution 4	107
27	Comparison of Solution with Experiments for Several Grashof Numbers	115
28	Comparison of Overall Heat Transfer Results	117

NOMENCLATURE

- A Rayleigh Number, $(Gr Pr)$
- a, b constants appearing in Equations 40 and 41
- B $\Delta\tau/(\Delta\gamma)^2$ as used in Equation 54.
- C $\Delta\tau/(\Delta R)^2$ as used in Equation 63
- C_p heat capacity, Btu/lb-°F
- D diameter of the cylinder, ft
- D $\Delta\tau/(R\Delta\epsilon)^2$ as used in Equation 63
- \mathcal{D} total differential operator
- div divergence operator
- g acceleration due to gravity, ft/sec²
- Gr Grashof Number: $g\beta\Delta T x^3/\nu^2$ for the flat plate
 $g\beta\Delta T r_0^3/\nu^2$ for the cylinder
- h heat transfer coefficient = heat flux divided by overall temperature drop
- j integer denoting grid position in the direction parallel to the boundary
- k thermal conductivity, Btu/lb-ft-°F
- k, k₁, k₂ integers in a term in a Fourier Series
- l integer denoting grid position normal to the boundary
- n integer denoting time increment
- Nu Nusselt Number: hx/k for the plate
 hD/k for the cylinder
- Pr the Prandtl number, ν/α .
- p pressure, lbs/ft-sec²
- p' excess in pressure above the initial condition, lbs/ft-sec²
- P' dimensionless excess pressure as defined in Equation 8 or 25
- r radial position, ft

- r_o radius of the boundary, ft
 R dimensionless radial position = r/r_o .
 R the gas law constant in Equation 71
 T temperature, $^{\circ}R$
 t time, sec
 u velocity parallel to the boundary, ft/sec
 U dimensionless velocity parallel to the boundary as defined in Equations 52 or Equations 26.
 v velocity normal to the boundary, ft/sec
 V dimensionless velocity normal to the boundary as defined in Equations 52 or Equations 26.
 \vec{V} the velocity vector, ft/sec
 x distance, parallel to the plate, ft
 X dimensionless distance as defined in Equations 52
 y distance normal to the plate, ft
 Y dimensionless distance as defined in Equations 52

Greek Letters

- α thermal diffusivity, ft^2/sec
 β coefficient in Equation 2, $^{\circ}R^{-1}$
 β either $|U/\Delta\tau/(R\Delta\theta)$ or $|U/\Delta\tau/\Delta X$ when used in discussions of stability
 γ either $|V/\Delta\tau/\Delta R$ or $|V/\Delta\tau/\Delta Y$ when used in discussions of stability
 ΔT overall temperature drop = $T_w - T_i$ for the plate and $T_H - T_C$ for the cylinder, $^{\circ}F$
 η, ξ amplification factors in a Fourier Series
 μ viscosity, $lb(mass)/ft\text{-}sec$
 ν kinematic viscosity, ft^2/sec
 Θ angle as indicated in Figure 1
 ϕ dimensionless temperature = $(T - T_i)/\Delta T$

τ dimensionless time as defined in Equation 26 or Equation 52

λ an eigenvalue

ρ density, lbs(mass)/ft³

Subscripts

C denotes the cold side of the cylinder

H denotes the hot side of the cylinder

i denotes the initial condition

j, ξ denotes position in the space grid

m denotes a mean value

o denotes a reference quantity

w denotes the condition at the flat plate

Superscript

(n) denotes the time increment

I. INTRODUCTION

Numerical finite difference methods for solving partial differential equations are of increasing interest and importance since the advent of high speed digital computers. The methods have been employed extensively in heat conduction (diffusion) problems. However, heat convection, which involves conduction plus fluid motion, has received very little attention.

The principal attraction of the finite difference approach to partial differential equations lies in the fact that the methods should yield solutions to the great class of problems which resist ordinary methods of analysis. In actual practice there are some difficulties associated with convergence and stability of the difference equations and with the relatively large amount of computation required. These difficulties have retarded the widespread application of the methods which would seem to be warranted by the great advances in computer technology of the last few years. However, the promise is there, and it seems almost certain that the methods will eventually be used for solving the most difficult problems in fluid mechanics and heat convection.

The purpose of this work is to investigate the solution of natural convection problems by difference methods. Methods and problems associated with the methods are studied, and two conditions are selected for illustrative calculations: the isothermal, vertical flat plate, and the region confined by an infinite, horizontal cylinder with the vertical halves of the walls at different uniform temperatures. These conditions

are chosen because of the availability of analytical solutions and experimental measurements to compare with the results.

In problems of the type considered in this thesis, there are two basic and difficult questions. First, does the system of equations under consideration adequately describe the actual physical phenomenon over the ranges of interest of the variables? Secondly, does the finite difference method of computation give the solution to the system of equations or an adequate approximation of the solution? The first question theoretically can be answered without ever solving the system of equations if the required derivatives are measured or obtained from measured quantities. Unfortunately, the precision of the measurements required to test the equations in this way is usually prohibitively high so that it is usually necessary to solve the equations and compare the solution with measurements. The second question in many cases can be answered by analysis. However, the mathematical theory is often inadequate and it is necessary to compare the approximate solution either with an exact solution or with measurements. The question of stability in initial value problems is a crucial part of the second basic question in that no meaningful results can be expected unless stable difference equations are used.

The flat plate problem was chosen for calculation because the results of the calculations could be compared with a solution which may be regarded as exact. Such a solution exists for very small time where conduction alone prevails and for very large time where the steady state is reached. The cylinder problem was selected as a more difficult problem for which an analytical solution is not available, but for which experimental data exist. The calculations would be of little value if it were

always necessary to have solutions or measurements by which to verify the calculations. Such verification is essential in exploratory investigations such as the present work, but once the validity of the result is established, the methods can be used to provide new information and to solve new problems.

This thesis is divided into seven parts:

1. Introduction.
2. Review of prior work and theoretical background.
3. A discussion of finite difference methods.
4. Results for the flat plate.
5. Results for the cylinder.
6. Discussion of related problems.
7. Summary of results.

II. REVIEW OF PRIOR WORK AND THEORETICAL BACKGROUND

A. The Mathematical Model

Conservation of mass, energy, and momentum are described by the equations given below. The thermal conductivity, viscosity and heat capacity are assumed to be constant, and viscous dissipation and work of compression are neglected.

$$\frac{\partial \rho}{\partial t} = -\rho \operatorname{div} \vec{V} \quad (1a)$$

$$\frac{\partial T}{\partial t} = \frac{k}{\rho c_p} \nabla^2 T \quad (1b)$$

$$\frac{\partial u}{\partial t} = -g - \frac{1}{\rho} \frac{\partial p}{\partial x} + \frac{\mu}{\rho} \left[\nabla^2 u + \frac{1}{3} \frac{\partial}{\partial x} \operatorname{div} \vec{V} \right] \quad (1c)$$

$$\frac{\partial v}{\partial t} = -\frac{1}{\rho} \frac{\partial p}{\partial y} + \frac{\mu}{\rho} \left[\nabla^2 v + \frac{1}{3} \frac{\partial}{\partial y} \operatorname{div} \vec{V} \right] \quad (1d)$$

The force of gravity is taken to be in the negative x direction. For three-dimensional or turbulent motion a third momentum balance should be included. However, for the purpose of dimensional analysis, it can be omitted since it is of the same form as Equation 1d. Associated with Equations 1 are boundary and initial conditions. In this work the initial condition is that the velocity is zero and the temperature is some constant, T_i . On the boundary the velocity is zero and the temperature is prescribed as either a constant or a function of position.

If density variations due to pressure are negligible, the following equation of state is a good approximation for most gases and liquids.

$$\rho = \frac{\rho_i}{1 + \beta(T - T_i)} \quad (2)$$

For ideal gases the coefficient, β , equals $1/T_i$.

The initial components of the pressure gradient are:

$$\frac{\delta p_i}{\delta x} = -g \rho_i \quad (3)$$

and

$$\frac{\delta p_i}{\delta y} = 0 \quad (4)$$

In natural convection it may be expected that the pressure gradient will depart very little from the initial, static pressure gradient. So it is desirable to divide the pressure into two parts: p_i , the initial pressure and p' the increase in pressure due to motion and variations in density. Later on it will be assumed that in some cases $p' \equiv 0$.

$$\begin{aligned} p &= p_i + p' \\ \frac{\delta p}{\delta x} &= \frac{\delta p_i}{\delta x} + \frac{\delta p'}{\delta x} = -g \rho_i + \frac{\delta p'}{\delta x} \end{aligned} \quad (5a)$$

$$\frac{\delta p}{\delta y} = \frac{\delta p_i}{\delta y} + \frac{\delta p'}{\delta y} = 0 + \frac{\delta p'}{\delta y} \quad (5b)$$

The expressions for the components of the pressure gradient given by Equations 5 may be substituted into equations 1c and 1d to give:

$$\frac{\partial u}{\partial x} = g \left(\frac{\rho_i}{\rho} - 1 \right) - \frac{1}{\rho} \frac{\partial p'}{\partial x} + \frac{\mu}{\rho} \left[\nabla^2 u + \frac{1}{3} \frac{\partial}{\partial x} \operatorname{div} \vec{V} \right] \quad (6a)$$

$$\frac{\partial v}{\partial x} = -\frac{1}{\rho} \frac{\partial p'}{\partial y} + \frac{\mu}{\rho} \left[\nabla^2 v + \frac{1}{3} \frac{\partial}{\partial y} \operatorname{div} \vec{V} \right] \quad (6b)$$

Now the density may be eliminated from all the conservation equations by use of the equation of state to give

$$\frac{\partial}{\partial x} \left[\frac{1}{1 + \beta(T - T_i)} \right] = - \frac{1}{1 + \beta(T - T_i)} \operatorname{div} \vec{V} \quad (7a)$$

$$\frac{\partial T}{\partial x} = \frac{k}{\rho c_i} [1 + \beta(T - T_i)] \nabla^2 T \quad (7b)$$

$$\frac{\partial u}{\partial x} = g \beta (T - T_i) - \left[\frac{1 + \beta(T - T_i)}{\rho_i} \right] \frac{\partial p'}{\partial x} + \frac{\mu}{\rho_i} [1 + \beta(T - T_i)] \left[\nabla^2 u + \frac{1}{3} \frac{\partial}{\partial x} \operatorname{div} \vec{V} \right] \quad (7c)$$

$$\frac{\partial v}{\partial x} = - \left[\frac{1 + \beta(T - T_i)}{\rho_i} \right] \frac{\partial p'}{\partial y} + \frac{\mu}{\rho_i} [1 + \beta(T - T_i)] \left[\nabla^2 v + \frac{1}{3} \frac{\partial}{\partial y} \operatorname{div} \vec{V} \right] \quad (7d)$$

Equations 7 may be considered as a general model for natural convection. The only assumption made to this point which seems subject to serious challenge is the assumption of constant viscosity which will not be a good approximation for viscous fluids under large temperature difference. However, Sparrow and Gregg (39) have investigated the effect of variable viscosity and their results tend to support the present practice among engineers of using a constant viscosity evaluated at a mean temperature.

It should be mentioned that there is some confusion in the literature regarding Equations 7. Many books and papers introduce the

term $g\beta(\rho_i/\rho - 1)$ by reference to "Archimedes' law of buoyancy" without noting that p' differs from p . Hermann (12) discusses this point and emphasizes that Archimedes' law applies only for a particle of a given density immersed in a fluid of uniform density, which is certainly not the case in natural convection. It is also a common practice to start with a system of equations like Equations 7 except that the terms $1 + \beta(T - T_i)$ are omitted along with the terms $\text{div } \vec{v}$. These simplifications will be used later in this work, but it should be noted that such simplifications imply that $(T - T_i) \ll 1/\beta$. That is to say, the maximum overall temperature difference must be small relative to $1/\beta$ (T_i for gases).

B. The Flat Plate

Consider an isothermal, vertical plate of infinite width, extending from $x = 0$ to $x = \infty$ immersed in a Newtonian fluid of infinite extent, initially at a uniform temperature, T_i , and at rest. At some time, $t = 0$, the plate instantaneously takes on a temperature T_w , different from the initial fluid temperature, T_i . Let $u \equiv u(x, y, t)$, then the boundary and initial conditions may be written

$$\begin{aligned}u(x, 0, t) &= u(x, \infty, t) = u(x, y, 0) = 0 \\v(x, 0, t) &= v(x, \infty, t) = v(x, y, 0) = 0 \\T(x, 0, t) &= T_w, \quad T(x, \infty, t) = T(x, y, 0) = T_i\end{aligned}$$

Notice that only two parameters, T_w and T_i , appear in these equations. If the variable T is replaced with a new variable, ϕ , such that $\phi = (T - T_i)/\Delta T$ where $\Delta T = T_w - T_i$, the two parameters are eliminated and the conditions on ϕ are:

$$\phi(x, 0, t) = 1, \quad \phi(x, \infty, t) = \phi(x, y, 0) = 0$$

Now if any of the variables u , v , x , y , or t (not ϕ) is replaced by a new variable differing from the old by only a constant multiplier, the boundary and initial conditions using the new variable will be the same as before. This fact gives one the freedom to choose new, dimensionless variables without introducing parameters into the boundary and initial conditions.

1. A General Model

A systematic technique for choosing dimensionless variables so that the number of parameters and independent variables in the problem is reduced to a minimum has been given by Hellums and Churchill (10), and the technique is discussed and illustrated later on a simple system of equations. For Equations 7 the dimensionless variables may be shown by this technique to be:

$$U = \frac{u}{(\nu g \beta \Delta T)^{1/3}} ; \quad V = \frac{v}{(\nu g \beta \Delta T)^{1/3}} ; \quad P' = \frac{P'}{(\nu g \beta \Delta T)^{2/3} l}$$

$$X = x \left(\frac{g \beta \Delta T}{\nu^2} \right)^{1/3} ; \quad Y = y \left(\frac{g \beta \Delta T}{\nu^2} \right)^{1/3} ; \quad \tau = t \frac{(g \beta \Delta T)^{2/3}}{\nu^{1/3}}$$

and the equations become

$$\frac{\partial}{\partial \tau} \left(\frac{1}{1 + \beta \Delta T \phi} \right) = \frac{-1}{1 + \beta \Delta T \phi} \left(\frac{\partial U}{\partial X} + \frac{\partial V}{\partial Y} \right) \quad (8a)$$

$$\frac{\partial \phi}{\partial \tau} = \frac{\alpha / \nu}{1 + \beta \Delta T \phi} \left(\frac{\partial^2 \phi}{\partial X^2} + \frac{\partial^2 \phi}{\partial Y^2} \right) \quad (8b)$$

$$\frac{\partial U}{\partial \tau} = \phi + (1 + \beta \Delta T \phi) \left(-\frac{\partial P'}{\partial X} + \frac{\partial^2 U}{\partial X^2} + \frac{\partial^2 U}{\partial Y^2} + \frac{1}{3} \frac{\partial^2 U}{\partial X^2} + \frac{1}{3} \frac{\partial^2 V}{\partial X \partial Y} \right) \quad (8c)$$

$$\frac{\partial V}{\partial \tau} = (1 + \beta \Delta T \phi) \left(-\frac{\partial P'}{\partial Y} + \frac{\partial^2 V}{\partial X^2} + \frac{\partial^2 V}{\partial Y^2} + \frac{1}{3} \frac{\partial^2 V}{\partial Y^2} + \frac{1}{3} \frac{\partial^2 U}{\partial X \partial Y} \right) \quad (8d)$$

Equations 8 with the boundary and initial conditions contain only two parameters: $\beta \Delta T$ and $\nu \alpha$, the Prandtl number. That is to say U ,

V , and ϕ depend on these two parameters in addition to X , Y and τ . The seven parameters which appeared in the original problem, T_w , T_i , μ , ρ_i , β , g , and α have been combined or included in the new variables such that only two parameters remain. Such a reduction in the number of parameters is of great value if the equations are to be solved numerically or if experimental data are to be correlated.

From these equations it is apparent that $(T - T_i)/\Delta T$, $u/(v g \beta \Delta T)^{1/3}$, $v/(v g \beta \Delta T)^{1/3}$ and $p'/\rho_i (v g \beta \Delta T)^{2/3}$ are functions only of $x(g \beta \Delta T/v^2)^{1/3}$, $y(g \beta \Delta T/v^2)^{1/3}$, $t(g \beta \Delta T)^{2/3}/v^{1/3}$, βT , and V/α .

The local heat transfer coefficient can be introduced and evaluated as follows:

$$h_{\Delta T} = -k \left(\frac{\partial T}{\partial y} \right)_{y=0} = -\frac{k \Delta T (g \beta \Delta T)^{1/3}}{v^{2/3}} \left(\frac{\partial \phi}{\partial Y} \right)_{Y=0} \quad (9)$$

hence

$$\frac{h}{k} \left(\frac{v^2}{g \beta \Delta T} \right)^{1/3} = F \left[\chi \left(\frac{g \beta \Delta T}{v^2} \right)^{1/3}, \frac{t (g \beta \Delta T)^{2/3}}{v^{1/3}}, \frac{V}{\alpha}, \beta \Delta T \right] \quad (10)$$

Equation (10) is a very general result. No assumption was made either explicitly or implicitly relative to the type of flow, and this functional relationship is presumed to hold for both laminar and turbulent flow. For a steady state, the time group may be dropped. For turbulent conditions the heat transfer coefficient then becomes the time mean value over a sufficient interval of time to dampen out the turbulent fluctuations.

The parameter $\beta \Delta T$ is observed to occur only in the form $1 + \beta \Delta T \phi$ in Equations 8. Since $0 \leq \phi \leq 1.0$, $\beta \Delta T$ may be dropped out of

the functional relationships if $\Delta T \ll 1/\beta$. The simplified result for steady state is

$$\frac{h}{k} \left(\frac{\gamma^2}{g\beta\Delta T} \right)^{1/3} = F \left[\chi \left(\frac{g\beta\Delta T}{\nu^2} \right)^{1/3}, \frac{\nu}{\alpha} \right] \quad (11)$$

The Prandtl number, ν/α , is the only parameter remaining in Equation 11. Therefore a single experiment or numerical calculation in which h is determined as a function of x should be sufficient to define the problem for a given Prandtl number if $\Delta T \ll 1/\beta$.

Equations 8 have been useful in the past only for dimensional analysis. The equations have never been solved in such a general form.

2. The Schmidt-Beckmann Model

Schmidt and Beckmann aided by a mathematician, Pohlhausen (31), made a number of simplifications of Equations 8 and obtained an analytical solution to the simplified equations. The simplifications, which are of the type now often referred to as of the boundary layer type, consist of dropping $\partial u^2/\partial x^2$, $\partial^2 T/\partial x^2$, $\partial p'/\partial x$ and the entire momentum balance in the y direction, and again assuming $\beta\Delta T$ to be negligible with respect to unity. Ostrach (26) gives a detailed discussion of the implications of the assumptions. The resulting equations are given below except that here the time derivatives are included. Schmidt and Beckmann worked only with the steady-state case.

$$\frac{\partial u}{\partial x} + \frac{\partial v}{\partial y} = 0 \quad (12a)$$

$$\frac{\partial \phi}{\partial x} = \alpha \frac{\partial^2 \phi}{\partial y^2} \quad (12b)$$

$$\frac{\partial u}{\partial t} = g\beta\Delta T \phi + \gamma \frac{\partial^2 u}{\partial y^2} \quad (12c)$$

The boundary and initial conditions for this system of equations have some implications which should be discussed. First, the velocity normal to the plate, v , cannot be restrained to zero for large y . At $y = 0$ v is zero but v approaches some non-zero function of x as y increases. Secondly, along the leading edge of the plate ($x = 0$) $u = 0$ and $v = 0$. The behavior of v does not correspond to that of a real fluid except at positions which in some sense are near the plate and far from the leading edge. The solution to the system of equations cannot be expected to be valid near the leading edge.

Dimensional analysis of this system of equations will be carried out in detail as an illustration of the technique mentioned before. A new set of variables will be adopted: $U = u/u_0$, $V = v/v_0$, $X = x/x_0$, $Y = y/y_0$ and $\tau = t/t_0$, where u_0 , v_0 , x_0 , and y_0 are constants or parameters. The variable ρ will be left unaltered since any multiplier would introduce a parameter into the boundary conditions as was mentioned above. It is important to note that the quantities u_0 , v_0 , x_0 , y_0 and t_0 are entirely arbitrary and can be chosen in such a way that the problem is simplified. That is to say the objective of the analysis is to eliminate as many as possible of the parameters and independent variables from the problem by appropriate choice of values for the arbitrary quantities. The equations in terms of the new variables are given below.

$$\frac{\partial U}{\partial X} + \left(\frac{x_0 v_0}{y_0 u_0} \right) \frac{\partial V}{\partial Y} = 0 \quad (13a)$$

$$\frac{\partial \phi}{\partial \tau} + \left(\frac{u_0 t_0}{x_0} \right) U \frac{\partial \phi}{\partial X} + \left(\frac{t_0 v_0}{y_0} \right) V \frac{\partial \phi}{\partial Y} = \frac{\alpha t_0}{y_0^2} \frac{\partial^2 \phi}{\partial Y^2} \quad (13b)$$

$$\frac{\partial U}{\partial \tau} + \left(\frac{u_0 t_0}{x_0} \right) U \frac{\partial U}{\partial X} + \left(\frac{t_0 v_0}{y_0} \right) V \frac{\partial U}{\partial Y} = \left(\frac{\rho \beta \Delta T t_0}{u_0} \right) \phi + \left(\frac{t_0 \gamma}{y_0^2} \right) \frac{\partial^2 U}{\partial Y^2} \quad (13c)$$

Now it is desired to eliminate as many as possible of the dimensionless groups in the equations. Each group can be equated to unity which gives a system of eight equations (not all independent) in the five arbitrary quantities u_0 , v_0 , x_0 , y_0 , and t_0 . These equations can be solved to give the arbitrary quantities in terms of the parameters of the original problem α , ν , g , β and ΔT . If all of the eight equations can be satisfied, all of the parameters can be eliminated from the partial differential equations. In the case at hand, the two equations $\alpha t_0 / y_0^2 = 1$ and $\nu t_0 / y_0^2 = 1$ cannot both be satisfied so one parameter will remain. The solution to the algebraic problem for the arbitrary quantities is

$$\left. \begin{aligned} u_0 &= (x_0 g \beta \Delta T)^{1/2} & ; & & v_0 &= (\nu^2 g \beta \Delta T / x_0)^{1/4} \\ x_0 &= (x_0 / g \beta \Delta T)^{1/2} & ; & & y_0 &= (\nu^2 x_0 / g \beta \Delta T)^{1/4} \\ x_0 &= \text{arbitrary} \end{aligned} \right\} \quad (14)$$

All the parameters in the problem except one can be eliminated without specifying x_0 , and the equations are not affected by the choice of a value for x_0 .

Substitution of the quantities of Equations 14 into Equations 13 gives

$$\frac{\partial U}{\partial X} + \frac{\partial V}{\partial Y} = 0 \quad (15a)$$

$$\frac{\partial^2 \phi}{\partial \tau^2} = \frac{\alpha}{\nu} \frac{\partial^2 \phi}{\partial Y^2} \quad (15b)$$

$$\frac{\partial U}{\partial \tau} = \phi + \frac{\partial^2 U}{\partial Y^2} \quad (15c)$$

in which ν/α , the Prandtl number, is the only parameter. So it is concluded that $u/(x_0 g \beta \Delta T)^{1/2}$, $v/(x_0 / \nu^2 g \beta \Delta T)^{1/4}$ and $(T - T_i)/(T_w - T_i)$ depend on

x/x_0 , $y(g\beta\Delta T/\nu^2 x_0)^{1/4}$, $t(g\beta\Delta T/x_0)^{1/2}$ and ν/α . The system of differential equations with the boundary and initial conditions is independent of the choice of x_0 . So it must be concluded that the solution is also independent of the choice of x_0 . A new set of variables which does not contain x_0 can be formed by multiplying each old variable by x/x_0 raised to an appropriate power. Birkhoff (2) has given a formal justification to such a procedure by much the same line of reasoning as given here. The revised conclusion is that $u/(xg\beta\Delta T)^{1/2}$, $v(x/\nu^2 g\beta\Delta T)^{1/4}$ and $(T - T_i)/(T_w - T_i)$ depend on $y/(g\beta\Delta T/\nu^2 x)^{1/4}$, $t(g\beta\Delta T/x)^{1/2}$ and ν/α . The validity of the new choice of variables can always be checked by computing the required derivatives and substituting them into the original system of equations.

The local heat transfer coefficient can be introduced in the same way as before to give

$$\frac{h}{k} \left(\frac{\nu^2 x}{g\beta\Delta T} \right)^{1/4} = f \left[\left(\frac{t/\nu\Delta T}{x} \right)^{1/2}, \frac{\nu}{\alpha} \right] \quad (16)$$

If attention is restricted to steady state, the terms involving time may be dropped; a single independent variable remains, and the partial differential equations can be reduced to ordinary differential equations. The system of ordinary differential equations was first developed and solved for a Prandtl number of 0.733 by Schmidt, Beckmann and Pohlhausen (31). The solution was found to agree well with the experimental data of Schmidt and Beckmann. The original solution was by series. Since that time others have solved the equations for a variety of conditions using numerical methods. References 7, 26, 30, 31, 33, 35, 36, 37, 38, 39 and 40 all pertain to solutions of this system of equations.

Transient free convection has been studied by Illingworth (13), Sugawara and Michiyoshi (41) and, most recently, Siegel (34). None of these workers obtained a solution which is valid over the whole range of time out to the steady state condition. Siegel used the Kármán-Pohlhausen approximation method in attacking the problem. He did not compute heat transfer coefficients beyond the short time when conduction alone prevails. However, he did produce an estimate of the time required to reach steady state.

3. A Highly Simplified Model

As a final case the further simplification of steady state and very slow motion such that the inertial terms in the momentum equations can be dropped will be examined. Morgan and Warner (23) indicate that this latter idealization is justifiable for fluids with large Prandtl numbers. The resulting equations are

$$\frac{\partial u}{\partial x} + \frac{\partial v}{\partial y} = 0 \quad (17a)$$

$$u \frac{\partial T}{\partial x} + v \frac{\partial T}{\partial y} = \alpha \frac{\partial^2 T}{\partial y^2} \quad (17b)$$

$$g\beta(T - T_i) + \nu \frac{\partial^2 u}{\partial y^2} = 0 \quad (17c)$$

Proceeding as before reveals that $(T - T_i)/\Delta T$, $u(\nu/\alpha g\beta\Delta T)^{1/2}$ and $v(x\nu/\alpha^3 g\beta\Delta T)^{1/4}$ are functions only of $y(g\beta\Delta T/\nu x)^{1/4}$ and hence that

$$\frac{h}{k} \left(\frac{\alpha \nu x}{g\beta\Delta T} \right)^{1/4} = C \quad (18)$$

where C is an unknown constant.

This result is practically as useful as a complete solution since a single experimental or computed value for the heat transfer coefficient defines the coefficient for all other positions and conditions within the range of the applicability of Equations 17. Equation 18 can be rearranged in the more familiar but less explicit form

$$N_u = C (Gr Pr)^{1/4} \quad (19)$$

This relationship, including the a value for C was first derived by Lorenz (19). However, Lorenz made more simplifications than were necessary in the analysis presented above. Morgan and Warner apparently were the first to derive Equation 19 from Equations 17.

4. Comparison of Models

It is interesting to compare the different functional representations obtained for the local, steady state, heat transfer coefficient for the successive idealizations. Equation 19 should be regarded as a first order approximation and would be expected to become a poorer representation as the Prandtl number is decreased. Equations 16, 11, and 10 should be successively better approximations. The dimensionless heat transfer groups on the left side of Equations 16, 11, and 10 can be changed to the same form as the heat transfer group on the left side of Equation 19 by multiplying through by the dimensionless groups on the right side to the appropriate powers, thus obtaining

$$\frac{h}{k} \left(\frac{\alpha \nu \chi}{g \beta \Delta T} \right)^{1/4} = F \left[\chi \left(\frac{g \beta \Delta T}{\nu^2} \right)^{1/3}, \nu/\alpha, \beta \Delta T \right] \quad (21)$$

$$\frac{h}{k} \left(\frac{\alpha \nu \chi}{g \beta \Delta T} \right)^{1/4} = F \left[\chi \left(\frac{g \beta \Delta T}{\nu^2} \right)^{1/3}, \nu/\alpha \right] \quad (22)$$

and

$$\frac{h}{k} \left(\frac{\alpha \nu x}{g \beta \Delta T} \right)^{1/4} = F \left[\frac{\nu}{\alpha} \right] \quad (23)$$

respectively. Thus the dimensionless heat transfer group $h(\alpha \nu x / g \beta \Delta T)^{1/4} / k$ can be regarded as invariant as a first approximation, as a function of ν / α as a better approximation, and as a function of the dimensionless position $x(g \beta \Delta T / \nu^2)^{1/3}$ and $\beta \Delta T$ in the more general case. This suggests plotting data in the form of $h(\alpha \nu x / g \beta \Delta T)^{1/4} / k$ versus α / ν or if necessary as $h(\alpha \nu x / g \beta \Delta T)^{1/4} / k$ versus $x(g \beta \Delta T / \nu^2)^{1/3}$ with α / ν and $\beta \Delta T$ as parameters. It should be remembered that the variation of μ , k and C_p with temperature and of ρ with pressure were neglected in all of the analyses. Analytical expressions for these variations would introduce additional dimensionless groups.

C. Confined Fluids - The Horizontal Cylinder

A large part of the prior work on natural convection has been on the flat plate problem discussed above. The flat plate is the simplest condition of practical importance from both the theoretical and experimental standpoints. A larger and more important class of conditions are those associated with confined fluids. Specific examples include air spaces within the walls and rooms of buildings, and within many refrigerators and heaters of both household and industrial use. Practically all problems in heating, cooling, boiling and insulating involve natural convection of confined fluids to some degree.

Analytical or numerical solutions to convection problems almost invariably are approximate solutions to simplified models so that it is highly desirable to compare the solution with experimental data. If the

solution agrees with experimental data, the inference is that the solution will provide information on conditions for which no experimental data exist. Comparison of heat transfer rates is necessary but such a comparison does not provide a critical test of the method. A critical test is provided by comparison of local velocity and temperature distributions.

1. Previous Experimental Measurements

The only experimental measurements of local velocities and temperatures for natural convection in an enclosed region seem to be those of Martini and Churchill (21). In the great majority of investigations only the overall rate of heat transfer or only the temperature distribution is measured.

Martini and Churchill studied natural convection of air inside a horizontal cylinder 36 inches long by 4.3 inches diameter. The cylinder was divided longitudinally at the vertical diameter and a small layer of insulation was inserted between the two halves so that the two sides of the cylinder could be maintained at different temperatures (see Figure 1). The length of the cylinder was sufficient so that near the center the motion of the air was considered to be two dimensional. Local air temperatures were measured directly by thermocouple traverses. Velocity data were obtained by taking multiple exposure pictures of small dust particles suspended in the air. This method of determining velocities gives both the flow lines and the magnitude of the velocity. The results

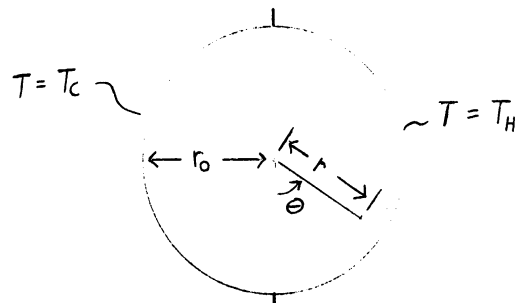


Figure 1. The Horizontal Cylinder

will be discussed in comparison with the calculations of the present work.

It should be mentioned that accurate measurement of local velocities is extremely difficult--which undoubtedly accounts for the dearth of such measurements. The problems of measurement are more difficult for confined fluids than for unconfined fluids, and the comparatively low velocities associated with natural convection pose more problems than cases of high velocity forced convection. Martini and Churchill considered their work to be exploratory in that they were seeking an effective method to make such measurements. The technique was only partly successful and they do not claim a high accuracy of measurement. Unfortunately, the difficulties of measurement by any technique are multiplied near the boundary where the results are of most interest.

Ostroumov (25) studied natural convection in a horizontal cylinder by an optical method. His discussion is limited for the most part to a description of the method. No data are reported except photographs showing lines of constant components of the temperature gradient. Natural convection in rectangular regions has been investigated by several workers. Jakob (14), Globe and Dropkin (8), Schmidt and Silveston (32), and de Graff and van der Held (3) give discussions and correlations. Natural convection in vertical tubes closed at one end has been studied by Hartnett and Welsh (9), Eckert and Diagula (5), Foster (6), and Martin (20). As was mentioned above, none of these workers measured local velocities.

2. Analytical Solutions

All efforts toward solving the confined fluid problem have been restricted to the case of steady, two dimensional, laminar flow.

Batchelor (1) considers a rectangular region such as an air space in the wall of a house with the two vertical walls at different temperatures. A single solution to the system of equations is not given as such, but three solutions each of which is expected to be a valid approximation for a limited range of the parameters. Working with the parameters' Rayleigh number, A (product of Grashof and Prandtl numbers), and aspect ratio, L/D (ratio of height to thickness of the air layer), solutions are developed for three limiting cases: (a) very small A , L/D not restricted; (b) very large A , L/D not restricted; and (c) L/D very large, A not restricted. The three solutions give a fairly complete overall qualitative view of the phenomenon, although the heat transfer coefficients so predicted are about 50 to 100% higher than those measured by Mull and Reiher (24).

Zhukhovitski (42) considers an infinitely long cylindrical cavity in a solid medium having a horizontal temperature gradient perpendicular to the axis of the cylinder. A solution is sought in terms of powers series in a modified Rayleigh number. The coefficients are determined by a method of successive approximation. The results of the calculations are compared with the measurements of Ostroumov and are found to be in qualitative agreement for a Rayleigh number of 500. Zhukhovitski indicates that there is no certainty that the method will apply to large Rayleigh numbers. The series may not converge for Rayleigh numbers greater than unity although it is asserted that calculations indicate convergence at least up to a Rayleigh number of 1,000. Batchelor (1) uses the power series approach in his solution for small Rayleigh numbers and gives an argument that 1,000 is the highest value of Rayleigh number for which the power series is useful. Unfortunately Rayleigh numbers of 1,000 or less

are of no practical interest in Batchelor's problem since most of the heat transfer is by conduction in this range. It can be concluded that Zhukhovitski's solution shows some promise, but more work is needed to determine the value of the method over wide ranges of the parameters and on conditions other than those of the original investigation.

Poots (27) gives a solution to the same problem considered by Batchelor--the rectangular region. The temperature and the stream function are expressed as double series of orthogonal functions of the space variables. By means of Fourier transforms the equations for the coefficients are reduced to two infinite sets of coupled simultaneous algebraic equations. An iterative method for solving the algebraic equations is outlined and numerical values of the coefficients are given for a Prandtl number of 0.73, aspect ratio of unity (a square region), and several Rayleigh numbers between 500 and 10,000. The calculations become more difficult with increasing Rayleigh number, and the number of coefficients required in the series also increases. It is indicated that the determination of the coefficients is impractically laborious for Rayleigh numbers greater than 10,000 or aspect ratios greater than 4. There are no data on square regions to compare with Poots' solution. However, for a Rayleigh number of 10,000, Poots' solution agrees with Jakob's (14) empirical formula for the overall heat transfer coefficient. Poots' method of solution seems to hold promise. However, more work is needed to determine if it can be adapted to larger values of the parameters Rayleigh number and aspect ratio.

Lighthill (18) has analyzed the case of natural convection in heated vertical tubes closed at the lower end and opening into a reservoir of cool fluid at the top. The Kármán-Pohlhausen integral approximation method is used on a system of equations in which it is assumed that the

Prandtl number is large so that the non-linear terms can be omitted from the momentum balance. In this method the shape of the velocity and temperature profiles must be assumed or deduced in advance by physical considerations.

It can be concluded that the methods of attack used to date on the equations governing natural convection in enclosed regions have had only limited success and that each method appears to be severely limited in its range of applicability.

3. A General Model

Equations 1 with appropriate boundary conditions apply to confined fluids as well as unconfined fluids. The calculations to be described later on were performed for a cylindrical region so it is desirable to consider the equations in cylindrical coordinates. The angle Θ is measured clockwise from the vertical such that the force of gravity is in the radial direction where $\Theta = 0$. The motion is assumed to be two dimensional so that all gradients in the z or axial direction are zero. The equations are given below where u is the velocity component in the Θ direction and v is the velocity component in the radial direction.

$$\frac{\partial u}{\partial t} + \frac{u}{r} \frac{\partial u}{\partial \Theta} + v \frac{\partial u}{\partial r} + \frac{vu}{r} = -g \sin \Theta - \frac{1}{\rho r} \frac{\partial p}{\partial \Theta}$$

$$+ \frac{\mu}{\rho} \left[\frac{\partial^2 u}{\partial r^2} + \frac{1}{r} \frac{\partial u}{\partial r} - \frac{u}{r^2} + \frac{1}{r^2} \frac{\partial^2 u}{\partial \Theta^2} + \frac{2}{r^2} \frac{\partial v}{\partial \Theta} + \frac{1}{3r} \frac{\partial}{\partial \Theta} \text{div } \vec{V} \right] \quad (24a)$$

$$\frac{\partial v}{\partial t} + v \frac{\partial v}{\partial r} + \frac{u}{r} \frac{\partial v}{\partial \Theta} - \frac{v^2}{r} = g \cos \Theta - \frac{1}{\rho} \frac{\partial p}{\partial r}$$

$$+ \frac{\mu}{\rho} \left[\frac{\partial^2 v}{\partial r^2} + \frac{1}{r} \frac{\partial v}{\partial r} - \frac{v}{r^2} + \frac{1}{r^2} \frac{\partial^2 v}{\partial \Theta^2} - \frac{2}{r^2} \frac{\partial u}{\partial \Theta} + \frac{1}{3} \frac{\partial}{\partial r} \text{div } \vec{V} \right] \quad (24b)$$

$$\frac{\partial T}{\partial t} + v \frac{\partial T}{\partial r} + \frac{u}{r} \frac{\partial T}{\partial \theta} = \alpha \left[\frac{\partial^2 T}{\partial r^2} + \frac{1}{r} \frac{\partial T}{\partial r} + \frac{1}{r^2} \frac{\partial^2 T}{\partial \theta^2} \right] \quad (24c)$$

$$\frac{\partial p}{\partial t} + \frac{1}{r} \frac{\partial (rvr)}{\partial r} + \frac{1}{r} \frac{\partial (ur)}{\partial \theta} = 0 \quad (24d)$$

The boundary and initial conditions for the problem are as indicated below and in Figure 1 where $u = u(r, \theta, t)$.

$$\begin{aligned} u(r_0, \theta, t) &= u(r, \theta, 0) = 0 \\ v(r_0, \theta, t) &= v(r, \theta, 0) = 0 \\ T(r_0, \theta, t) &= T_H \text{ if } 0 < \theta < \pi \\ T(r_0, \theta, t) &= T_C \text{ if } \pi < \theta < 2\pi \\ T(r, \theta, 0) &= T_i \end{aligned}$$

In the cases for which calculations were performed, the initial temperature T_i was taken to be $(T_H + T_C)/2$.

Equations 24 can be simplified somewhat if attention is restricted to cases of small temperature differences (see the discussion just after Equations 7 in Part II). Making this assumption, dividing pressure into two components in the same way as was done in obtaining Equations 7, and putting the equations into dimensionless form gives

$$\begin{aligned} \frac{\partial U}{\partial \tau} + \frac{U}{R} \frac{\partial U}{\partial \theta} + V \frac{\partial U}{\partial R} + \frac{UV}{R} &= Gr \phi \sin \theta - \frac{1}{R} \frac{\partial P'}{\partial \theta} \\ + \frac{\partial^2 U}{\partial R^2} + \frac{1}{R} \frac{\partial U}{\partial R} - \frac{U}{R^2} + \frac{1}{R^2} \frac{\partial^2 U}{\partial \theta^2} + \frac{2}{R^2} \frac{\partial V}{\partial \theta} & \end{aligned} \quad (25a)$$

$$\begin{aligned} \frac{\partial V}{\partial \tau} + V \frac{\partial V}{\partial R} + \frac{U}{R} \frac{\partial V}{\partial \theta} - \frac{V^2}{R} &= -Gr \phi \cos \theta - \frac{\partial P'}{\partial R} \\ + \frac{\partial^2 V}{\partial R^2} + \frac{1}{R} \frac{\partial V}{\partial R} - \frac{V}{R^2} + \frac{1}{R^2} \frac{\partial^2 V}{\partial \theta^2} - \frac{2}{R^2} \frac{\partial U}{\partial \theta} & \end{aligned} \quad (25b)$$

$$\frac{\partial \phi}{\partial z} + v \frac{\partial \phi}{\partial R} + \frac{u}{R} \frac{\partial \phi}{\partial \Theta} = \frac{\alpha}{V} \left[\frac{\partial^2 \phi}{\partial R^2} + \frac{1}{R} \frac{\partial \phi}{\partial R} + \frac{1}{R^2} \frac{\partial^2 \phi}{\partial \Theta^2} \right] \quad (25c)$$

$$\frac{\partial(RV)}{\partial R} + \frac{\partial U}{\partial \Theta} = 0 \quad (25d)$$

where the dimensionless variables are as indicated below

$$\phi = \frac{T - T_i}{T_H - T_C}, \quad U = \frac{ur_0}{V}, \quad V = \frac{vr_0}{V}$$

$$= \frac{tV}{r_0^2} \quad \text{and} \quad P' = \left(\frac{p - \rho_i g r \cos \Theta}{\rho_i V^2} \right) r_0^2$$

The two parameters are $Gr, r_0^3 g \beta \Delta T / V^2$, a Grashof number based on the radius of the cylinder, and V/α , the Prandtl number. In the case of the unconfined fluid the corresponding set of equations contain only a single parameter. Here, the boundary conditions are slightly more complex and two parameters are required. For a still more complicated boundary such as a rectangle, a third parameter involving the ratio of the two dimensions of the rectangle is required.

4. A Simplified Model

The variable P' in Equations 25 represents the deviation of the pressure from the initial hydrostatic pressure distribution and the gradient of P' should be in some sense small. Equation 25a is a momentum balance in the Θ direction, the direction of principal motion, and U and the derivatives of U with respect to R should be large compared to V and the derivatives of V which appear in Equation 25b. If it is assumed that $\partial P' / \partial \Theta$ is negligible compared to the largest terms of Equation 25a, Equations 25a, 25c, and 25d

are sufficient for the determination of U, V, and ϕ . Equation 25b could then be used to determine P' if desired. As a second simplification the Coriolis force term, UV/R, will be neglected in Equation 25a along with the term $(2/R^2)(\partial V/\partial \Theta)$ to give the system of equations which were used in the computation part of this work.

$$\frac{\partial U}{\partial t} + \frac{U}{R} \frac{\partial U}{\partial \Theta} + V \frac{\partial U}{\partial R} = G \alpha \phi \sin \Theta + \frac{\partial^2 U}{\partial R^2} + \frac{1}{R} \frac{\partial U}{\partial R} - \frac{U}{R^2} + \frac{1}{R^2} \frac{\partial^2 U}{\partial \Theta^2} \quad (26a)$$

$$\frac{\partial \phi}{\partial t} + \frac{U}{R} \frac{\partial \phi}{\partial \Theta} + V \frac{\partial \phi}{\partial R} = \frac{\alpha}{V} \left[\frac{\partial^2 \phi}{\partial R^2} + \frac{1}{R} \frac{\partial \phi}{\partial R} + \frac{1}{R^2} \frac{\partial^2 \phi}{\partial \Theta^2} \right] \quad (26b)$$

$$\frac{\partial (RV)}{\partial R} + \frac{\partial U}{\partial \Theta} = 0 \quad (26c)$$

The boundary conditions are now that at $R = 1$: U and V are zero, $\phi = 1/2$ for $0 < \Theta < \pi$, and $\phi = -1/2$ for $\pi < \Theta < 2\pi$. Initially U, V, and ϕ are zero.

The implications of the idealizations given above deserve some discussion. Dropping the terms UV/R and $(2/R^2)(\partial V/\partial \Theta)$ can be justified very simply by estimating the magnitude of the terms in relation to other terms in the equation by use of Martini's data and by use of solutions of Equations 26. Neglecting $\partial P'/\partial \Theta$ in Equation 25a leads to anomalies which are analogous to those of the flat plate, Equations 12. The radial velocity, V, is that velocity required to satisfy the continuity equation without regard to momentum changes in the radial direction. Outside the boundary layer where U and its derivatives are small, the quantity RV becomes a non-zero function of Θ , and at the center V is infinite. This behavior of V away from the boundary, as in the case of the flat plate, need not prevent the model from being useful. It is postulated that $\partial U/\partial R$,

$\partial^2 U / \partial R^2$, $\partial \phi / \partial R$ and $\partial^2 \phi / \partial R^2$ are large near the boundary and U approaches zero with increasing distance from the boundary after going through a maximum. Beyond the point where U is small, values of V predicted by Equations 26 are meaningless, but they are of no interest. Values of U , V , and ϕ from the equations should be valid in the region near the boundary where U and ϕ differ appreciably from zero. In the central region values of U and ϕ should be valid (approximately zero) and values of V are meaningless.

The idealization required to simplify Equation 26 to the form of Equations 25 are discussed in more detail in Appendix A. It is shown there that the validity of the idealizations depends on the Grashof number. The model should approximate the actual behavior of fluids more closely as the Grashof number increases. For very small Grashof numbers the model should be expected to be inadequate.

5. A Highly Simplified Model

It is instructive to consider a highly simplified model from which a first approximation of the effect of the parameters is obtained. Suppose that the motion is in some sense slow such that the inertial terms in Equations 26 may be neglected and that U and ϕ are different from zero only in a narrow region near the boundary so that $r d\Theta \approx r_0 d\Theta$ where r_0 is the radius of the boundary. As additional simplifications, suppose that $1/r^2 \partial^2 u / \partial \Theta^2$ and $(1/r^2) (\partial^2 \phi / \partial \Theta^2)$ are negligible compared to $\partial^2 u / \partial r^2$ and $\partial^2 \phi / \partial r^2$. The resulting simplified equations are given below for steady state.

$$g \beta \Delta T \phi \sin \Theta + \nu \frac{\partial^2 u}{\partial r^2} = 0 \quad (27a)$$

$$\nu \frac{\partial \phi}{\partial r} + \frac{u}{r_0} \frac{\partial \phi}{\partial \Theta} = \alpha \frac{\partial^2 \phi}{\partial r^2} \quad (27b)$$

$$\frac{\partial \nu}{\partial r} + \frac{1}{r_0} \frac{\partial u}{\partial \Theta} = 0 \quad (27c)$$

If the variable r is replaced by $y = r_0 - r$, the distance from the boundary, the equations are unchanged except that some terms change sign. By the postulation of narrow boundary layer it is possible to neglect the curvature of the wall when thinking of the boundary conditions associated with y . For example one condition where $U = 0$, is at $y = 0$ and the other condition where $U = 0$ may be taken to be at $y = \infty$. Multiplying y by any constant will not alter the two conditions so a new dimensionless variable, y/y_0 , may be chosen in which y_0 is completely arbitrary. Using this freedom and carrying out dimensional analysis in the manner illustrated before leads to the result that u ($V/r_0 g \beta \Delta T \alpha$)^{1/2}, v ($r_0 V / g \beta \Delta T \alpha^3$)^{1/4}, and ϕ depend on Θ and $(1 - r/r_0) \cdot (g \beta \Delta T r_0^3 / \nu \alpha)$ ^{1/4}; and h/k ($\nu \alpha r_0 / g \beta \Delta T$)^{1/4} depends only on Θ . This result can be rearranged in terms of the Grashof, Nusselt and Prandtl numbers and in terms of the variables of Equations 26 as indicated below

$$\frac{u \sqrt{r_0}}{V} = \left(\frac{Gr}{Pr} \right)^{1/2} f_1 \left[\Theta, (1 - r/r_0) (Gr Pr)^{1/4} \right] \quad (28)$$

$$\frac{v \sqrt{r_0}}{V} = \left(\frac{Gr}{Pr^3} \right)^{1/4} f_2 \left[\Theta, (1 - r/r_0) (Gr Pr)^{1/4} \right] \quad (29)$$

$$\phi = f_3 \left[\Theta, (1 - r/r_0) (Gr Pr)^{1/4} \right] \quad (30)$$

$$\frac{h \sqrt{r_0}}{k} = (Gr Pr)^{1/4} f_4 \left[\Theta \right] \quad (31)$$

Equations 28 through 31 are extremely useful in predicting the qualitative effect of the Grashof and Prandtl parameters. As will be shown in the discussion of results the simple model agrees well with the computations based on a more complex model. The equations can even serve

in a limited way to establish the conditions under which the simplifying assumptions by which the equations were devised may be expected to be valid. Such a procedure admittedly involves circuitous reasoning. However, the procedure seems to give the right answers so it will be outlined.

For simplicity in the notation, let Z be the second argument of f_1 in Equation 28 and let $U = ur_0/\nu$, $V = vr_0/\nu$, and $R = r/r_0$ as in Equations 26. As a first example, consider the assumption of a thin boundary layer. This assumption tends to fail as the Rayleigh number decreases since for Z to have a fixed value $1 - r/r_0$ must increase as the Rayleigh number decreases. The boundary layer thickness is proportional to $(GrPr)^{-1/4}$. As a second example consider the assumption that $(1/R^2)(\partial^2 U/\partial \theta^2)$ may be neglected compared to $\partial^2 U/\partial R^2$. From Equation 28

$$\frac{\partial^2 U}{\partial R^2} = Gr \frac{\partial^2 f_1}{\partial Z^2}$$

$$\frac{\partial^2 U}{\partial \theta^2} = \frac{\partial^2 f_1}{\partial \theta^2}$$

which shows that the maximum radial derivative increases with the Grashof number whereas the azimuthal derivative does not. The assumption then tends to fail as the Grashof number decreases. By a similar argument it can be shown that other of the idealizations tend to fail for small Prandtl numbers. These conclusions must be tempered by the knowledge that if the Grashof number is very large, turbulent flow occurs and the model also fails. Herman (11,12) Merk and Prins (22), and Morgan and Warner (23) give other discussions of the idealizations used here.

In the analysis given here the effects of both the Grashof and Prandtl numbers are taken into account. By Equation 31 the Nusselt number is proportional to the product of the two numbers to the one-quarter power.

In Appendix A the analysis is given in more detail. The analysis given there shows:

1. The dependence of the solution on the Grashof number can be established by assuming only a large Grashof number--it is not necessary to neglect the inertial terms. In other words the asymptotic solution for large Grashof numbers is that $Nu \propto Gr^{\frac{1}{4}}$.

2. The inertial terms in the momentum balance become less and less important relative to the other terms as the Prandtl number increases. In other words the analysis given above in which $Nu \propto (GrPr)^{\frac{1}{4}}$ is the asymptotic solution for both large Gr and large Pr.

III. FINITE DIFFERENCE METHODS

It has been mentioned that finite difference methods hold promise for solution of problems which are too difficult for ordinary methods of analysis. In this section the methods will be discussed in some detail. It should be mentioned at the outset that basic questions of convergence and stability can not be resolved with mathematical rigor because the theory is generally inadequate. Nevertheless it is possible to cope with the major difficulties and produce an apparently satisfactory solution for the system of equations under consideration.

The basic idea of finite difference approximation comes directly from the definition of the derivative. Suppose $u \equiv f(x, y, t)$ and its first derivatives are continuous; then the definition of the partial derivative with respect to x may be written in three different ways:

$$\begin{aligned} \frac{\partial u(x_0, y_0, t_0)}{\partial x} &= \lim_{h \rightarrow 0} \frac{f(x_0+h, y_0, t_0) - f(x_0, y_0, t_0)}{h} = \lim_{h \rightarrow 0} \frac{f(x_0, y_0, t_0) - f(x_0-h, y_0, t_0)}{h} \\ &= \lim_{h \rightarrow 0} \frac{f(x_0+h, y_0, t_0) - f(x_0-h, y_0, t_0)}{2h} \end{aligned}$$

in which the alternate definitions are identical. If the limit process is not carried out, h is finite and the result is called a divided difference approximation to the derivative:

$$\begin{aligned} \frac{\partial U}{\partial x}(x_0, y_0, t_0) &\approx \frac{f(x_0+h, y_0, t_0) - f(x_0, y_0, t_0)}{h} \approx \frac{f(x_0, y_0, t_0) - f(x_0-h, y_0, t_0)}{h} \\ &\approx \frac{f(x_0+h, y_0, t_0) - f(x_0-h, y_0, t_0)}{2h} \end{aligned}$$

in which the alternate forms may not be expected to be the same. The three differences in the numerator of the equation are called forward, backward and central differences, respectively. From Taylor's formula the central difference would be expected to be the best of the three from the standpoint of accuracy. However, there are other factors to consider in selecting the form of the difference as will be discussed later. The error in the approximation clearly depends on the size of the increment, h , as well as on the behavior of the function.

An approximation to the second derivative can be obtained by repeating the process whereby the first derivative was approximated. A different method which illustrates the use of Taylor's formula is outlined below

$$\begin{aligned} f(x_0+h, y_0, t_0) &= f(x_0, y_0, t_0) + h \frac{\partial f}{\partial x}(x_0, y_0, t_0) + \frac{h^2}{2} \frac{\partial^2 f}{\partial x^2}(x_0, y_0, t_0) + \frac{h^3}{3!} \frac{\partial^3 f}{\partial x^3}(x_0, y_0, t_0) \\ f(x_0-h, y_0, t_0) &= f(x_0, y_0, t_0) - h \frac{\partial f}{\partial x}(x_0, y_0, t_0) + \frac{h^2}{2} \frac{\partial^2 f}{\partial x^2}(x_0, y_0, t_0) - \frac{h^3}{3!} \frac{\partial^3 f}{\partial x^3}(x_0, y_0, t_0) \end{aligned}$$

where $x_0 < x^+ < x_0 + h$ and $x_0 - h < x^- < x_0$ (the values x^+ and x^- are chosen to satisfy the equality). Adding the two formulas and rearranging gives:

$$\frac{\partial^2 f}{\partial x^2}(x_0, y_0, t_0) = \frac{f(x_0+h, y_0, t_0) - 2f(x_0, y_0, t_0) + f(x_0-h, y_0, t_0)}{h^2} + \frac{h}{3!} \left[\frac{\partial^3 f}{\partial x^3}(x^-, y_0, t_0) - \frac{\partial^3 f}{\partial x^3}(x^+, y_0, t_0) \right] \quad (32)$$

The first term on the right hand side of Equation 32 is called a central difference approximation of the second derivative, and the other term represents the truncation error incurred by replacing the derivative by the divided difference. The truncation error vanishes as $h \rightarrow 0$ and is zero for any h if the third derivative is identically zero.

The basic concept of the finite difference approach can be stated in very simple terms. The derivatives in a system of equations are replaced by divided differences giving a system of algebraic equations which presumably can be solved by some method. The solution to the difference equations is expected to approximate the solution to the differential equations. In actual practice there are some difficulties which are to be discussed below. It is clear that if the increment size is in some sense large the solution to the difference equations might be a very poor approximation to the solution to the original problem.

A. Methods of Attack

In the problems under consideration there are two space variables, x and y ; a time variable, t , and three dependent variables u , v , and T . If it is supposed that at large times a steady state is reached such that u , v , and T no longer depend on time and that this steady state solution is of primary interest, then there are two alternate methods of attacking the problem: the steady state approach and the unsteady state approach.

1. The Steady State Approach

In the steady state approach the derivatives with respect to time in the equations are dropped reducing the number of independent variables from three to two. If the x and y dimensions of the region of interest are divided into $M - 1$ and $N - 1$ increments, respectively, there will be MN "grid points." At each grid point there are the three independent variables so that there are $3MN$ algebraic equations to be solved. As an indication of the enormity of the task, the number $3MN$ was as high as 6,000 in this work. The algebraic equations are not linear. Methods of solving non-linear algebraic equations, in contrast to those for linear equations, are not highly developed.

There is a stability problem associated with unsteady state calculations which is not present in the steady state approach. It might therefore be expected that the steady state approach is preferable if only the steady state solution is desired. However, the system of algebraic equations will almost certainly have to be solved by some iterative procedure, and the problems associated with finding a method of iteration which converges with some rapidity are considerable. Douglas and Peaceman (4) indicate that, even for conduction problems which involve only linear equations, the unsteady state approach is preferable to the steady state approach. In view of the difficulties involved in solving non-linear algebraic equations and for the reasons given below, the unsteady state approach was used throughout this work.

2. The Unsteady State Approach

In the unsteady state approach, the equations are written as an initial value problem in which the velocities and the temperature are computed as functions of space and time starting from some initial condition. There are several advantages to this method of attack:

1. Both the transient and steady state solutions are obtained; the steady state solution being the limiting value of the transient solution.

2. The unsteady state calculations may be thought of as an iterative method of solving the steady state problem in which the intermediate values of the dependent variables have physical significance. If the transient solution is not desired, the initial condition can be replaced by an estimate of the steady state solution thereby reducing the amount of computation required. The steady state solution is independent of the choice of initial conditions.

3. No direct assumption of laminar flow is required. The steady state approach is clearly limited to laminar flow. In the unsteady state approach the time dependent form of the equations is preserved along with the intriguing possibility of actually computing the fluctuations which characterize turbulent flow. The direct calculation of turbulent flow is very likely more difficult than laminar flow by orders of magnitude and even may be essentially impossible. However, it is a matter of such interest and importance that it is desirable to learn as much as possible about the behavior of the difference equations with respect to time in the hope that the work may constitute a step in the direction of computing turbulence.

The main difficulty in the unsteady state method is that the difference equations may be unstable unless care is taken in selecting the form of the differences and the size of the time step.

B. Stability and Convergence

The remainder of this section is based for the most part on Richtmyer's book on difference methods (28) in which work by Lax, von

Neumann and others is presented along with a number of examples. The reader is referred to this book for an excellent discussion of the theory and practice. Richtmyer gives the development of the theory for a class of linear equations with constant coefficients, but points out that the theory is inadequate for complicated problems of the most interest. He then shows that the von Neumann method of stability analysis can be applied successfully to problems for which a rigorous stability analysis is unknown. The stability criterion so predicted is shown to be an excellent approximation of the necessary condition for stability in several cases by actually performing experimental calculations and observing the behavior of the solution.

Stability is a necessary condition for the solution of the difference problem to converge to solution of the differential problem as the size of the increments, Δx , Δy and Δt tend to zero. Convergence is essential for the results to be meaningful in that the fundamental idea of an approximation is that the error can be made as small as one wishes. In practice an unstable scheme of calculation usually yields meaningless numbers which overflow the accumulator of the computer after a relatively few time steps. The essence of stability is that there should be a limit to the extent to which any part of the initial data can be amplified in the numerical procedure.

Suppose the x and y dimensions of the region of interest are divided into increments of size Δx and Δy respectively such that $x = j\Delta x$ and $y = l\Delta y$ where j and l are integers. Let n , an integer, denote the number of time steps starting from the initial condition such that $t = n\Delta t$. Let $u_{j,l}^{(n)}$ be an independent variable associated with the n^{th} time step (n here is a superscript not an exponent) and the position denoted by the subscripts. Now in the scheme of calculations a new set of the variables,

$u_{j,l}^{(n+1)}$, is somehow calculated from the old, $u_{j,l}^{(n)}$, perhaps using values of other dependent variables and perhaps using values of the variables at other time levels (for example, $u_{j,l}^{(n-1)}$). However the calculations are carried out the scheme will be said to be stable if the following inequality holds for any choice of initial data:

$$\max_{(j,l)} |u_{j,l}^{(n+1)}| \leq \left(\max_{(j,l)} |u_{j,l}^{(n)}| \right) (1 + M_1 \Delta t) + M_2 \Delta t \quad (33)$$

for some $M_1 \geq 0$, $M_2 \geq 0$.

The numerical procedure should be thought of as one of a sequence in which Δx , Δy , and Δt are made smaller and smaller with the expectation of convergence. For stability it is required that the values of u at some time, t , be bounded independent of the increment sizes. By repeated application of the inequality, $u_{j,l}^{(n)}$ can be bounded in terms of the initial data $u_{j,l}^{(0)}$ and the time, t as indicated below:

$$\begin{aligned} \max_{(j,l)} |u_{j,l}^{(n)}| &\leq \left[\left(\max_{(j,l)} |u_{j,l}^{(n-1)}| \right) (1 + M_1 \Delta t) + M_2 \Delta t \right] (1 + M_1 \Delta t) + M_2 \Delta t \\ &\leq \left[\max_{(j,l)} |u_{j,l}^{(0)}| \right] \left[(1 + M_1 \Delta t)^n + M_2 \Delta t \left[(1 + M_1 \Delta t) + (1 + M_1 \Delta t)^2 + \dots + (1 + M_1 \Delta t)^{n-1} \right] \right] \\ &\leq (1 + M_1 \Delta t)^n \left[\max_{(j,l)} |u_{j,l}^{(0)}| + M_2 \Delta t \right] = (1 + M_1 \Delta t)^n \left[\max_{(j,l)} |u_{j,l}^{(0)}| + t M_2 \right] \end{aligned}$$

Using the fact that $(1 + M_1 \Delta t)^n \leq e^{n \ln(1 + M_1 \Delta t)}$ and that $\ln(1 + M_1 \Delta t) \leq M_1 \Delta t$ gives

$$\max_{(j,l)} |u_{j,l}^{(n)}| \leq e^{t M_1} \left[\max_{(j,l)} |u_{j,l}^{(0)}| + t M_2 \right] \quad (34)$$

which is the desired result. For a fixed t as $\Delta t \rightarrow 0$ the number of time steps, n , becomes infinite, but the solution is bounded independent of t .

In problems for which the theory is well developed stability implies convergence under fairly general circumstances if the truncation error incurred by replacing derivatives by divided differences vanishes as Δx , Δy , and $\Delta t \rightarrow 0$. It should be mentioned that stability is defined in different ways by some workers. The definition given above is essentially the same as that originated by Fritz John (16) and used by Richtmyer (28).

C. Stability Analysis

The importance of the concept of stability has been indicated above. In this section methods of stability analysis will be discussed in association with some examples. It will be shown that the choice of the form of the differences used to approximate the derivatives is of crucial importance. Some choices lead to schemes which are unconditionally unstable. As a general rule a stability criterion involves a restriction on Δt in terms of Δx , Δy and the parameters of the system of equations. However, there are schemes which are unconditionally stable or unconditionally unstable. In the case of non-linear problems the stability criterion may also involve the dependent variables.

As a very simple example of a non-linear problem, consider the equation given below in which only the leading terms of a momentum balance are included.

$$\frac{\partial u}{\partial t} = -u \frac{\partial u}{\partial x} \quad (35)$$

In association with Equation 35 it is supposed that u is specified on a boundary and initially although it is not necessary to think of the equation as representing a physical situation.

Consider three different approximations to Equation 35 in which $\partial u / \partial t$ is replaced by a forward divided difference and $\partial u / \partial x$ is replaced by a forward, central or backward divided difference.

$$\frac{u_j^{(m+1)} - u_j^{(m)}}{\Delta t} = -u_j^{(m)} \frac{u_{j+1}^{(m)} - u_j^{(m)}}{\Delta x} \quad (36)$$

$$\frac{u_j^{(m+1)} - u_j^{(m)}}{\Delta t} = -u_j^{(m)} \frac{u_{j+1}^{(m)} - u_{j-1}^{(m)}}{2\Delta x} \quad (37)$$

$$\frac{u_j^{(m+1)} - u_j^{(m)}}{\Delta t} = -u_j^{(m)} \frac{u_j^{(m)} - u_{j-1}^{(m)}}{\Delta x} \quad (38)$$

The three schemes are called explicit since the values of u at the $n + 1^{\text{th}}$ time level can be solved for directly from those at the n^{th} time level. It will be shown that Equation 37 is unconditionally unstable; that Equation 36 can be stable only if $u \leq 0$, and that Equation 38 can be stable only if $u \geq 0$. In the stable cases it is required that

$\left| u_j^{(n)} \right| \Delta t / \Delta x \leq 1$. It is interesting to notice that Equation 37 which would intuitively be expected to be preferred is completely useless because of instability.

1. Positive Type Difference Equations

A useful method of stability analysis is based on the use of difference equations in which all the coefficients are positive. In such cases a sufficient condition for stability can often be established by inspection. By way of illustration Equation 36 can be rearranged to give

$$u_j^{(m+1)} = u_j^{(m)} \left(1 + \frac{\Delta t}{\Delta x} u_j^{(m)} \right) - u_{j+1}^{(m)} \left(\frac{\Delta t}{\Delta x} u_j^{(m)} \right)$$

from which no conclusions are obvious unless $u_j^{(n)} < 0$. Considering $u_j^{(n)} < 0$ the equation can be rewritten

$$u_j^{(m+1)} = u_j^{(m)} \left(1 - \frac{\Delta t}{\Delta x} |u_j^{(m)}| \right) + u_{j+1}^{(m)} \left(\frac{\Delta t}{\Delta x} |u_j^{(m)}| \right)$$

Now the sum of coefficients of $u_j^{(n)}$ and $u_{j+1}^{(n)}$ is unity and each coefficient is positive or zero providing $\Delta t / \Delta x |u_j^{(n)}| \leq 1$. Then $u_j^{(n+1)}$ always falls between $u_j^{(n)}$ and $u_{j+1}^{(n)}$. Hence Equation 36 is stable if $u_j^{(n)} \leq 0$ and $\Delta t / \Delta x |u_j^{(n)}| \leq 1$. Notice that the stability criterion depends on the solution so that it is not generally possible to select a time step in advance which will insure stability. The computer must test the criterion and alter the time step as necessary to maintain stability.

The simple way of looking at the stability problem outlined above is useful for only a small class of problems. There is a much more general method of stability analysis due to von Neumann.

2. The von Neumann Method of Stability Analysis

The von Neumann method of stability analysis employing Fourier series can be applied to a great variety of problems. Theoretically the method only applies to a small class of linear equations with constant coefficients. In practice it has been found to give a good approximation to the stability criterion even for non-linear problems. The method can be applied to explicit or implicit schemes involving any number of time levels and any number of variables. By way of introduction the method will be used to show that Equation 37 is unstable as previously asserted.

$$\frac{u_j^{(m+1)} - u_j^{(m)}}{\Delta t} = -u_j^{(m)} \left(\frac{u_{j+1}^{(m)} - u_{j-1}^{(m)}}{2\Delta x} \right) \quad (37)$$

The equation could be made linear by writing $u + \dot{u}$ in place u , where \dot{u} is a small quantity of the first order, and dropping quantities of the second and higher order. For Equation 37 this only amounts to thinking of the coefficient of the derivative as a constant, so the notation of the equation will be retained except the subscript and superscript on the coefficient will be dropped. By rearrangement

$$u_j^{(m+1)} = u_j^{(m)} - \beta \left(u_{j+1}^{(m)} - u_{j-1}^{(m)} \right) \quad (38)$$

where $\beta = u \Delta t / 2\Delta x$.

Now it is assumed that the solution of the equation can be written in the form

$$u_j^{(m)} = \sum_K \xi^{(k)} e^{ikj\Delta x}$$

By the assumption of separation of variables each term in the series grows or decays independently and a general term of the series can be considered.

Substitution of $\xi e^{ikj\Delta x}$ into equation gives

$$\xi^{m+1} e^{ikj\Delta x} = \xi^m e^{ikj\Delta x} - \beta \xi^m \left(e^{ik(j+1)\Delta x} - e^{ik(j-1)\Delta x} \right)$$

which can be solved for ξ .

$$\xi = 1 - \beta \left(e^{ik\Delta x} - e^{-ik\Delta x} \right) = 1 - 2i\beta \sin(k\Delta x) \quad (39)$$

The absolute value of ξ determines the rate of growth of u with time: $|\xi| < 1$ corresponds to no growth and $|\xi| \leq 1 + M\Delta t$ (M not dependent on k) corresponds to exponential growth which is permissible by the

definition of stability. However, by Equation 39, $|\xi| > 1$ without regard to Δt for all values of k except those where $\sin k \Delta x = 0$. In other words at a fixed t , as $\Delta t \rightarrow 0$ and $n \rightarrow \infty$ with β fixed, some terms of the series are amplified without bound. Therefore, the scheme is unstable.

The technique is easily adapted to systems of equations in several space variables. Consider a simple example to illustrate the method. The example is too simple to represent a physical situation, but contains terms of the type of interest.

$$\frac{\partial u}{\partial t} = -u \frac{\partial u}{\partial x} + a \phi \quad (40)$$

$$\frac{\partial \phi}{\partial t} = -u \frac{\partial \phi}{\partial x} + b \frac{\partial^2 \phi}{\partial y^2} \quad (41)$$

In this example u is taken to be positive and the difference equations are given below in which u is treated as a constant where it is a coefficient in the manner of the first example

$$\frac{u_{j,l}^{(n+1)} - u_{j,l}^{(n)}}{\Delta t} = -u \frac{u_{j,l}^{(n)} - u_{j-1,l}^{(n)}}{\Delta x} + a \phi_{j,l}^{(n)}$$

$$\frac{\phi_{j,l}^{(n+1)} - \phi_{j,l}^{(n)}}{\Delta t} = -u \frac{\phi_{j,l}^{(n)} - \phi_{j-1,l}^{(n)}}{\Delta x} + b \frac{\phi_{j,l+1}^{(n)} - 2\phi_{j,l}^{(n)} + \phi_{j,l-1}^{(n)}}{(\Delta y)^2}$$

It will be supposed that the general terms of the series for u and ϕ are of the form $\xi^n e^{ik_1 j \Delta x} e^{ik_2 l \Delta y}$ and $\eta^n e^{ik_1 j \Delta x} e^{ik_2 l \Delta y}$, respectively. Substitution and rearrangement gives

$$\xi^{n+1} = \xi^n [1 - \beta(1 - e^{-ik_1 \Delta x})] + \eta^n a \Delta t \quad (42)$$

$$\rho^{n+1} = \rho^n \left[1 - \beta(1 - e^{-ik_1 \Delta x}) \right] + \rho^n \gamma \left[e^{ik_2 \Delta y} - 2 + e^{-ik_2 \Delta y} \right] \quad (43)$$

where $\beta = u \Delta t / \Delta x$ and $\gamma = b \Delta t / (\Delta y)^2$.

In a more general problem it would not be possible to solve the equations directly. The system of equations might be of the form

$$A \vec{V}_1 = B \vec{V}_2$$

or

$$\vec{V}_1 = A^{-1} B \vec{V}_2$$

where \vec{V}_1 is the vector with components ξ^{n+1} and ρ^{n+1} and \vec{V}_2 is the vector with components ξ^n and ρ^n . Let $G = A^{-1}B$; G is called the amplification matrix and it plays the part of ξ in the first example. From Equation 42 and 43 for this example

$$G = \begin{pmatrix} C_1 & a \Delta t \\ 0 & \gamma + C_2 \end{pmatrix}$$

where $C_1 = 1 - \beta(1 - e^{-ik_1 \Delta x})$ and $C_2 = \gamma \left[e^{ik_2 \Delta y} - 2 + e^{-ik_2 \Delta y} \right] = 2\gamma [\cos k_2 \Delta y - 1]$.

The von Neumann necessary condition for stability is that $|\lambda| \leq 1 + M \Delta t$ for some $M \geq 0$, where λ is the largest eigenvalue of G . The eigenvalues of G in the example are

$$\lambda_1 = C_1 = 1 - \beta(1 - e^{-ik_1 \Delta x})$$

$$\lambda_2 = \gamma + C_2 = 1 - \beta(1 - e^{-ik_1 \Delta x}) + 2\gamma(\cos k_2 \Delta y - 1)$$

If $\beta + 2\gamma \leq 1$ both the eigenvalues lie within or on the unit circle

($\beta \geq 0$, $\gamma \geq 0$). The stability requirement then is that $u \Delta t / \Delta x + 2b \Delta t /$

$(\Delta y)^2 \leq 1$, where $u \geq 0$. If $u < 0$ the equations are unconditionally unstable.

It should be mentioned that known sufficient conditions for stability may be more stringent than necessary conditions. However, Richtmyer asserts that the von Neumann condition has always been found to be both necessary and sufficient in those cases where the gap between the two has been narrowed.

Almost every step in the procedure of stability analysis given above is unsatisfactory from the mathematical standpoint. Nevertheless the procedure has been found to give the correct answers to the stability question in many cases. Richtmyer (28) gives a number of examples wherein the stability criterion is determined by experiment and found to agree with that predicted by the procedure given above.

Round off error has not been mentioned at all in this section despite the fact that many workers define stability in terms of round off error. It can be shown that the alternate definitions of stability are essentially the same for linear equations as well as non-linear equations in those cases for which the theory is well developed. Richtmyer states that in his opinion round off error is generally not of much importance.

IV. THE FLAT PLATE

The flat plate problem was selected for finite difference calculations partially because a solution to the problem exists both for small time where practically all the heat transfer is by conduction and for large time where steady state is reached. The results of the calculations will be compared with the existing solutions at both ends of the time scale. In the intermediate time range the problem has never been solved before so the results represent new information. The existing solutions will be reviewed very briefly before discussion of the finite difference solution.

Initially in the flat plate problem there is no fluid motion, and after the motion starts for some time the motion is essentially one dimensional. During this initial interval the heat transfer is almost entirely by conduction for which the classical solution is

$$\phi = 1 - \operatorname{erf}\left(\frac{y}{2\sqrt{\alpha t}}\right) \quad (50)$$

where ϕ is the dimensionless temperature as before. By differentiating Equation 50 the heat transfer coefficient is found to be

$$h = \frac{k}{\sqrt{\pi\alpha t}} \quad (51)$$

which will be used later in a comparison of results.

At very large times the steady state solution of Schmidt, Beckmann and Pohlhausen which was discussed earlier applies. The original solution was by series in which the coefficients were determined numerically by iteration. More recent solutions have been by numerical integration.

Numerical methods of solving ordinary differential equations yield accurate results with very little computation so such a solution will be regarded here as exact. Ostrach's solution (26) will be used in the comparison with results. Ostrach gives a comparison of the solution with the measurements of Schmidt and Beckmann. Excluding points near the leading edge and those where turbulent flow may be starting, the agreement is good. The velocities and temperatures agree remarkably well near the plate where they are of the most interest. The deviation in the velocity increases with distance from the plate. The velocity of the solution seems to approach zero more quickly with distance than the measured velocity.

A. The Differential Problem

The equations of the Schmidt-Beckmann model used in the finite difference calculations are given below in dimensionless form.

$$\frac{\partial U}{\partial \tau} + U \frac{\partial U}{\partial X} + V \frac{\partial U}{\partial Y} = \phi + \frac{\partial^2 U}{\partial Y^2} \quad (52a)$$

$$\frac{\partial \phi}{\partial \tau} + U \frac{\partial \phi}{\partial X} + V \frac{\partial \phi}{\partial Y} = \frac{\alpha}{\nu} \frac{\partial^2 \phi}{\partial Y^2} \quad (52b)$$

$$\frac{\partial U}{\partial X} + \frac{\partial V}{\partial Y} = 0 \quad (52c)$$

The boundary and initial conditions are:

$$X=0: \quad U = \phi = 0$$

$$Y=0: \quad U = V = 0; \quad \phi = 1$$

$$Y=\infty: \quad U = V = \phi = 0$$

$$\tau=0: \quad U = V = \phi = 0$$

and the dimensionless variables are:

$$U = \frac{u}{(\nu g \beta \Delta T)^{1/3}} ; \quad V = \frac{v}{(\nu g \beta \Delta T)^{1/3}} ; \quad X = x \left(\frac{g \beta \Delta T}{\nu^2} \right)^{1/3}$$

$$Y = y \left(\frac{g \beta \Delta T}{\nu^2} \right)^{1/3} ; \quad \tau = t \frac{(g \beta \Delta T)^{2/3}}{\nu^{1/3}}$$

B. The Difference Problem

It is possible to approximate Equations 52 by a system of explicit difference equations. The difference equations will be stable for sufficiently small time steps only if certain types of differences are used for the non-linear terms. The terms $U \partial U / \partial X$, $V \partial U / \partial Y$, $U \partial \phi / \partial X$, and $V \partial \phi / \partial Y$ must be approximated using either a forward or backward difference depending on the sign of U or V , whichever appears as a coefficient of the derivative. A forward difference is used where the coefficient velocity is negative and a backward difference is used where the coefficient velocity is positive. This method of dealing with terms of this type is due to Lelevier according to Richtmyer (28). In general the velocities may be expected to change sign in the space-time region of interest so that four different sets of equations are required and the machine must determine the signs of U and V at each point and select the equations to be used. However, the flat plate problem is somewhat simpler than the most general problem in that U is always positive or zero and V is always negative or zero. As a result a single system of difference equations can be used.

1. The Space Grid

The space grid used for the problem is shown in Figure 2. The point $j = 1$, $l = 1$ corresponds to the origin, $X = (j - 1) \Delta X$ and $Y =$

$(\ell - 1)\Delta Y$. The line $Y = 0$ corresponds to the plate with $X = 0$ being the leading edge. The plate is of infinite extent in the X direction and the fluid is of infinite extent in the Y direction. It is also assumed here that the plate is of infinite extent in the direction normal to the $X - Y$ plane. In the numerical procedure it is necessary to work with a finite region.

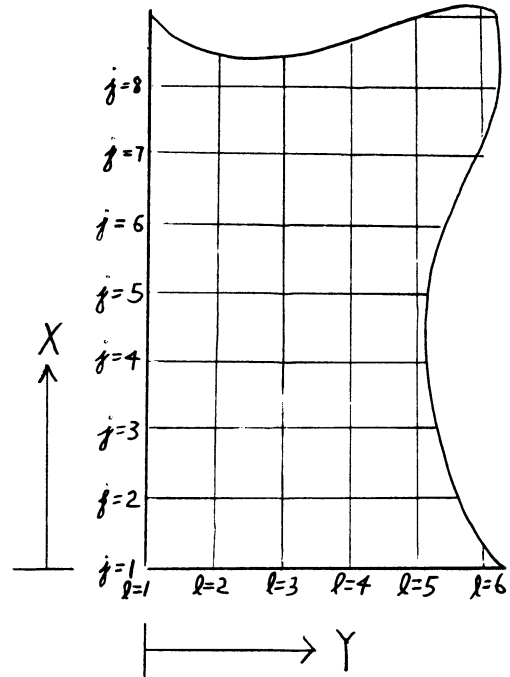


Figure 2. The Space Grid.

In this work the X dimension of the region was 100 which corresponds to a Grashof number of 10^6 . The choice

of the X dimension is somewhat arbitrary since the solution can be rearranged into a form valid for all X . The integers j ranged up to 40. That is $j = 40$ corresponds to $X = 100$ so that $\Delta X = 100/39$.

In the Y direction there are conditions that U and ϕ are zero at $Y = 0$ so that some finite Y dimension which can be regarded as infinite must be used. An infinite distance may be thought of as some distance so large that it no longer matters how large it is. The problem was first solved forcing U and ϕ to be zero at $Y = 25$ corresponding to $\ell = 40$ so that $\Delta Y = 25/39$. To determine the effect of the choice of the Y dimension the problem was reworked forcing U and ϕ to be zero at $Y = (25)(49)/39$ which corresponds to $\ell = 50$ using the same ΔY . It was found that the velocities and temperatures near the plate were the same in the two cases

to at least four significant figures. It is concluded that either case is a satisfactory solution with respect to the infinite condition.

2. The Difference Equations

The difference equations corresponding to Equations 52 are given below.

$$\begin{aligned} \frac{U'_{j,l} - U_{j,l}}{\Delta\tau} + U_{j,l} \frac{U_{j,l} - U_{j-1,l}}{\Delta X} + V_{j,l} \frac{U_{j,l+1} - U_{j,l}}{\Delta Y} \\ = \phi'_{j,l} + \frac{U_{j,l+1} - 2U_{j,l} + U_{j,l-1}}{(\Delta Y)^2} \end{aligned} \quad (53a)$$

$$\begin{aligned} \frac{\phi'_{j,l} - \phi_{j,l}}{\Delta\tau} + U_{j,l} \frac{\phi_{j,l} - \phi_{j-1,l}}{\Delta X} + V_{j,l} \frac{\phi_{j,l+1} - \phi_{j,l}}{\Delta Y} \\ = \frac{\alpha}{V} \frac{\phi_{j,l+1} - 2\phi_{j,l} + \phi_{j,l-1}}{(\Delta Y)^2} \end{aligned} \quad (53b)$$

$$\frac{U_{j,l} - U_{j-1,l}}{\Delta X} + \frac{V_{j,l} - V_{j,l-1}}{\Delta Y} = 0 \quad (53c)$$

The primed variables are at the time level $\tau + \Delta\tau$ and the unprimed variables are at the time τ . The procedure of calculation using the equations is very simple. Starting from the initial condition, values of U' and ϕ' are computed using Equations 53a and 53b, respectively for the whole grid excluding the boundary. Then the corresponding values of V are computed from Equation 53c, working from the boundary, where $V = 0$, outward. The procedure is repeated over and over giving the velocity and temperature distribution for increasing values of time.

3. The Stability Criterion

The criterion for stability of Equations 53 can be obtained by either of the methods described earlier. The simple approach using a positive

type of difference equation applies here and gives the same results as the von Neumann method. First consider the energy balance, Equation 53b, which can be rearranged to give:

$$\begin{aligned} \phi'_{j,l} = & \phi_{j,l} \left(1 - \beta - \gamma - \frac{2B\alpha}{V} \right) + \phi_{j-1,l} \beta + \phi_{j,l-1} \frac{\alpha B}{V} \\ & + \phi_{j,l+1} \left(\frac{\alpha B}{V} + \gamma \right) \end{aligned} \quad (54)$$

where $\beta = U_{j,l} \frac{\Delta \tau}{\Delta X}$, $\gamma = |V_{j,l}| \frac{\Delta \tau}{\Delta Y}$ and $B = \frac{\Delta \tau}{(\Delta Y)^2}$

The absolute value of V is used where V is a coefficient so that β , γ and B all exceed or equal zero. The coefficients of Equation 54 add up to unity and the coefficients are all positive or zero if $\beta + \gamma + 2B\alpha/V \leq 1$, in which case $\phi'_{j,l}$ is always between the extreme of $\phi_{j,l}$ and three neighboring temperatures at the previous time. Initially, all the temperatures are zero except those on the boundary which are unity. Then ϕ at any point at any time cannot exceed unity nor be less than zero, and stability is assured. The stability requirement for the energy equation is then

$$\frac{U \Delta \tau}{\Delta X} + |V| \frac{\Delta \tau}{\Delta Y} + \frac{2\alpha \Delta \tau}{V(\Delta Y)^2} \leq 1 \quad (55)$$

The momentum balance can be treated in exactly the same way. It is found that $U'_{j,l}$ cannot exceed $\Delta \tau \phi'_{j,l}$, plus the largest of $U_{j,l}$ and neighboring values of U providing

$$\frac{U \Delta \tau}{\Delta X} + |V| \frac{\Delta \tau}{\Delta Y} + \frac{2\alpha \Delta \tau}{(\Delta Y)^2} \leq 1 \quad (56)$$

If inequalities 55 and 56 are both satisfied, $0 \leq \phi \leq 1$ and $0 \leq U \leq \infty$ which assures stability. Inequality 55 is more restrictive for Prandtl numbers of less than unity, whereas inequality 56 is more restrictive for Prandtl numbers greater than unity.

4. The Calculations

Equations 53 were solved on an IBM 704 computer for a Prandtl number of 0.733. This Prandtl number was selected since it was used by Schmidt and Beckmann (31) as well as by Ostrach (26), and one purpose of the flat plate work was to provide a comparison of a finite difference solution with exact solutions. The maximum values of U and V to be expected were estimated and on this basis a time step of $\Delta\tau = 0.1$ was used. It will be shown in the discussion of results that steady state was reached after about 400 time steps although the calculations were carried out for 680 time steps to be sure that no further change occurred. For the first ten time steps all the independent variables which differed from zero were printed by the machine; then selected values were printed after 20, 40, 80, 120 . . . time steps. A total of about six million values of the independent variables were calculated during the work so it was not practical to print them all.

The "Fortran" language was used for all the programs in this work. The procedure of calculation for the flat plate is very simple relative to that for the cylinder problem. The basic procedure was given in the discussion of the difference equations. It should be mentioned that in the calculations numbers smaller than 10^{-38} were encountered since U and ϕ tend to zero at large Y. Such numbers are below the capacity of the machine used so that an error is incurred unless some corrective action is taken. All numbers less than 10^{-10} were set identically equal to zero. By this

procedure the generation in the calculation of numbers between 10^{-38} and zero was avoided.

The first solution using the 40 by 40 space grid was terminated after 680 time steps. Then the Y dimension corresponding to $Y = \infty$ was extended by 25 per cent as indicated in the discussion of the space grid. The calculations were then continued for 240 time steps using the extended (40 by 50) space grid. The calculations on the extended grid were for the purpose of determining if the choice of the Y dimension influenced the solution near the plate. As indicated earlier there was no significant difference in the results. Tabular results are given in the appendix for both cases.

It is highly significant that by modern standards very little calculation was required to obtain an excellent solution to the system of equations. The solution was essentially complete after less than two hours of computing time. Much more than two hours computer time was actually used in investigating the effect of the conditions at $Y = \infty$ and in continuing the calculations past the time where steady state was reached. By making use of the knowledge gained in this work the steady state solution of a problem of similar difficulty could probably be obtained in about one hour of calculation on the IBM 704 or some similar machine. The amount of calculation could be reduced by using a more coarse grid at large distances from the boundary where derivatives are small. Also, the size of the time step could be increased by about 50% if the derivatives $U \partial U / \partial X$, $U \partial \phi / \partial X$, $V \partial U / \partial Y$ and $V \partial \phi / \partial Y$ were approximated using implicit differences. This procedure will be discussed in a later section of this thesis where it will be shown that using implicit differences for these terms does not complicate the calculations. The larger time step was not used in the calculations since it would presumably reduce the accuracy of the transient

solution. The transient solution was considered to be of particular importance in this work since such a solution has not been obtained before.

C. Results

The direct results of the calculations are values of U , V , and ϕ as functions of X , Y , and Z , the dimensionless variables of Equations 52. The results can be placed in a more compact form by use of the analysis previously given in Part II. In terms of the dimensionless variables of Equation 52 for a fixed Prandtl number $U/X^{1/2}$, $VX^{1/4}$, and ϕ depend on $Y/X^{1/4}$ and $Z/X^{1/2}$ or, in terms of the variables of the original problem $u/(xg\beta\Delta T)^{1/2}$, $V(x/\nu^2g\beta\Delta T)^{1/4}$ and $(T-T_i)/(T_w-T_i)$ depend on $y(g\beta\Delta T/\nu^2x)^{1/4}$ and $t(g\beta\Delta T/x)^{1/2}$; and $h/k(\nu^2x/g\beta\Delta T)^{1/4}$ depends on $t(g\beta\Delta T/x)^{1/2}$.

The heat transfer coefficient, h , was defined as follows

$$h(T_w - T_i) = -k \left(\frac{\partial T}{\partial y} \right)_{y=0} = -k(T_w - T_i) \left(\frac{\partial \theta}{\partial y} \right)_{y=0} \quad (57)$$

The derivative in Equation 57 was evaluated by simply taking a straight line through the point corresponding to the plate and the point nearest the plate. Inspection of the computed temperatures subsequently confirms that the temperature does vary almost linearly with distance near the plate. A parabola passed through three points instead of the straight line through two points, yields values of h differing only about 0.2%, providing the points under consideration are not near the leading edge. The effect of the leading edge is discussed below.

1. The Leading Edge

It has been mentioned before that Equations 52 cannot be expected to describe the actual behavior of fluids near the leading edge of the plate. Nevertheless there is a solution to Equations 52 near the leading

edge whether it is physically meaningful or not. There is some difficulty in approximating this solution at the leading edge by finite difference methods. The solution to the difference problem will depart from the solution to the differential problem more and more as the leading edge of the plate is approached from values of x above the leading edge. The reason for this departure is that v and h are infinite at the leading edge in the true solution. This behavior of v and h causes no difficulty in a solution where one works with quantities of the form $vx^{1/4}$ and $hx^{1/4}$ which are bounded at $x = 0$. In the numerical procedure where v and h are computed directly, the variables cannot be obtained at all at the leading edge of the plate, and the variables have some large but finite value at the level of the first x increment above the leading edge.

The departure of the solution of difference problem from the solution of the difference problem near the leading edge is not of consequence providing the final solution is taken at some distance from the leading edge. In terms of the variables used in the calculations the space-time grid is three dimensional. However, according to the analysis given earlier, the number of independent variables can be reduced from three to two. Therefore, the solution along any line $X = \text{constant}$ must be the same as that along any other line $X = \text{constant}$ providing the solutions are expressed in terms of the composite variables. Deviations from the analysis can only be due to error. If there were no error the values of the dependent variables taken along any line of constant X would constitute a complete solution valid for all X . Figure 3 shows steady state values of $h/k (\nu^2 x / g \beta \Delta T)^{1/4}$ versus position. The group $h/k (\nu^2 x / g \beta \Delta T)^{1/4}$ would be a constant at steady state if there were no error and its deviation at small j represents the departure mentioned above. Figure 4 shows steady state velocity profiles at

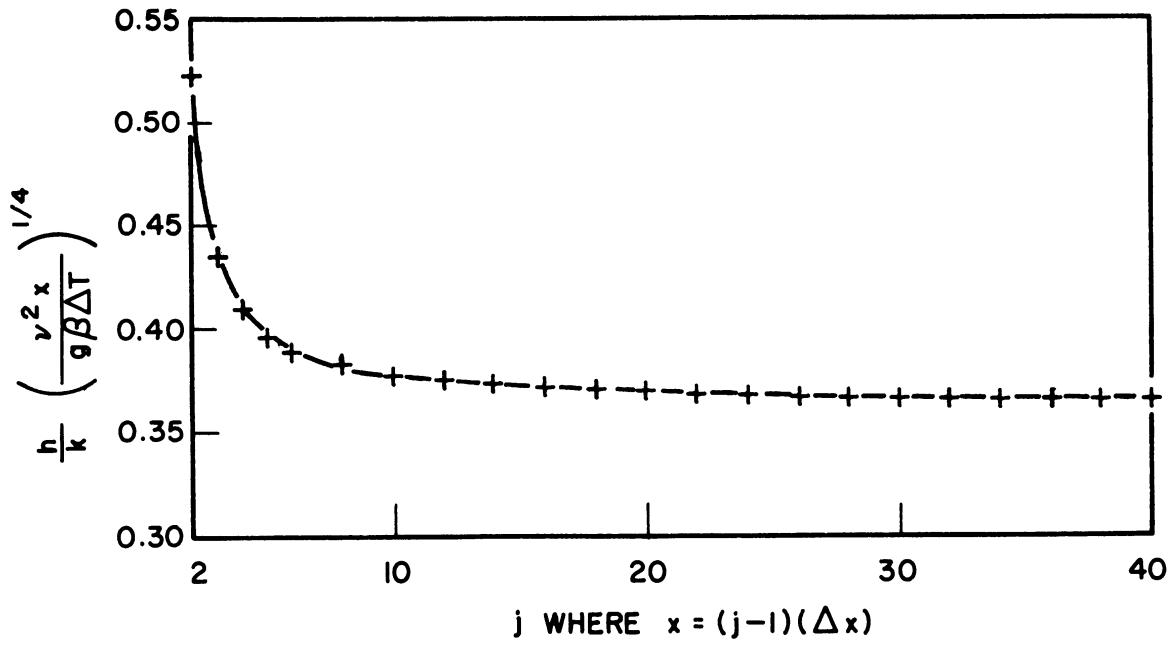


Figure 3. Effect of Leading Edge Error on Heat Transfer Group.

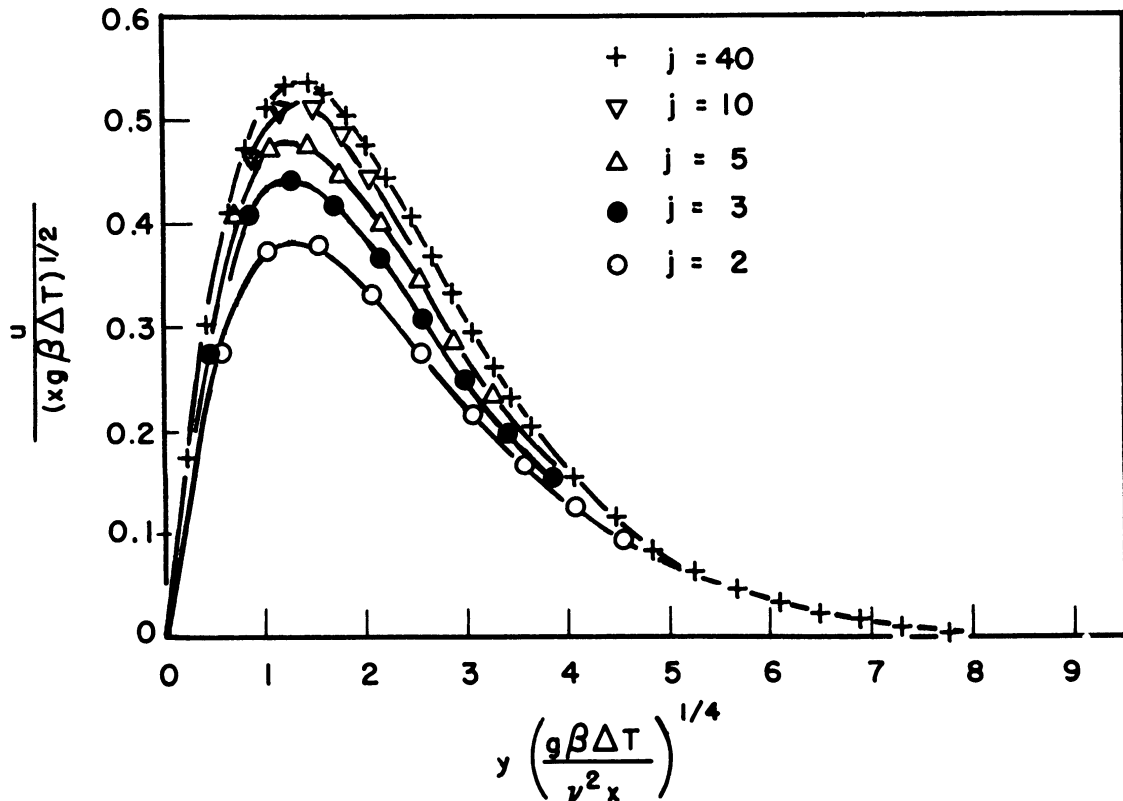


Figure 4. Effect of Leading Edge Error on Velocity Profile.

various positions. The profiles would all be the same if there were no error and the deviations at small values of j also represent the departure mentioned above. It can be seen in both figures that the error due to the leading edge is confined to small values of j . The results to be presented henceforth are all at large j where the results are independent of j .

It should be mentioned that the leading edge error is easily avoided only because the number of dependent variables can be reduced from three to two in this particular problem. Otherwise it would be necessary to subdivide the grid near the leading edge to obtain a better approximation to the solution. However, the function v could never be approximated at the leading edge in a problem such as the one at hand since the function is not defined there. In problems of more nearly complete physical significance the velocity would be everywhere finite.

2. Principal Results

The results of the calculations on the flat plate are given in Figures 5, 6, 7 and 8. Figure 5 shows the velocity profile at various times. Starting from the initial, motionless condition the velocity at a given point increases uniformly with time until a maximum is reached, and then decreases slightly to its steady state value. The triangular points were taken from Ostrach's steady state solution (26). It can be seen that the agreement between the calculations and Ostrach's work is excellent. The largest difference between the two is about 2%.

Figure 6 shows the temperature profile at various times. Starting from an initial value of zero, the temperature at a given point increases with time, goes through a maximum, and then decreases slightly to a steady state value. The triangular points again are from Ostrach's solution for steady state and the agreement can be seen to be excellent.

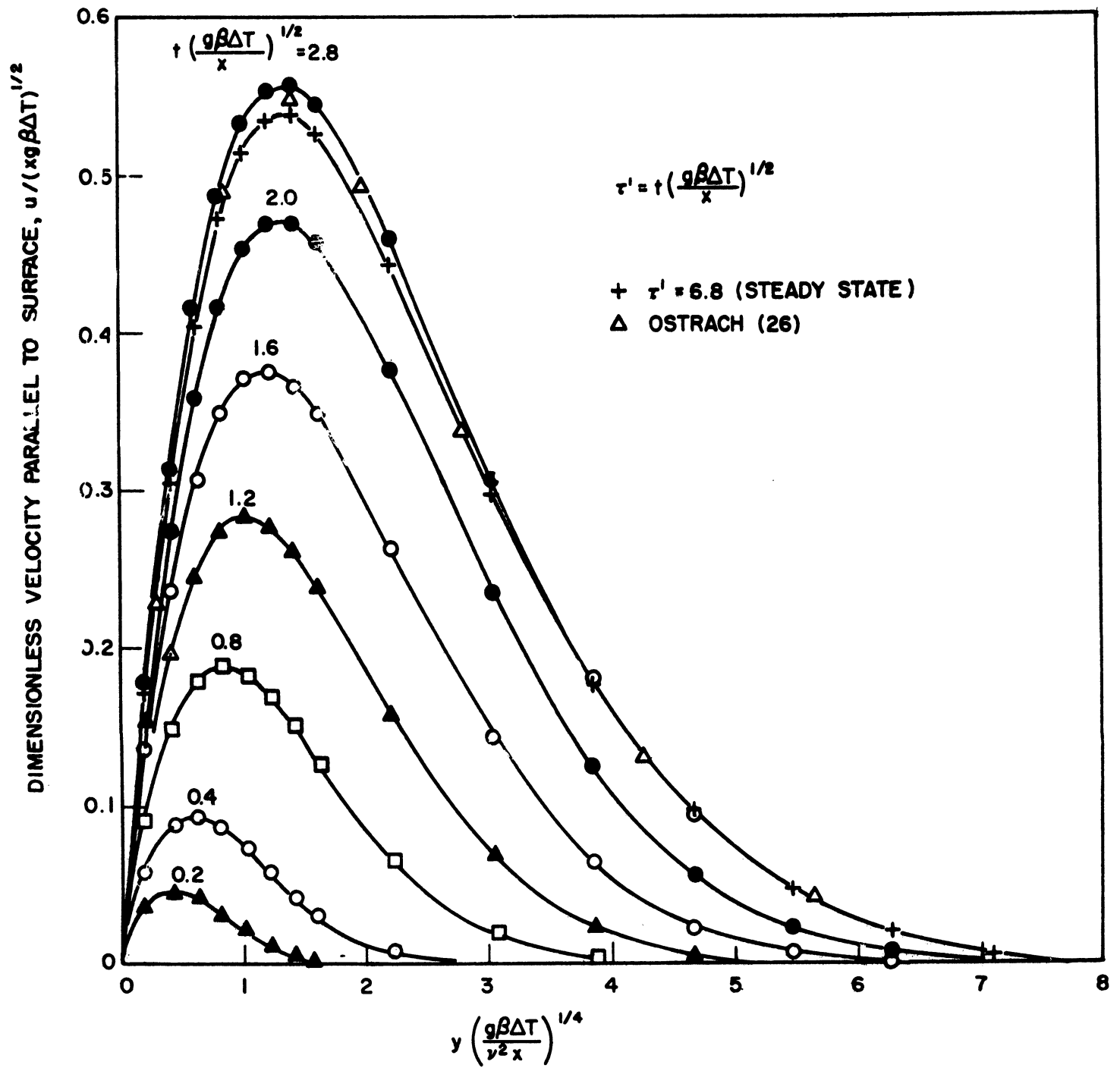


Figure 5. Transient Velocity Profiles.

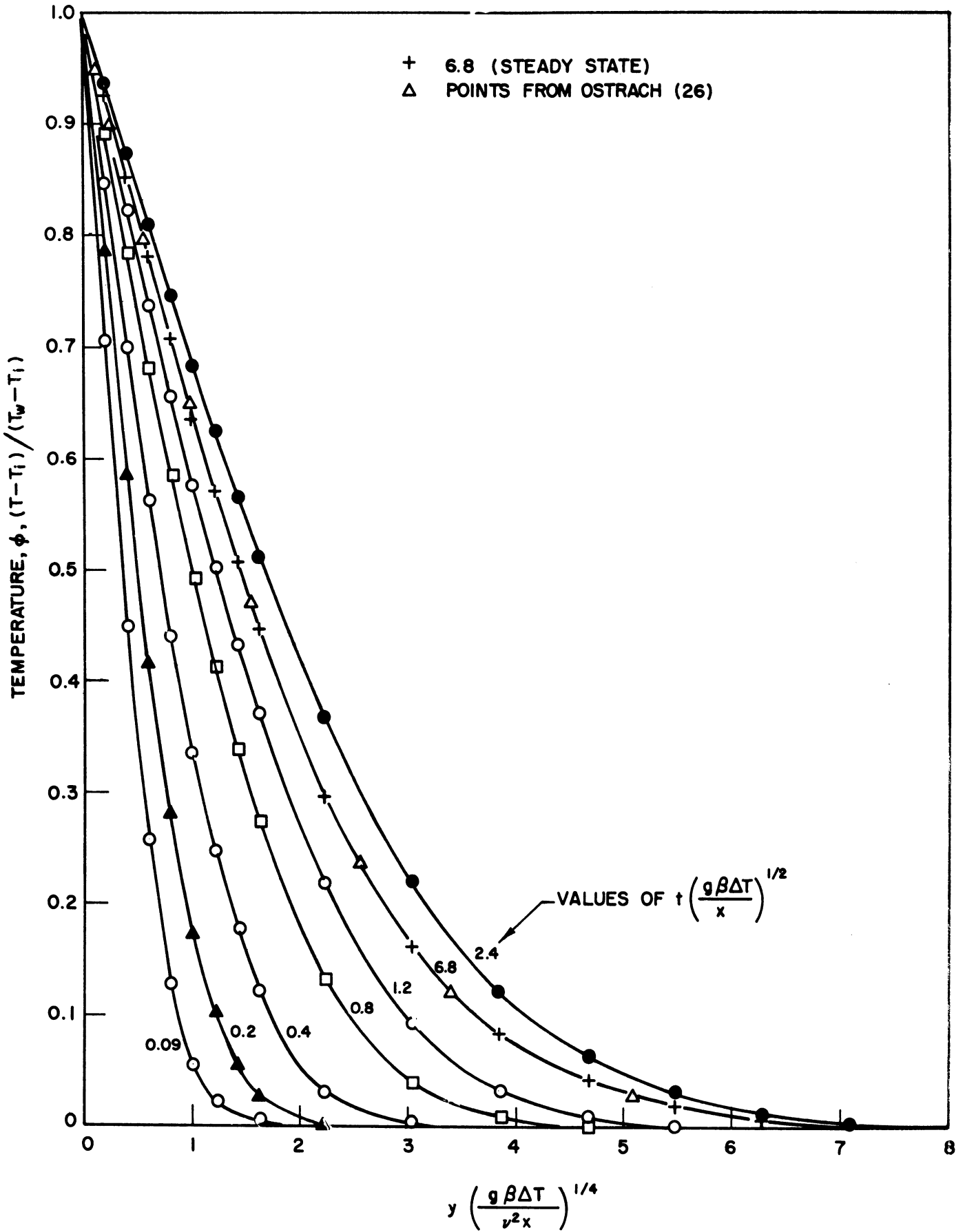


Figure 6. Transient Temperature Profiles.

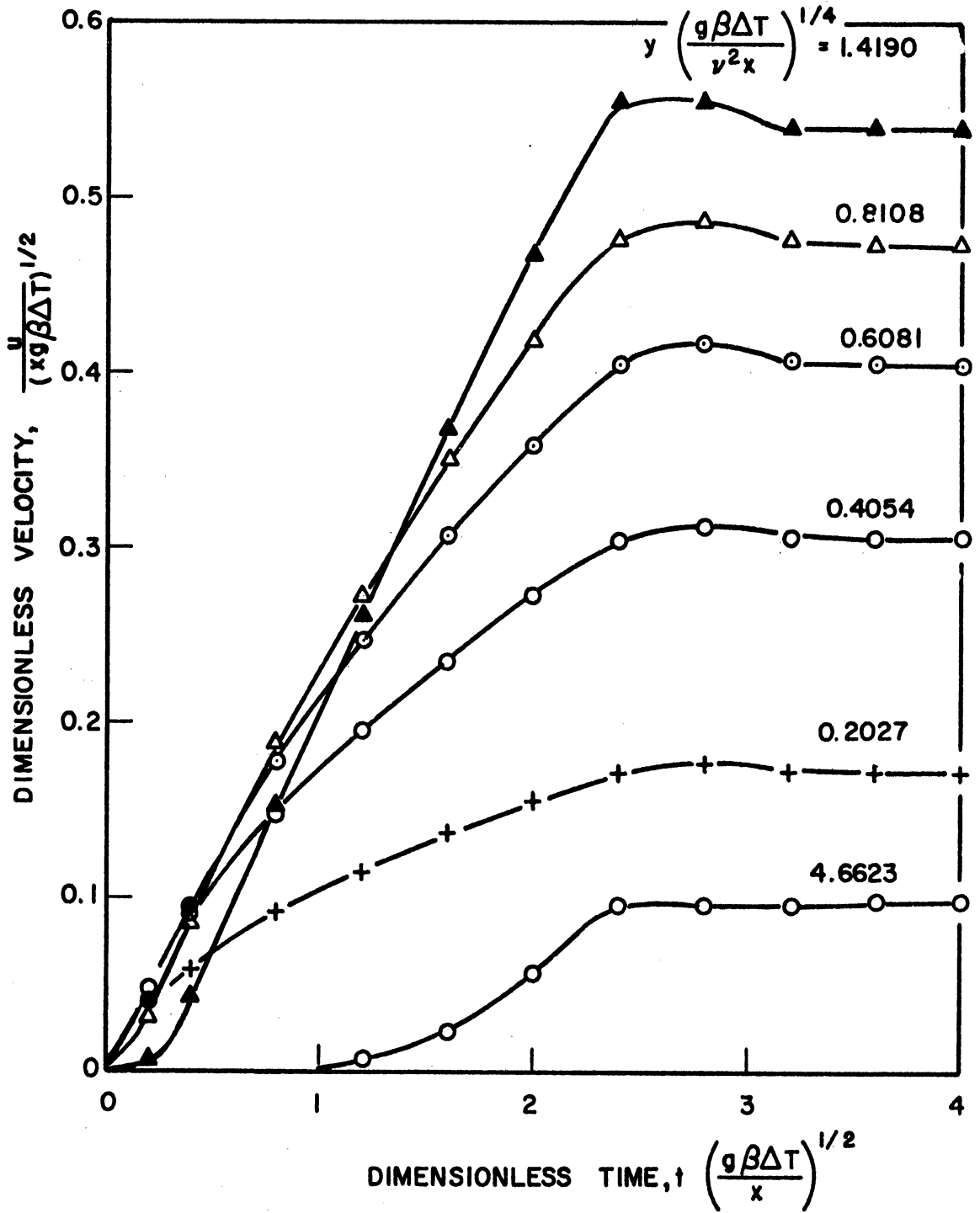


Figure 7. Transient Velocity at Various Positions.

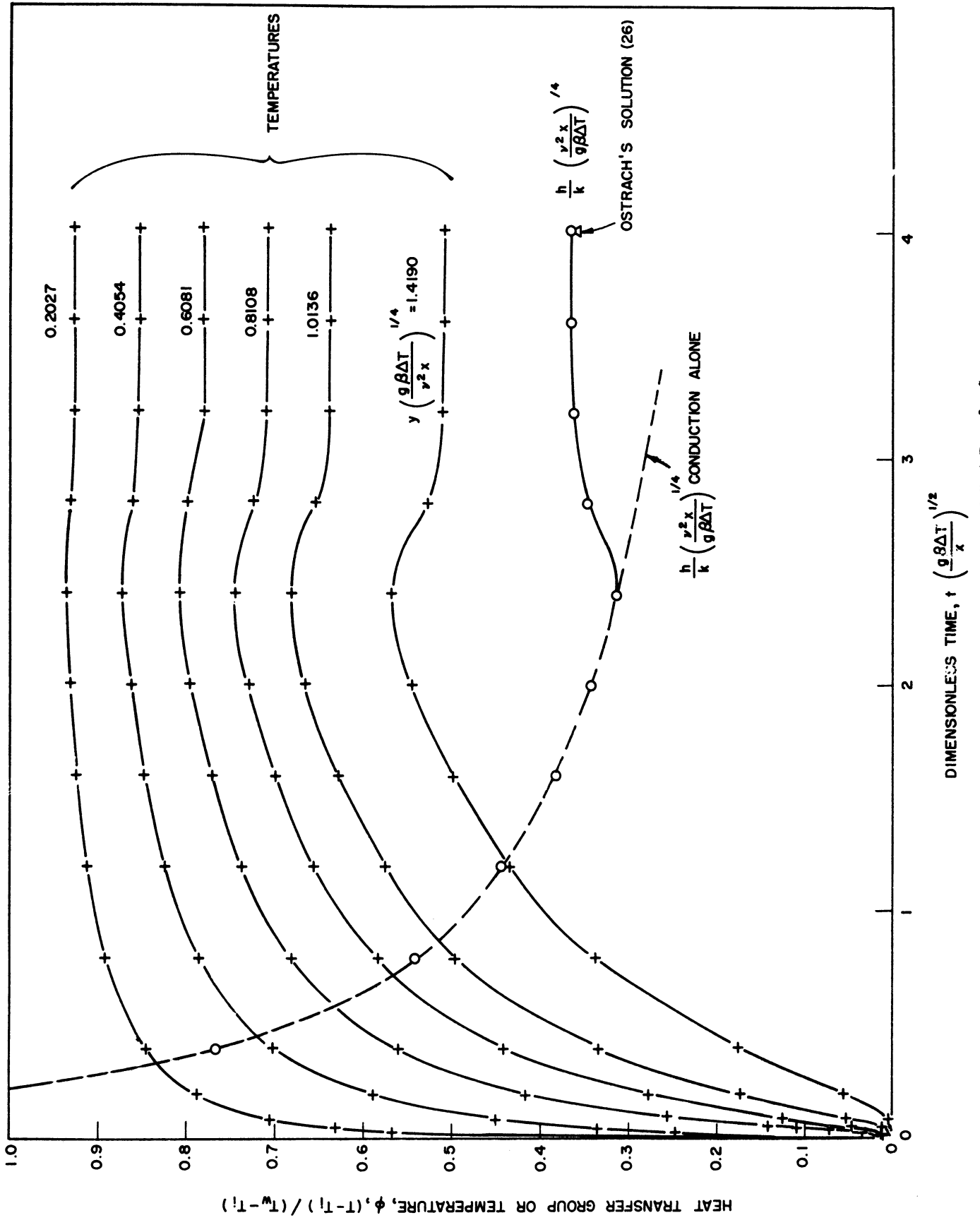


Figure 8. Transient Temperatures and Heat Transfer Group.

Figures 7 and 8 show more clearly the variation of velocity and temperature with time. In these figures the points given at intervals of time represent one fortieth of the points actually calculated. The time scale on the figures terminates where the time group equals 4.0 since there are essentially no changes in the variables beyond this point. The calculations were actually carried out to a value of the time group of 6.8. Each curve may be thought of as showing the variation of velocity or temperature at a fixed point with time although in this and the other figures the composite variables are used for compact presentation of the results. Figure 8 also gives the most important part of the results from an engineering standpoint: the variation of the heat transfer group with time. The heat transfer group is infinite initially since the wall temperature changes discontinuously at time zero. The group then decreases with time, goes through a minimum, and finally increases to a steady state value. Ostrach's steady state value is denoted in Figure 8 by a triangle. The difference between this work and Ostrach's is about 2% which again constitutes excellent agreement. The cause of the 2% difference is not clear. It might be due to the influence of the leading edge error discussed earlier or it might be due to the size of the increments used in the finite difference method of calculations. There is of course no assurance that Ostrach's solution is more accurate than the solution presented here. However, it seems likely that finite difference method is the less accurate.

The heat transfer coefficient for the initial interval was previously given from the analytical solution to be

$$h = \frac{k}{\sqrt{\pi \alpha t}}$$

which can be put into the form of the variables of this work to give:

$$\frac{h}{R} \left(\frac{v^2 x}{g \beta \Delta T} \right)^{1/4} = \left[\frac{v}{\pi \alpha} \right]^{1/2} \left[x \left(\frac{g \beta \Delta T}{x} \right)^{1/2} \right]^{-1/2} = 0.4830 \left[x \left(\frac{g \beta \Delta T}{x} \right)^{1/2} \right]^{-1/2} \quad (58)$$

Equation 58 which is expected to hold for small times is represented in Figure 8 as a dashed curve. The dashed curve departs from the full curve representing the numerical solution for values of the time group greater than 2.4. For times below this value of 2.4 the two curves are indistinguishable. It is remarkable that the solution for conduction alone holds for times up to fairly near the time at which steady state is reached.

Siegel (34) studied the transient convection problem using the Kármán-Pohlhausen approximation method, and developed expressions for the time at which steady state is reached and for the time at which the initial interval ends. Equation 59 is Siegel's formula for the end of the initial interval and Equation 60 is his formula for the time to reach steady state.

$$x \left(\frac{g \beta \Delta T}{x} \right)^{1/2} = (0.90)(1.5 + Pr)^{1/2} + (1.24)(0.6 + Pr)^{1/2} \quad (59)$$

$$x \left(\frac{g \beta \Delta T}{x} \right)^{1/2} = (2.62)(0.952 + Pr)^{1/2} + (3.55)(0.377 + Pr)^{1/2} \quad (60)$$

According to Equation 59 the initial interval should end when the time group equals 2.7 as compared to a value of about 2.4 from inspection of Figure 8. According to Equation 60 steady state should be reached when the time group equals 7.1, as compared to a value of about 3.5 or 4.0 from inspection of Figure 8. Siegel's estimate of the time at which the initial interval ends must be considered as good. His estimate of the time to reach steady state is high but even here the estimate is of the right order

and could be considered to be good depending on how one wishes to define the time at which steady state is reached. Siegel did not obtain a direct solution for the transient problem. He estimated the times at which the two existing solutions should be valid as outlined above, and then simply interpolated between the two limiting solutions.

The confirmation of the existence of a minimum with respect to time in the heat transfer group and corresponding maximums in the temperature and velocity are of particular interest. The only experimental work on transient natural convection seems to be the limited work of Klei (17) in which such a minimum in the heat transfer coefficient was found. Klei's measurements were for a plate with constant energy input rather than constant temperature so his results are not comparable on a quantitative basis with those of this work. The existence of the minimum was also predicted by Siegel in his analysis.

V. THE HORIZONTAL CYLINDER

The horizontal cylinder problem was selected for finite difference calculations as a problem for which no solution is available, but for which experimental data exist. The measurements of Martini and Churchill (21) which were discussed earlier will be compared with the results of the calculations. In the case of the flat plate the finite difference solution was compared with a more exact solution and the validity of the finite difference calculations was immediately evident. Comparing a finite difference solution with experimental data is less conclusive verification of the method of calculation because there are several additional uncertainties:

1. The results of the numerical procedure will always deviate from the exact solution of the difference problem because of rounding error, and because the calculations may not be continued until steady state is reached.
2. The exact solution to the difference problem will differ from the solution to the differential problem because of truncation error.
3. The exact solution of the differential problem may not adequately describe the physical situation. This remark applies to the conservation equations even in their most general form since they have never been tested critically; extensive simplifications of the equations have always been required to obtain a solution.
4. The mathematical model selected for the calculations may differ from the physical situation. For example, in the cylinder model

the wall temperature change discontinuously at two points, whereas the wall temperature changes continuously in the physical situation. The discontinuous change can only be approximated in the physical situation.

5. There is always an unknown experimental error.

In this section the method of calculation and the results for the horizontal cylinder will be discussed and compared with measurements. The results will be shown to be in general good agreement with the measurements. There are deviations for some ranges of the Grashof number which seem to be due mostly to the model rather than to the finite difference method of calculation or to experimental errors.

A. The Differential Problem

The differential equations used in the calculations are Equations 26 which were discussed in Part IIC. The equations are repeated below in dimensionless form.

$$\frac{\partial U}{\partial \tau} + \frac{U}{R} \frac{\partial U}{\partial \theta} + V \frac{\partial U}{\partial R} = Gr \phi \mu \theta + \frac{\partial^2 U}{\partial R^2} + \frac{1}{R} \frac{\partial U}{\partial R} - \frac{U}{R^2} + \frac{1}{R^2} \frac{\partial^2 U}{\partial \theta^2} \quad (26a)$$

$$\frac{\partial \phi}{\partial \tau} + \frac{U}{R} \frac{\partial \phi}{\partial \theta} + V \frac{\partial \phi}{\partial R} = \frac{\alpha}{\nu} \left[\frac{\partial^2 \phi}{\partial R^2} + \frac{1}{R} \frac{\partial \phi}{\partial R} + \frac{1}{R^2} \frac{\partial^2 \phi}{\partial \theta^2} \right] \quad (26b)$$

$$\frac{\partial(RV)}{\partial R} + \frac{\partial U}{\partial \theta} = 0 \quad (26c)$$

The boundary and initial conditions are:

$$\begin{aligned} R=1, 0 < \theta < \pi & : U=V=0, \phi = 1/2 \\ R=1, \pi < \theta < 2\pi & : U=V=0, \phi = -1/2 \\ \tau = 0 & : U=V=\phi=0 \end{aligned}$$

and the dimensionless variables and parameters are:

$$U = u\sqrt{\nu_0}/V, \quad V = v\sqrt{\nu_0}/V, \quad \tau = tV/\sqrt{\nu_0}^2$$

$$R = r/\sqrt{\nu_0}, \quad Gr = \frac{g\beta\Delta T\sqrt{\nu_0}^3}{\nu^2}, \quad \nu/\alpha \quad \text{is the Prandtl number.}$$

The angle, θ , is measured from the vertical.

Equations 26 are symmetrical in a certain sense and this symmetry can be used to reduce the amount of calculation required to solve the equations. The functions U and V are periodic with period π , and the function ϕ at a given angle is the negative of ϕ at some angle different by π :

$$U(R, \theta, \tau) = U(R, \theta + \pi, \tau) \quad (61a)$$

$$V(R, \theta, \tau) = V(R, \theta + \pi, \tau) \quad (61b)$$

$$\phi(R, \theta, \tau) = -\phi(R, \theta + \pi, \tau) \quad (61c)$$

Equations 61 are satisfied initially by the choice of initial conditions, and they can be shown to hold for subsequent times by formally integrating Equations 26 with respect to time. The important result of Equations 61 is that only half of the cylinder need be considered in the calculations. In a more general problem in which physical properties of the fluid vary, the equations would not be symmetrical.

B. The Difference Problem.

Equations 26 can be approximated using explicit difference equations providing care is used in selecting the form of the difference. However, it does not seem to be possible to use a single system of explicit

equations over the whole space-time region of interest. Four separate systems of equations were used in this work corresponding to the combinations of signs of the velocity components: $U > 0, V > 0$; $U > 0, V < 0$; $U < 0, V > 0$; and $U < 0, V < 0$. The use of several alternate sets of equations causes no particular difficulty although the calculations are complicated very slightly by the fact that the machine must determine which equations are to be used at every stage in the process. The equations and their application will be discussed after the space grid is described.

1. The Space Grid

The space grid used in the calculations is shown in Figures 9 and 10. As indicated in Figure 9 the integers ℓ denote radial position with $\ell = 1$ being the origin and $\ell = 26$ being the boundary such that ΔR is $1/25$. The integers j denote angle with $j = 2$ corresponding to $\Theta = 0$ and $j = 10$ corresponding to $\Theta = \pi$ such that $\Delta\Theta = \pi/8$. Near the boundary the radial increments are smaller than the angular increments: $(R)(\Delta\Theta)$ is about ten times ΔR . The increments were so selected in expectation of radial gradients being much larger than aximuthal gradients in which case the finer divisions are required to maintain accuracy.

The half cylinder $j = 2$ through $j = 10$ was used in the calculations. From the symmetry $U, V,$ and ϕ at a given radius on the ray $j = 1$ are always equal to $U, V,$ and $-\phi$, respectively, at the same radius on the ray $j = 9$. Values of the variables along the ray $j = 11$ are related to those along $j = 3$ in the same way. The rays $j = 1$ and 11 serve the same purpose as a boundary in providing exterior points where the values of the independent variables are always known. The use of these rays in the calculations will be explained later.

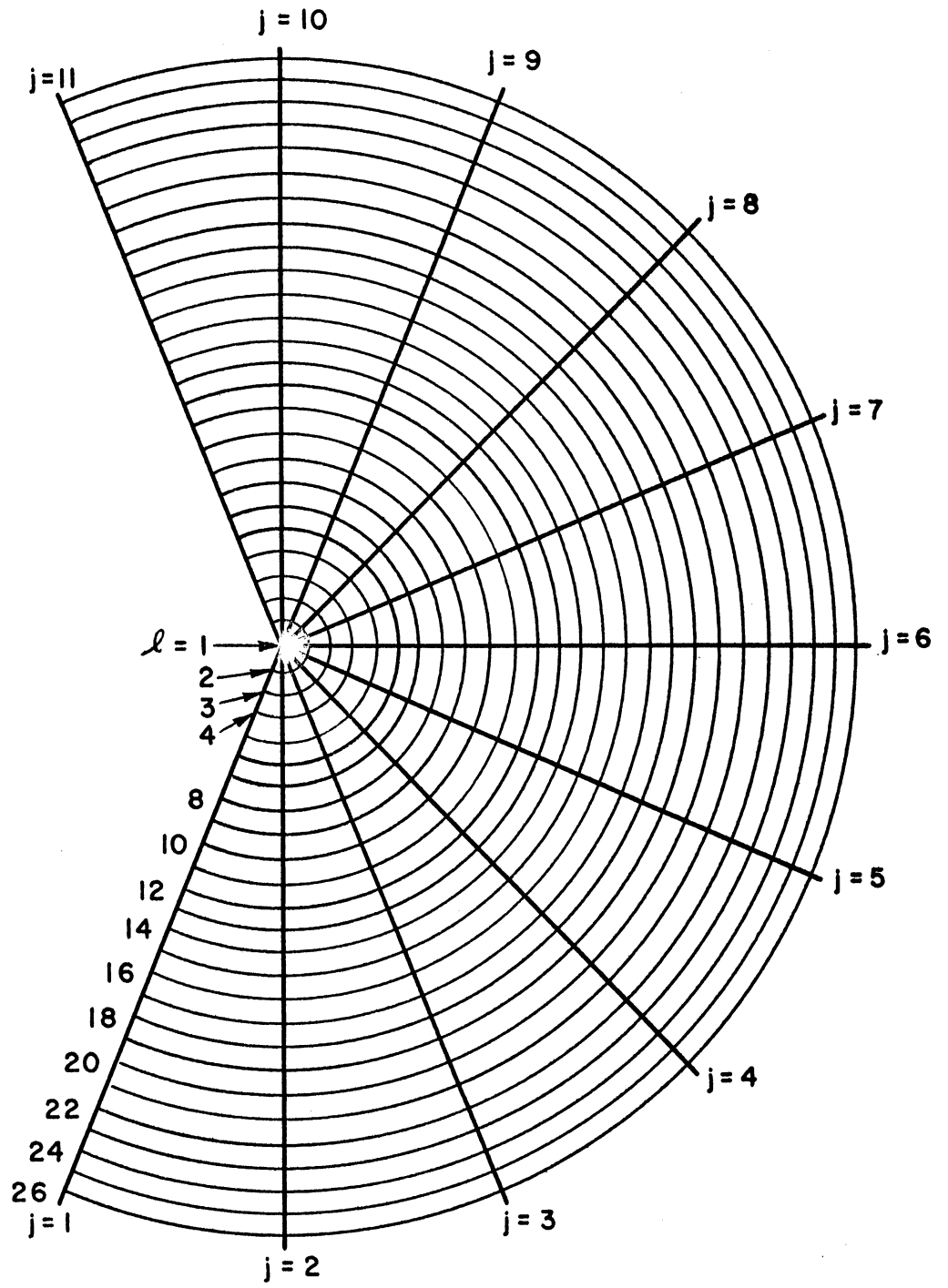


Figure 9. The Cylindrical Spare Grid.

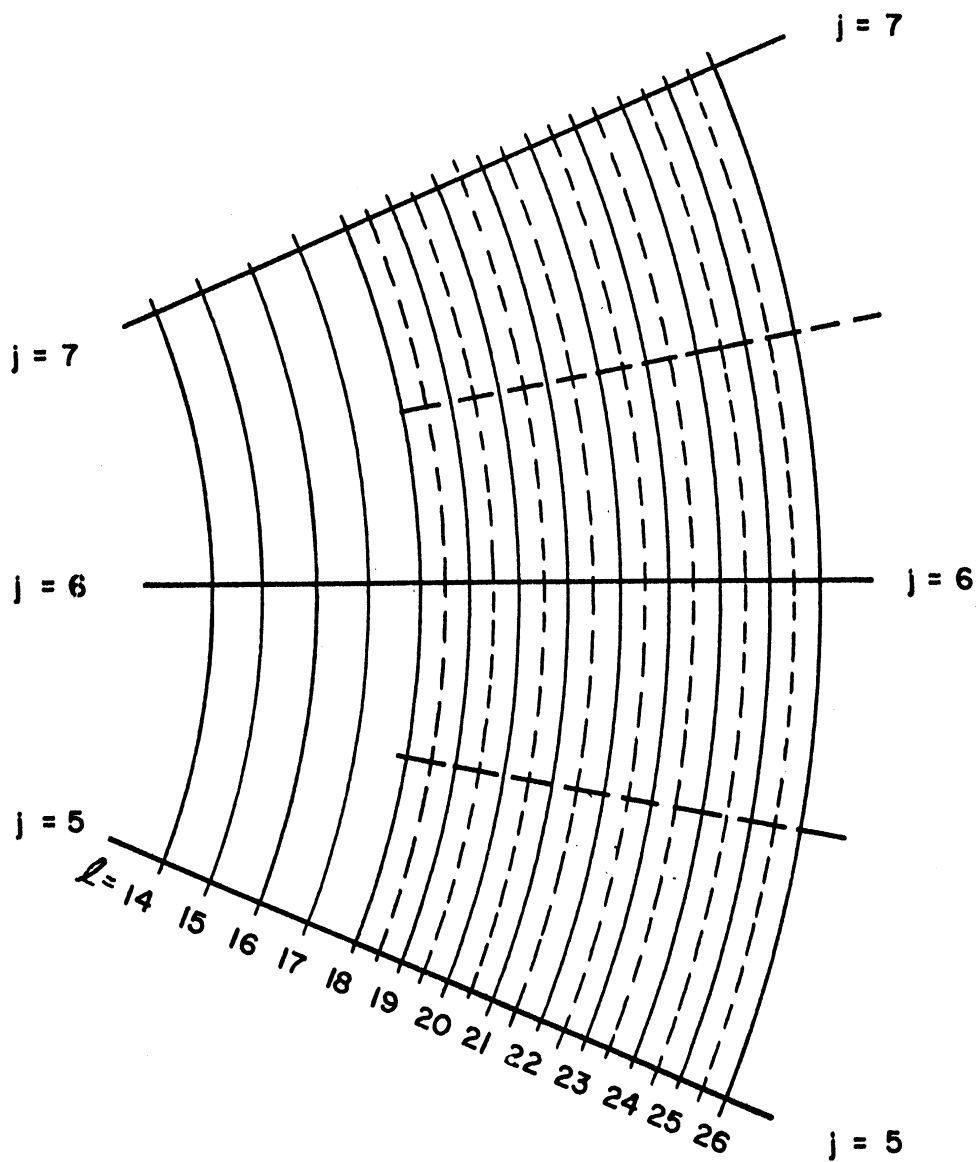


Figure 10. Subdivision of Outer Grid.

The solution to the system of equations using the space grid of Figure 9 was considered to be a first approximation and the outer part of the grid was subdivided in most cases to obtain a better approximation. Subdivision of the grid in this way not only gives an improved solution but gives an indication of the truncation error. Figure 10 is a fragment of the grid showing how the subdivision was carried out. The full lines are those from the first grid and the broken lines are those added in subdivision. The increment sizes for the outer third of the cylinder were cut in half. The unsubdivided solution to the temperature and velocity distributions in the inner region was accepted as valid when the grid was subdivided. That is to say U and ϕ were held constant at the inner boundary of the subdivided region using the values from the first approximation. This procedure is acceptable since U and ϕ and their derivatives are small in the inner region and a first approximation to the values here should suffice.

In the differential problem the temperature on the boundary changes discontinuously at $\Theta = 0$ from the value $-1/2$ to the value $+1/2$ and the temperature at $\Theta = 0$ is not defined. Similarly there is a discontinuity at $\Theta = \pi$. In the difference problem the temperature is specified only at discrete points and, since any number of functions could be passed through these points, the function being described by the discrete values of the variable is somewhat arbitrary. The method by which the grid is subdivided determines which wall temperature distribution is being approximated. By way of illustration, Figure 11 gives the values of the wall temperature near $\Theta = 0$ for the two grids in comparison with the wall temperature distribution of the differential problem. If one looks at the grids individually, a function with two discontinuities (the full line), or a continuous function (the broken line) are among the many which could be thought

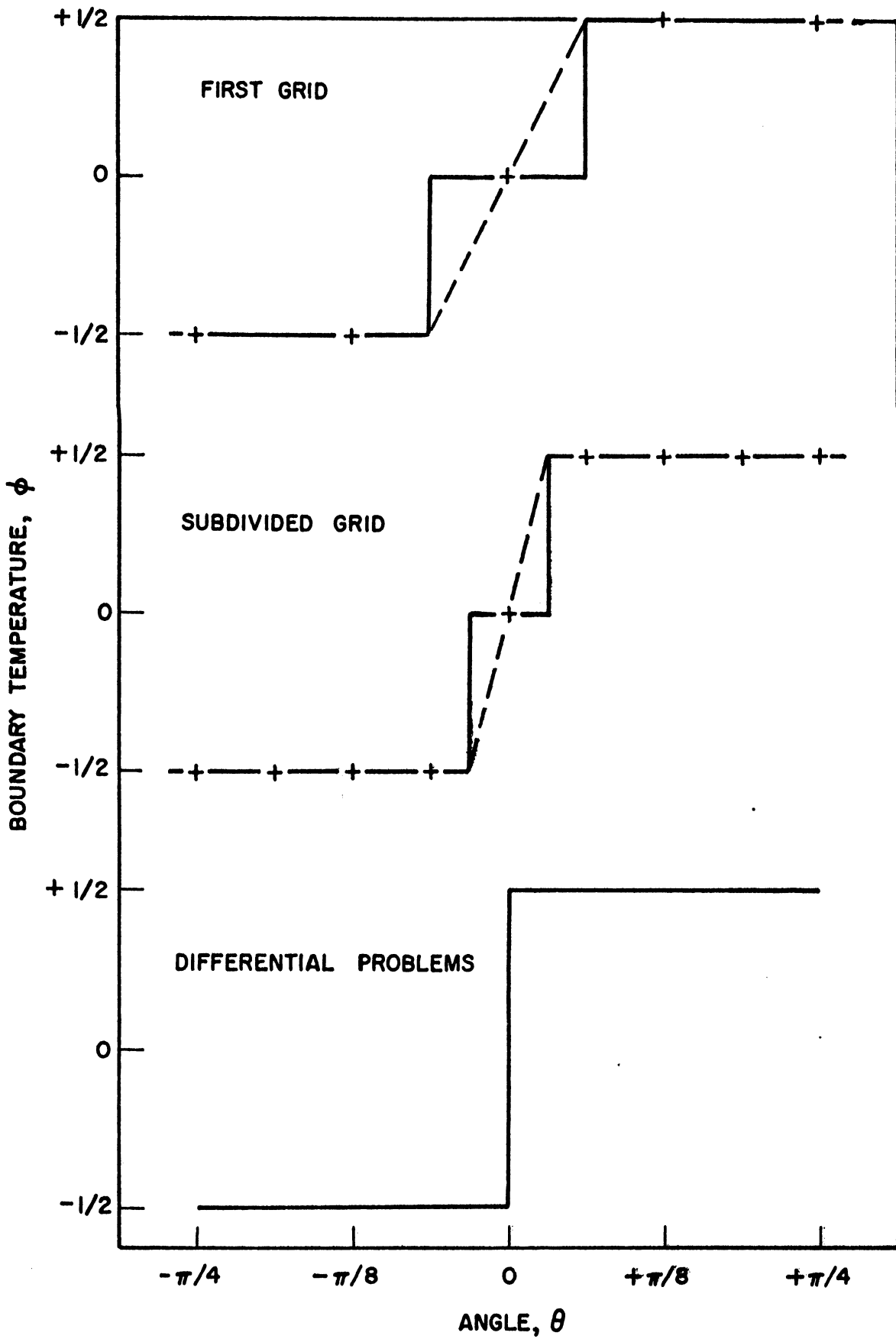


Figure 11. Approximation of Boundary Temperature.

of as the function being approximated. However, in the problem at hand the grids should be thought of as two of a sequence of smaller and smaller increment sizes such that the single discontinuity of the differential problem is approached. As would be expected from inspection of Figure 11 the subdivision of the grid makes a difference in the solution near the discontinuity since the boundary conditions are actually different after the grid is subdivided.

2. The Difference Equations

The difference equations corresponding to Equations 26 are given in this section for the case where $U \geq 0$ and $V \geq 0$. In this case the terms where U and V appear as coefficients are approximated using backward differences. The equations used in the other cases are obtained by simply replacing the backward difference by a forward difference whenever the coefficient velocity is less than zero.

Three of the terms in the momentum balance, Equation 26a, can be combined into a single term as indicated below.

$$\frac{\partial^2 U}{\partial R^2} + \frac{1}{R} \frac{\partial U}{\partial R} - \frac{U}{R^2} = \frac{\partial}{\partial R} \left[\frac{1}{R} \frac{\partial (UR)}{\partial R} \right]$$

Then the single term can be approximated:

$$\begin{aligned} \frac{1}{\Delta R} \left[\frac{1}{R} \frac{\partial (UR)}{\partial R} \right] &\approx \frac{(U_{j+1})(R+\Delta R) - (U_j)R}{(R+\Delta R/2)(\Delta R)^2} - \frac{(U_j)R - (U_{j-1})(R-\Delta R)}{(R-\Delta R/2)(\Delta R)^2} \\ &\approx \frac{1}{(\Delta R)^2} \left[(U_{j+1}) \left(\frac{R+\Delta R}{R+\Delta R/2} \right) + (U_{j-1}) \left(\frac{R-\Delta R}{R-\Delta R/2} \right) - (U_j) \left(\frac{R}{R+\Delta R/2} + \frac{R}{R-\Delta R/2} \right) \right] \end{aligned}$$

Two of the terms in the energy balance, Equation 26b, can be combined into a single term as indicated below.

$$\frac{\partial^2 \phi}{\partial R^2} + \frac{1}{R} \frac{\partial \phi}{\partial R} = \frac{1}{R} \frac{\partial}{\partial R} \left[R \frac{\partial \phi}{\partial R} \right]$$

Then the single term can be approximated

$$\begin{aligned} \frac{1}{R} \frac{\partial}{\partial R} \left[R \frac{\partial \phi}{\partial R} \right] &\approx \frac{(R+\Delta R/2)(\phi_{j,l+1} - \phi_{j,l}) - (R-\Delta R/2)(\phi_{j,l} - \phi_{j,l-1})}{R(\Delta R)^2} \\ &\approx \frac{1}{(\Delta R)^2} [\phi_{j,l+1} - 2\phi_{j,l} + \phi_{j,l-1}] + \frac{1}{2R\Delta R} [\phi_{j,l+1} - \phi_{j,l-1}] \end{aligned}$$

The complete difference equations are given below where A denotes the approximation of $\partial/\partial R [1/R \partial(Ur)/\partial R]$ and B denotes the approximation of $(1/R) \{ \partial/\partial R [R \partial \phi/\partial R] \}$.

$$\begin{aligned} \frac{U'_{j,l} - U_{j,l}}{\Delta \tau} + \frac{U_{j,l}}{R} \frac{U_{j,l} - U_{j-1,l}}{\Delta \theta} + V_{j,l} \frac{U_{j,l} - U_{j,l-1}}{\Delta R} \\ = G\pi \phi'_{j,l} \sin \theta + A + \frac{1}{R^2} \frac{U_{j+1,l} - 2U_{j,l} + U_{j-1,l}}{(\Delta \theta)^2} \end{aligned} \quad (62a)$$

$$\begin{aligned} \frac{\phi'_{j,l} - \phi_{j,l}}{\Delta \tau} + \frac{U_{j,l}}{R} \frac{\phi_{j,l} - \phi_{j-1,l}}{\Delta \theta} + V_{j,l} \frac{\phi_{j,l} - \phi_{j,l-1}}{\Delta R} \\ = \frac{\alpha}{V} B + \frac{\alpha}{VR^2} \frac{\phi_{j+1,l} - 2\phi_{j,l} + \phi_{j-1,l}}{(\Delta \theta)^2} \end{aligned} \quad (62b)$$

$$\frac{(R+\Delta R)(V'_{j,l+1}) - (R)(V_{j,l})}{\Delta R} + \frac{U_{j+1,l+1} - U_{j-1,l+1} + U_{j+1,l} - U_{j-1,l}}{4\Delta \theta} = 0 \quad (62c)$$

The primed variables are at the time level $\tau + \Delta \tau$ as before and the unprimed variables are at the time τ . The procedure of calculation using the equations is much the same as for the flat plate problem: the energy equation is used to determine values of ϕ at a new time level over the whole grid; the momentum balance is then used to similarly advance the values of U. Finally, the corresponding values of V are computed using

Equation 62c, working from the boundary in toward the center. The procedure is repeated over and over again giving values of U , V , and ϕ for increasing values of time. The use of the equations will be given in more detail after the stability requirement is discussed.

3. The Stability Criterion

Sufficient conditions for stability of Equations 62 can be established by either of the methods described earlier. In the case of the energy equation, the two methods give the same condition. However, in the case of the momentum equation, the results are slightly different. As would be expected, the von Neumann method of analysis permits a slightly larger time step. The von Neumann condition is supposed here to be necessary and sufficient for stability* whereas the condition from the simple analysis using a positive type difference equation is only sufficient for stability.

The stability analysis using a positive type difference equation will be omitted since such an analysis involves only rearranging the equation and inspecting the coefficients as was illustrated in the flat plate problem. From the analysis of the energy equation, it can be shown that the temperature will always fall between the extremes of the boundary temperature ($-1/2 \leq \phi \leq 1/2$) providing

$$\frac{U/\Delta\tau}{R\Delta\theta} + \frac{V/\Delta\tau}{\Delta R} + \frac{2\Delta\tau\alpha}{(\Delta R)^2\nu} + \frac{2\Delta\tau\alpha}{(R\Delta\theta)^2\nu} \leq 1 \quad (63)$$

It will be shown that the stability requirement for the momentum equation is the same as inequality 63 except that α/ν is replaced by unity. Equations 62a and 62b can be rearranged to give

*The condition actually is known to be sufficient only for a small class of problems as indicated in Part III.

$$\phi_{j,l}^{(m+1)} = a_1 \phi_{j,l}^{(m)} + a_2 \phi_{j+1,l}^{(m)} + a_3 \phi_{j+2,l}^{(m)} + a_4 \phi_{j,l+1}^{(m)} + a_5 \phi_{j,l}^{(m)} \quad (64)$$

$$J_{j,l}^{(m)} = b_1 U_{j,l}^{(m)} + b_2 U_{j+1,l}^{(m)} + b_3 U_{j+2,l}^{(m)} + b_4 U_{j,l+1}^{(m)} + b_5 U_{j,l}^{(m)} + \Delta \tau G_N \phi_{j,l}^{(m)} \Theta \quad (65)$$

The superscripts in the equations denote time level to be consistent with the notation of Part III. The coefficients a_i and b_i are

$$a_1 = 1 - \beta - \gamma - 2C \frac{\alpha}{V}; \quad b_1 = 1 - \beta - \gamma - 2D - 2C \left[\frac{R}{R + \Delta R/2} + \frac{R}{R - \Delta R/2} \right]$$

$$a_2 = D \frac{\alpha}{V} + \beta; \quad b_2 = D + \beta$$

$$a_3 = C \frac{\alpha}{V}; \quad b_3 = C \left(\frac{R + \Delta R}{R + \Delta R/2} \right)$$

$$a_4 = C \frac{\alpha}{V} + \gamma; \quad b_4 = C \left(\frac{R - \Delta R}{R - \Delta R/2} \right) + \gamma$$

$$a_5 = D \frac{\alpha}{V}; \quad b_5 = D$$

where $\beta = \frac{IV \Delta \tau}{R \Delta \Theta}$, $\gamma = \frac{IV \Delta \tau}{\Delta R}$, $C = \frac{\Delta \tau}{(\Delta R)^2}$ and $D = \frac{\Delta \tau}{(R \Delta \Theta)^2}$

Now the amplification matrix can be formed in exactly the same way as in the example of Part III and the eigenvalues are, by inspection

$$\lambda_1 = a_1 + a_2 e^{-ik_1 \Delta X} + a_3 e^{ik_2 \Delta Y} - a_4 e^{-ik_2 \Delta Y} + a_5 e^{ik_1 \Delta X} \quad (66)$$

$$\lambda_2 = b_1 + b_2 e^{-ik_1 \Delta X} + b_3 e^{ik_2 \Delta Y} + b_4 e^{-ik_2 \Delta Y} + b_5 e^{ik_1 \Delta X} \quad (67)$$

The coefficients are all real and they are all positive except a_1 and b_1 which may be either positive or negative. Therefore the largest absolute values of λ_1 and λ_2 will occur when all the terms in Equations 66 and 67 are real. That is to say when $k_1 \Delta X = k_2 \Delta Y = 2\pi$ or when $k_1 \Delta X = k_2 \Delta Y = \pi$.

Consider the maximum real value of λ_2 :

$$\lambda_{2(max)} = b_1 + b_2 + b_3 + b_4 + b_5$$

Substituting the definitions of the coefficients and simplifying gives

$$\lambda_{2(max)} = 1 + \left[\frac{\Delta R}{R + \Delta R/2} - \frac{\Delta R}{R - \Delta R/2} \right]$$

Since R is never less than ΔR (the equations are not used at the origin) it is concluded that the largest real value of λ_2 cannot exceed unity. If there is to be a stability restriction, it will be to prevent λ_2 from being less than -1 . To examine this possibility, consider the minimum real value of λ_2 .

$$\lambda_{2(min)} = c_1 - b_2 - b_3 - c_4 - b_5$$

Substituting for the coefficients and simplifying gives

$$\lambda_{2(min)} = 1 - 2\beta - 2\gamma - 4C - 4D$$

which will be less than -1 unless

$$\beta + \gamma + 2C + 2D \leq 1 \quad (68)$$

Inequality 68 is the condition for stability.

By applying the same technique to λ_1 , the condition is found to be Equation 63 as was asserted previously.

In summary, the results of the stability analysis are that the following inequality must be satisfied if the Prandtl number (ν/α) is less than unity.

$$\frac{W/\Delta T}{R\Delta\theta} + \frac{W/\Delta T}{\Delta R} + \frac{2\Delta T\alpha}{(R\Delta\theta)^2 V} + \frac{2\Delta T\alpha}{(R\Delta\theta)^2 V} = 1 \quad (69)$$

If the Prandtl number exceeds unity, α/ν in the inequality should be replaced by unity.

The analysis given above was for the case of $U \geq 0$, $V \geq 0$. The stability criterion so obtained holds irrespective of the sign of U or V providing the absolute values of U and V are used in the inequalities as indicated, and providing the difference equations are changed according to the sign of U or V as prescribed in Section 2, above.

4. The Calculations

Equations 62 were first solved for a Prandtl number of 0.70 and a Grashof number (based on radius) of 6.15×10^5 . These conditions were selected to correspond to the conditions of the experiment which Martini and Churchill presented in most detail so that a direct comparison with the measurements could be made. The equations were then solved for the same Prandtl number and two additional values of the Grashof number. Finally, the equations were solved for a Prandtl number of 10 and the original value of the Grashof number. Transient results were obtained in the first solution. For subsequent solutions the velocity and temperature distributions were estimated by use of the highly simplified model discussed earlier so that the amount of computation was reduced. In all cases except that of the lowest Grashof number, the grid was subdivided to improve on the solution obtained by the first grid. The incentive for subdividing the grid decreases with decreasing Grashof number as will be seen later.

A summary of the calculations is given in Table I. Solutions 1, 2, 3, 4 are the solutions mentioned above. Solution 1A is the same as solution 1 except that certain terms were omitted from the equations as will be discussed later on. The machine time required for most solutions was between one and two hours which is surprisingly small considering the complexity of the problem. A machine time requirement of 3.5 hours is shown in Table I for Solution 4. This larger amount of machine time was used in Solution 4 because the behavior of the solution in this case was somewhat different from the others as will be discussed later.

The procedure for computing U , V , and ϕ at time $\tau + \Delta\tau$ from the variables at time τ is given below.

(1) The values of U , V , and ϕ along the rays $j = 1$ and $j = 11$ are established from those along $j = 9$ and $j = 3$, respectively in the way indicated in the discussion on the symmetry of the equations. The variables are specified on the boundary and U and ϕ are equal to zero at the origin by symmetry. Hence values of U and ϕ at points exterior to the part of the grid to be advanced ($j = 2$ through 10 and $l = 2$ through 25, inclusive) are now fixed.

(2) The quantity $|U/\Delta\tau/R\Delta\theta + |V/\Delta\tau/\Delta R + 2\alpha\Delta\tau/V(R\Delta\theta)^2 + 2\alpha\Delta\tau/V(R\Delta\theta)^2$ is calculated for the interior points, the largest value of the quantity is found, and the time increment is altered as necessary to assure stability. This step would not be needed if a very good estimate of U and V could be made in advance. However, the extra work involved in the step is well spent and actually saves computer time in most cases. A conservatively small value of $\Delta\tau$ would have to be used if the criterion were not tested.

TABLE I
SUMMARY OF CALCULATIONS FOR THE CYLINDER

	Solution 1	Solution 1A	Solution 2	Solution 3	Solution 4
Grashof Number	6.15×10^5	6.15×10^5	4.5×10^4	10^7	6.15×10^5
Prandtl Number	0.7	0.7	0.7	0.7	10.0
<u>First Grid</u>					
Number of time steps	960	400	800	480	1280
Time increment at end of calculations	3.4×10^{-5}	2.8×10^{-5}	7.4×10^{-5}	2.7×10^{-5}	4.1×10^{-5}
Elapsed time, tr_0^2/ν	0.047	0.0121	0.030	0.0125	0.070
Machine time, hours	1.5	0.5	1.0	0.5	1.5
<u>Subdivided Grid</u>					
Number of time steps	480	---	---	480	1920
Time increment, tr_0^2/ν	6.0×10^{-5}	---	---	3.0×10^{-5}	5.0×10^{-5}
Elapsed time, tr_0^2/ν	0.029	---	---	0.0144	0.096
Machine time, hours	0.5	---	---	0.5	2.0
<u>Total</u>					
Machine time, hours	2.0	0.5	1.0	1.0	3.5

(3) The new values of ϕ and U are computed at each interior point using Equations 62a and 62b. The values of ϕ are computed first since U appears in the stability criterion and an increase in U would make the energy equation unstable. The calculations proceed one ray at a time and the values calculated are not substituted directly into the ray where they belong until after the next ray in the sequence is completed. This "holding out" of the values is required so that all of the values used in computing a given difference are from the same time level. Before advancing any given point the machine must determine the sign of U and V and select the equations to be used accordingly.

(4) The new values of V are computed from Equation 62c. V is specified as zero on the boundary and starting here the new values of V are computed working in toward the origin.

(5) The procedure starting with item 1 above is repeated. The calculations were continued as long as any of the independent variables changed appreciably with time.

It will be recalled from the discussion of the stability requirement that the time step depends on both U and V . In the central region of the cylinder U and its derivatives are small and RV is a constant at any fixed angle. At the origin V would be infinite but since U and ϕ were specified as equal to zero at the origin the equations are not applied here and the value of V at the origin is not needed in the calculations. However, the values of V near the origin are large and these values contribute heavily to the restriction on the time step imposed by the stability criterion. For example in the first solution at $R = 0.08$ the largest value of $|V| \Delta \tau / \Delta R$ is about 0.83 which indicates that the allowable time step is almost directly proportional to V . There is no point in carrying out

the calculations very near the origin because no information is gained and the time step is restricted. In this work the smallest value of R for which the calculations were carried out was 0.08 in every solution except solution 3, the case of the largest Grashof number. In the case of solution 3 the smallest value of R was selected as 0.16 based on the analysis given before which indicated that the boundary layer thickness is proportional to $Gr^{\frac{1}{4}}$. The ratio of $Gr^{\frac{1}{4}}$ in this case to $Gr^{\frac{1}{4}}$ of solution 1 is about two. Use of a larger minimum radius for the larger Grashof number compensates for the fact that the velocities increase with Grashof number which reduces the allowable time step.

After the solution using the first grid was completed the solution was used as input for the calculations using the subdivided grid. The calculations using the subdivided grid were carried out in the same way as those using the first grid with two exceptions: the minimum radius was much larger as indicated before, and the time step was held constant since the first solution gave excellent estimates of the maximum magnitudes of U and V for use in determining the allowable time step.

C. Results

The direct results of the calculations are values of U , V , and ρ as functions of R , θ , and ϕ , the dimensionless variables of Equations 62. The heat transfer coefficient is calculated from the temperature distribution in the same way as for the flat plate.

In the first parts of this section the results of the calculations will be presented in terms of U , V , and ρ . In the final part of this section in which the effects of the Grashof and Prandtl parameters are discussed, different variables will be used: $(ur_0/\gamma)(Pr/Gr)^{\frac{1}{2}}$,

$(\nu r_0/\nu)(P_r^3/Gr)^{\frac{1}{4}}$ and ϕ are expressed as function of Θ and $(1 - r/r_0)(GrPr)^{\frac{1}{4}}$. These variables from the analysis of a highly simplified model of Part IIC are expected to take the parameters into account to a first approximation so that the results can be presented in compact form.

1. The Transient Solution

The transient solution for the cylinder problem was obtained for a Grashof number, $(g\beta\Delta Tr_0^3/\nu^2)$, of 6.15×10^5 and a Prandtl number of 0.7. The initial condition was that of a motionless isothermal cylinder in which one half of the wall suddenly assumes a high temperature ($\phi = + 1/2$) and the other half assumes a low temperature ($\phi = - 1/2$). After the change in temperature of the boundary the fluid near the hotter part of the boundary tends to rise and that near the colder part tends to fall. Eventually a steady state is reached where, according to the observations of Martini and Churchill (21), as well as the results to be presented here, a narrow layer of fluid near the boundary circulates while the inner part of the fluid is practically isothermal and motionless. The steady state solution is of primary interest and is independent of the choice of initial conditions. The transient solution obviously depends on the choice of initial conditions. The initial conditions used in the cylinder problem were chosen primarily to facilitate obtaining the steady state solution rather than to correspond to any condition of actual engineering importance. For this reason only the most important results of the transient solution will be given here.

Figure 12 shows the velocity as a function of time at various positions. The points shown are for every fortieth time step as in the case of the flat plate. The calculations were carried out using the space grid shown in Figure 9. The first and most important conclusion from

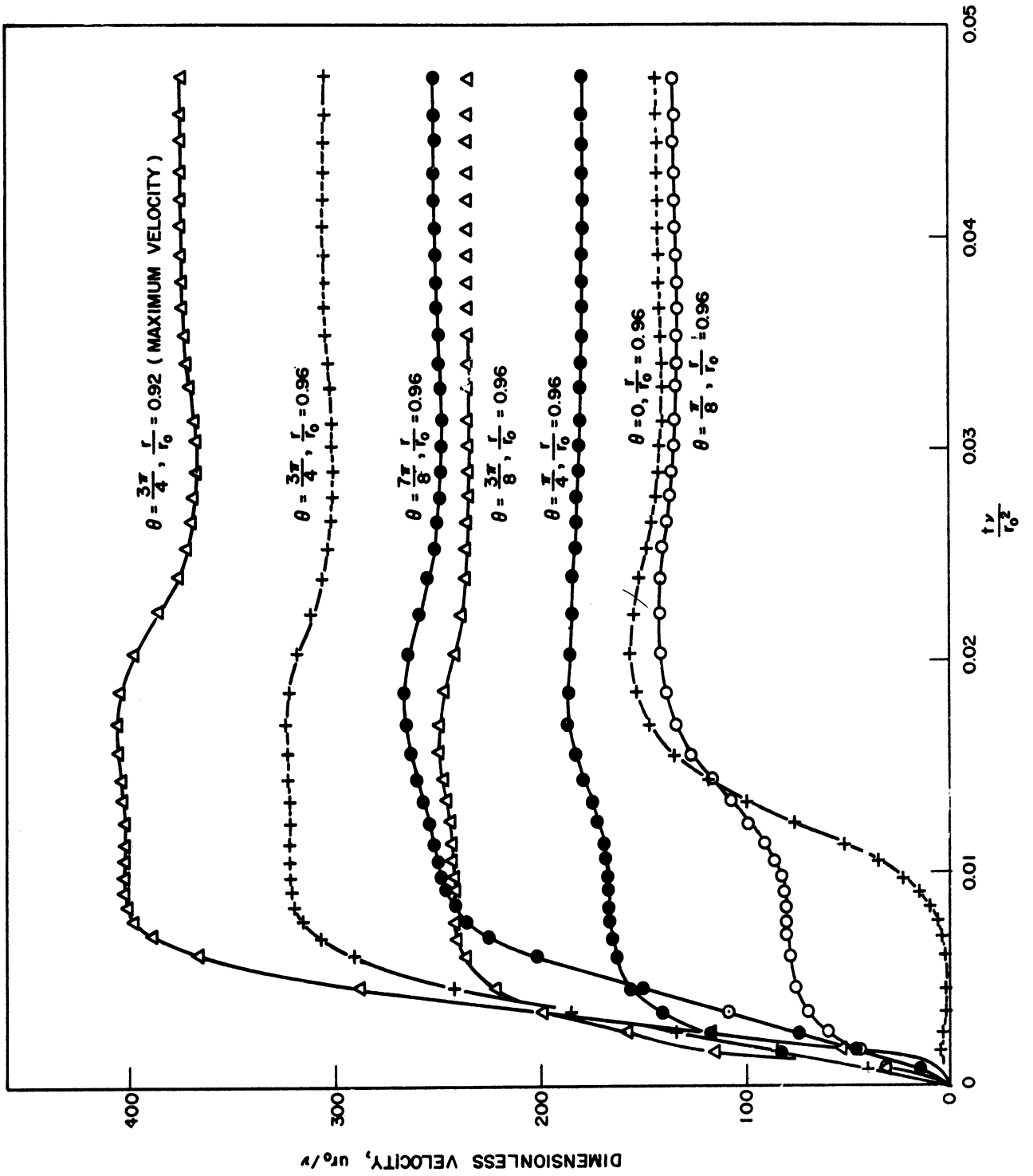


Figure 12. Transient Velocities in the Cylinder.

inspection of Figure 12 is that steady state was reached at a value of the time group of about 0.04.

The somewhat erratic behavior with time of the velocity at various points as shown in Figure 12 is interesting. The system seems to almost reach a steady state early in the calculations while the velocity at $\theta = 0$ (and $\theta = \pi$) is practically zero. Then the velocity at $r = 0$ (and $\theta = \pi$) increases and adjusts to its equilibrium value causing adjustments in the velocities elsewhere. This behavior can be explained by the fact that the fluid on the rays $r = 0$ and $\theta = \pi$ near the boundary has no incentive to move. That is to say the "buoyant force" on these rays acts perpendicular to the boundary. Eventually the fluid motion elsewhere is carried across the rays $r = 0$ and $\theta = \pi$ by momentum.

Figure 13 gives the most important results of the transient solution: the variation of the Nusselt number at various positions with time. Notice that the Nusselt number appears to reach steady state somewhat earlier than the velocity as given in Figure 12. This behavior is characteristic of all the calculations: the Nusselt number depends on the velocity distribution, but is insensitive to small variations in the velocity distribution. For this reason the approach to steady state is best judged by observing the variation of velocity with time. When the velocity becomes steady, the temperature distribution and the Nusselt number certainly also will be steady.

The Nusselt numbers vary less with time than the velocities except at small times. The boundary temperature changes discontinuously when $\tau = 0$ everywhere except at $\theta = 0$ and $\theta = \pi$; at these two points the

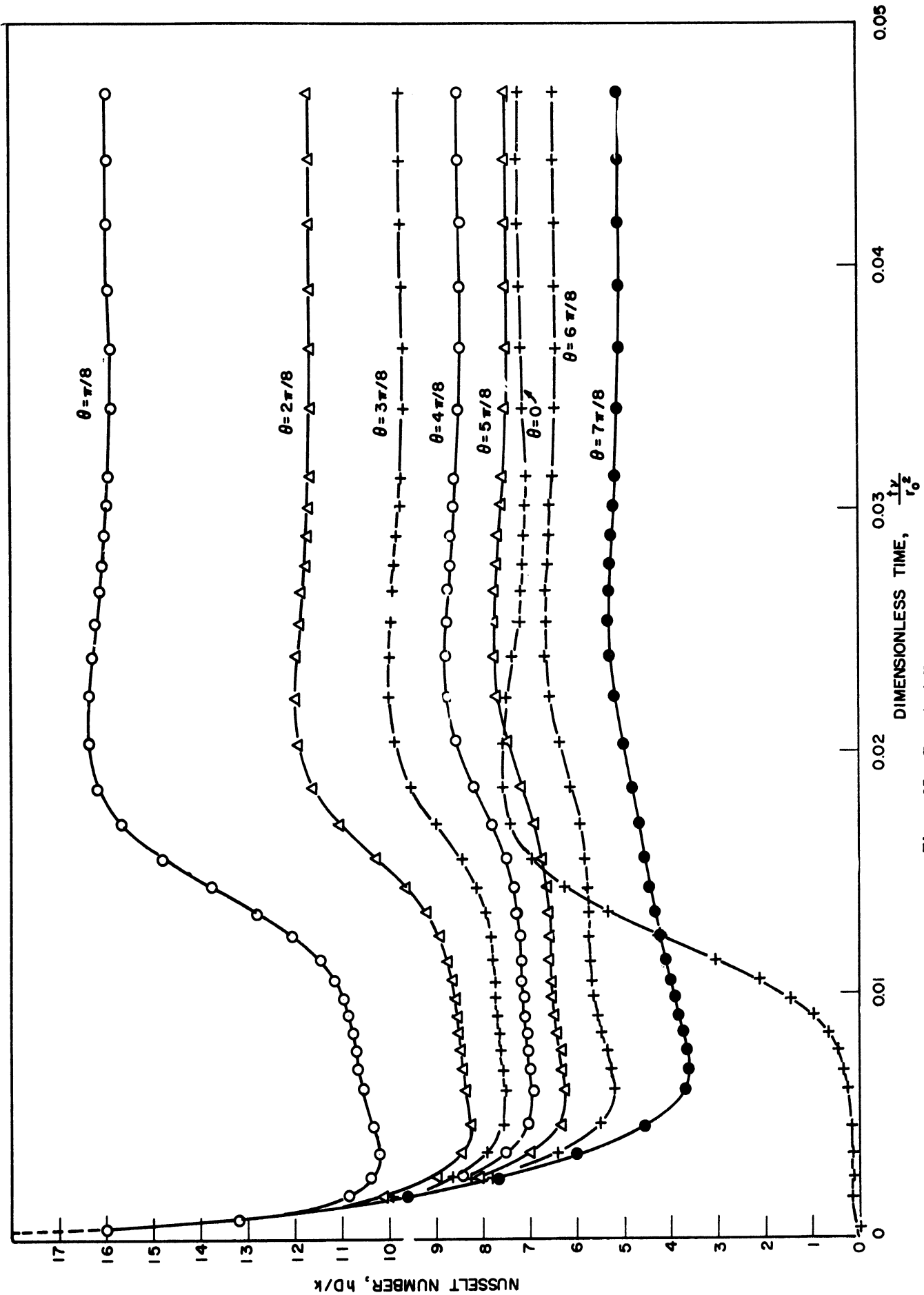


Figure 13. Transient Nusselt Numbers for the Cylinder.

Nusselt number is zero at $\gamma = 0$. Elsewhere the Nusselt number is infinite at $\gamma = 0$.

2. Comparison of Two Models

It will be recalled that in the development of Equations 26 it was postulated that radial gradients are large relative to azimuthal gradients so it might be expected that the terms $1/R^2 \partial^2/\partial\theta^2$ and $1/R^2 \partial^2 U/\partial z^2$ as well as U/R^2 are negligible. This expectation was investigated by solving the equations with and without these terms. There is no difficulty associated with the terms in finite difference calculations--as opposed to other methods of attack in which retaining the terms is often not possible if a solution is to be obtained. Finite difference methods are thus well suited for testing the validity of the idealizations which are often used in fluid mechanics.

Figure 14 gives a comparison of velocity and temperature profiles at various positions obtained by solving Equations 62 with and without the terms mentioned above. The solution of the simpler equations is denoted by broken curves and the solution of the more general equations by full curves. Near the boundary the two solutions are virtually indistinguishable and the deviations in the central region are slight. Hence, the expectation is confirmed.

The comparison of Figure 14 is based on solutions using the first (unsubdivided) space grid. At some positions, especially near $\theta = 0$, there are relatively few points near the boundary where the temperature changes rapidly with position so the need for subdivision of the space is evident. However, it will be shown in the next section that the results of Figure 14 constitute a surprisingly good solution despite the apparently coarse space grid used. The solution of Figure 14 is for the same values of the Grashof and Prandtl numbers as the transient solution.

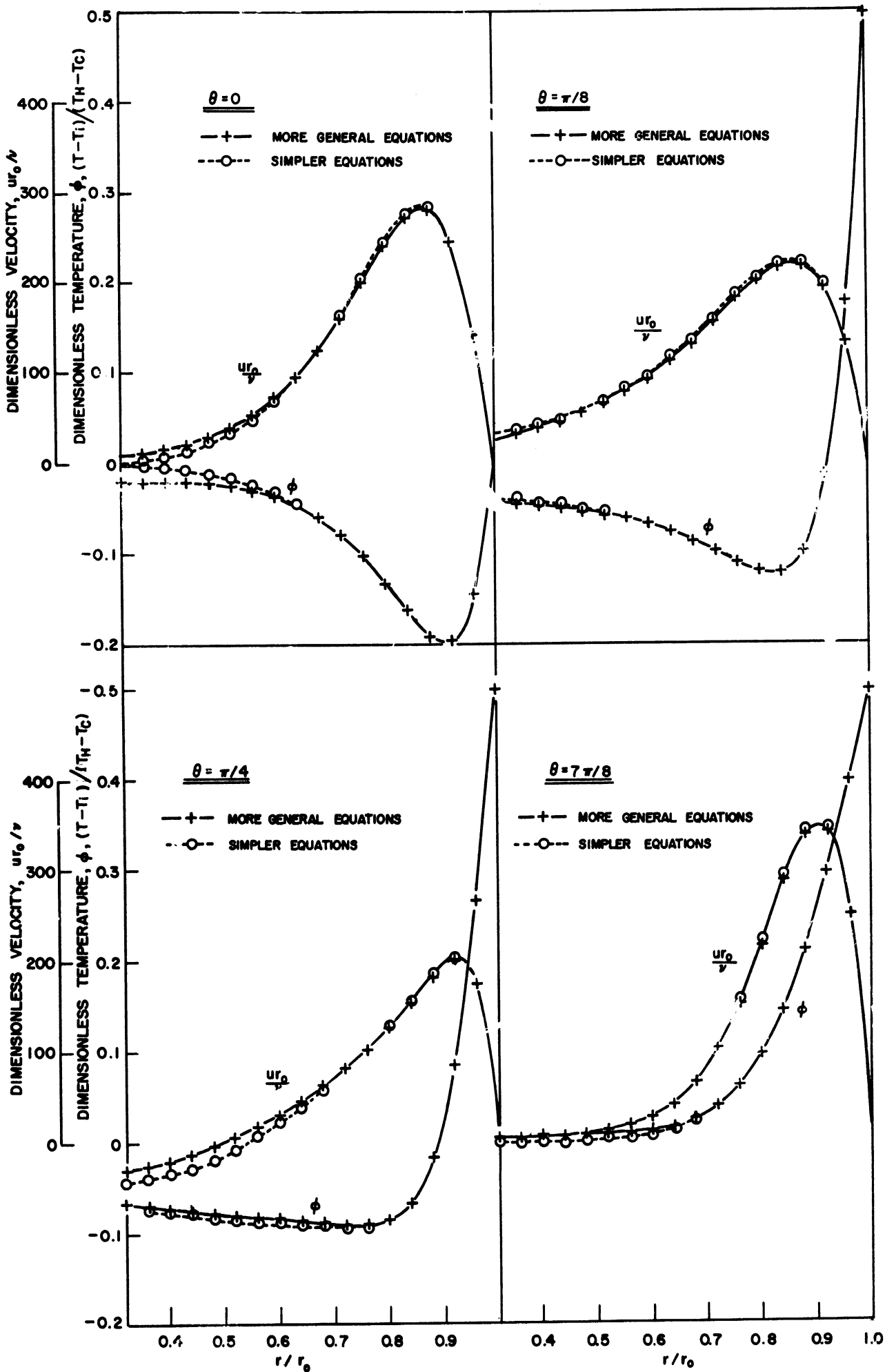


Figure 14. Velocity and Temperature Profiles from First Grid.

The temperature profile at various positions is interesting. Consider the fluid moving near the boundary in the direction of increasing Θ . Just before the fluid gets to the bottom of the cylinder ($\Theta = 0$) the fluid has passed the entire cold side of the cylinder and the temperature profile is "well developed;" it is monotone decreasing from the center ($\phi = 0$) out to the boundary ($\phi = -1/2$). The profile at $\Theta = -\pi/8$ is the reflection across the line $\phi = 0$ of the profile at $\Theta = 7\pi/8$. At $\Theta = 0$ the boundary temperature abruptly changes from $\phi = -1/2$ to $\phi = 0$, then at $\Theta = \pi/8$ the boundary changes temperature abruptly again to $\phi = 1/2$. The fluid heats as it passes up the hot side of the cylinder until, near the top, the temperature is monotone increasing with radius. At $\Theta = \pi$ the same sequence of changes starts only in the opposite direction.

3. Effect of Subdivision of the Grid

It has been mentioned before that subdivision of the space grid is expected to give an improved solution, and also to give an indication of the error involved in the approximation. This later expectation deserves some discussion. Suppose some function, f , satisfies a differential problem. This function in general will not satisfy the difference equations used to approximate the differential problems. By use of Taylor's formula as was illustrated before, it is possible to compute differences in f , substitute them into the difference equations and find an expression for the truncation error. For any consistent approximation the truncation error must vanish as the increment sizes approach zero. In the problems of this work the truncation error varies linearly with increment size from which it is inferred that the change in the solution on subdividing the grid by half is of the same order as the error in the resulting solution. This approach gives some indication of the error in the finite difference approximation

despite its obvious weaknesses. There is no other general method of estimating the error for complicated problems of the most interest.

There is some difficulty in considering the temperature profile near the boundary at $\Theta = 0$. It will be recalled that here the temperature varies discontinuously with both R and Θ at the boundary in the differential problem. There is no reason to try to approximate a function where the function is not defined and it must be concluded that the heat transfer coefficients computed at $\Theta = 0$ are meaningless. It is instructive to consider the behavior of the solution near the discontinuity, however, since the approximation is intended to be useful everywhere except at $\Theta = 0$ (and $\Theta = \pi$).

The results of Figure 14 for $\Theta = 0, \pi/8,$ and $\pi/4$ are shown again in Figure 15 in comparison with the solution to the same problem after subdivision of the grid. The fluid is generally colder after the grid is subdivided than before. This difference comes about because the boundary conditions on the difference problem were altered on subdivision as indicated earlier. The fraction of the boundary surface at the mean temperature ($\phi = 0$) is $1/16$ as opposed to $1/8$ before subdivision. Consequently the fluid passes by more cold surface in traversing the cold side and more hot surface in traversing the hot side. The result is that the minimum and maximum temperatures in the fluid are both increased in magnitude. The effect of subdivision on the solution is seen to be small even along the ray $\Theta = \pi/8$ which is the ray nearest the discontinuity which is common to both grids. The effect of the subdivision is less for rays farther removed from the discontinuity. For values of Θ greater than $\pi/4$ the solutions are practically indistinguishable. The subdivision has very little effect on the velocity profile. Only two points from the

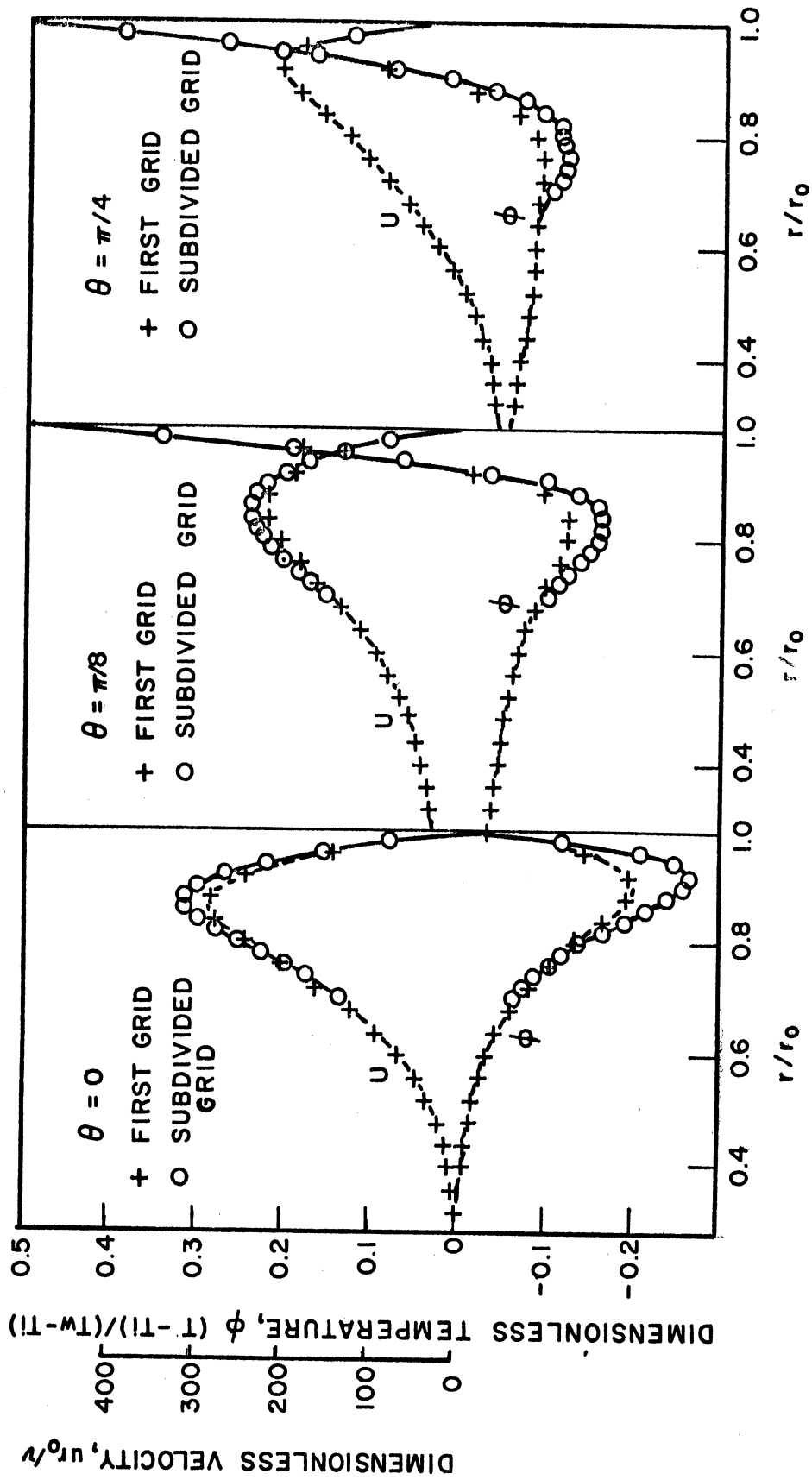


Figure 15. Effect of Subdivision on Velocity and Temperature Profiles for Solution 1 ($Gr = 6.15 \times 10^5$).

subdivided solution are given along the ray $\Theta = \pi/4$ because the points are coincident to the points from the first grid.

The effect of subdivision would have been much less if the boundary conditions on temperature had been treated differently. An alternate way of treating the conditions would involve avoiding placing a grid point at the discontinuity. Suppose the first grid contained points to the left and right of the discontinuity but not at the discontinuity. Then it could be supposed that the temperature changes discontinuously half way between two points. The angular increments should not be subdivided in half in this case because this would entail specification of the temperature at the discontinuity. However, the angular increments could be subdivided by one third and the discontinuity would again fall half way between two points. This procedure is preferable to the one used in this work. The procedure used in this work is sound and the difference between the two procedures diminishes with diminishing increment size. However, the alternate procedure outlined above is superior for large increment sizes.

The effect of the subdivision on the heat transfer coefficient is shown in Figure 16. In drawing Figure 16 the Nusselt number at $\Theta = 0$ and $\Theta = \pi$ was taken to be unbounded as in the differential problem despite the fact that finite heat transfer coefficients are actually calculated in the difference problem as indicated on the figure. It was mentioned earlier that the interpretation of the results near discontinuities is somewhat arbitrary. From inspection of Figure 16 it is concluded that the subdivision of the grid has practically no influence on the solution which in turn indicates that there is little error in the approximate solution.

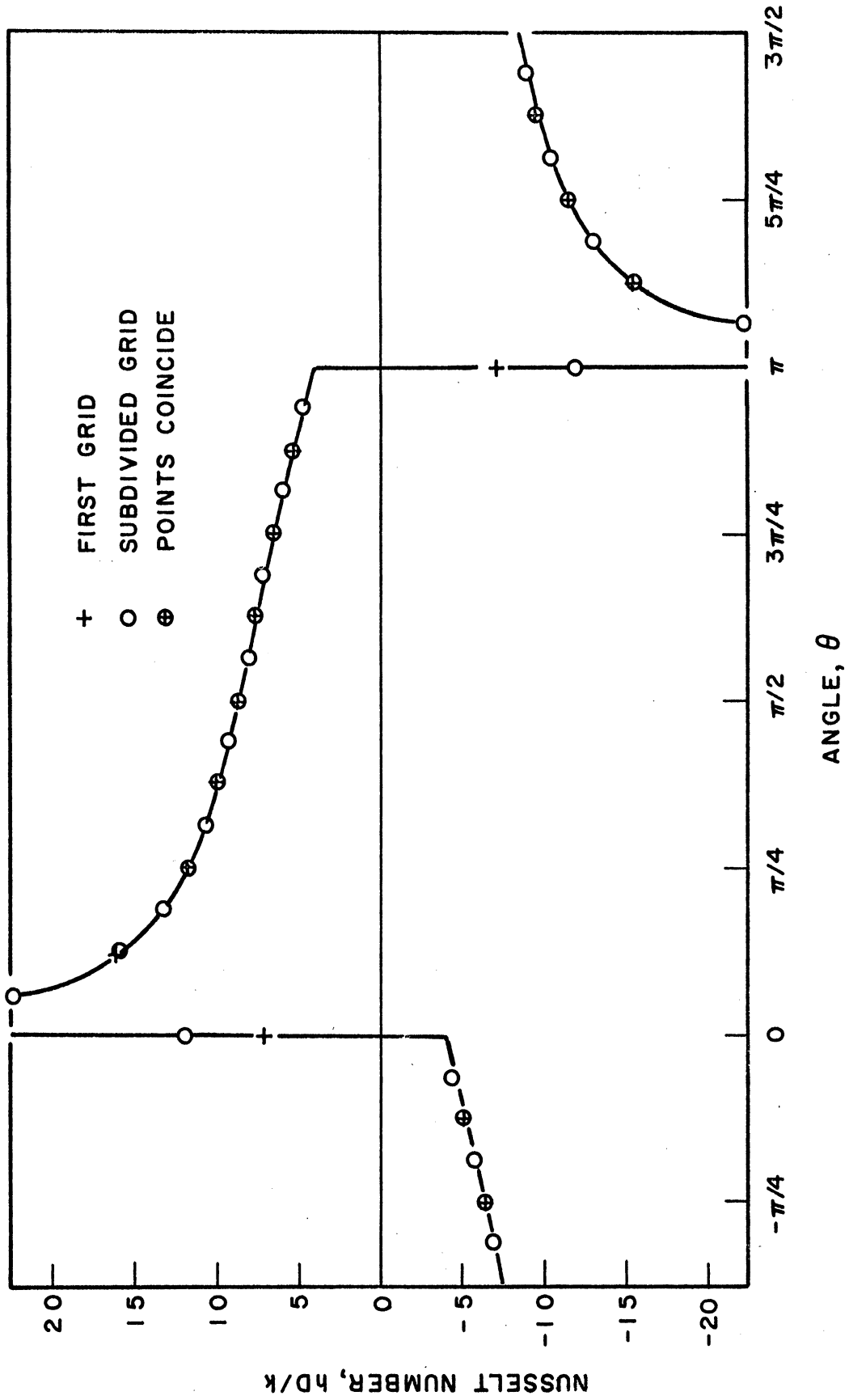


Figure 16. Effect of Subdividing the Grid on Nusselt Number for Solution 1 ($Gr = 6.15 \times 10^5$).

The necessity for subdividing the grid depends on the Grashof and Prandtl parameters. An increase in either of these parameters results in a decrease in the boundary layer thickness so that a finer mesh size is desired near the boundary to maintain accuracy. For this reason the subdivided grid was used in the calculations for the cases to be described in which either of the parameters exceeded the values in the solution of Figure 16 ($Gr = 6.15 \times 10^5$, $Pr = 0.7$).

The subdivision of the space grid should be most important for solutions of the largest Grashof number. Not only does the boundary layer thickness decrease, but the maximum velocity increases with increasing Grashof number. The effect of subdivision on Solution 3 ($Gr = 10^7$) is shown in Figures 17 and 18.

The velocity and temperature profiles given in Figure 17 are very similar in appearance to those discussed earlier from Solution 1 ($Gr = 6.15 \times 10^5$). This similarity is not due to coincidence: the ratio of the Grashof numbers for the two cases is about 16 to 1 from which it is to be expected that the boundary layer would be one half as thick and the maximum velocity would be four times as great. The distance scale in Figure 17 is twice that of Figure 15 and the velocity scale is four times as great. As a result the two figures look much alike. The effect of the Grashof number will be discussed in more detail later on.

The comments given earlier on the subdivision of Solution 1 apply to Solution 3 except that the subdivision alters the large Grashof solution slightly more as was expected. The difference between the first grid solution and the subdivided solution is given in Figure 18 in terms of the Nusselt number. Here, in contrast to Solution 1, there is a discernable difference in the Nusselt number near the discontinuity. At

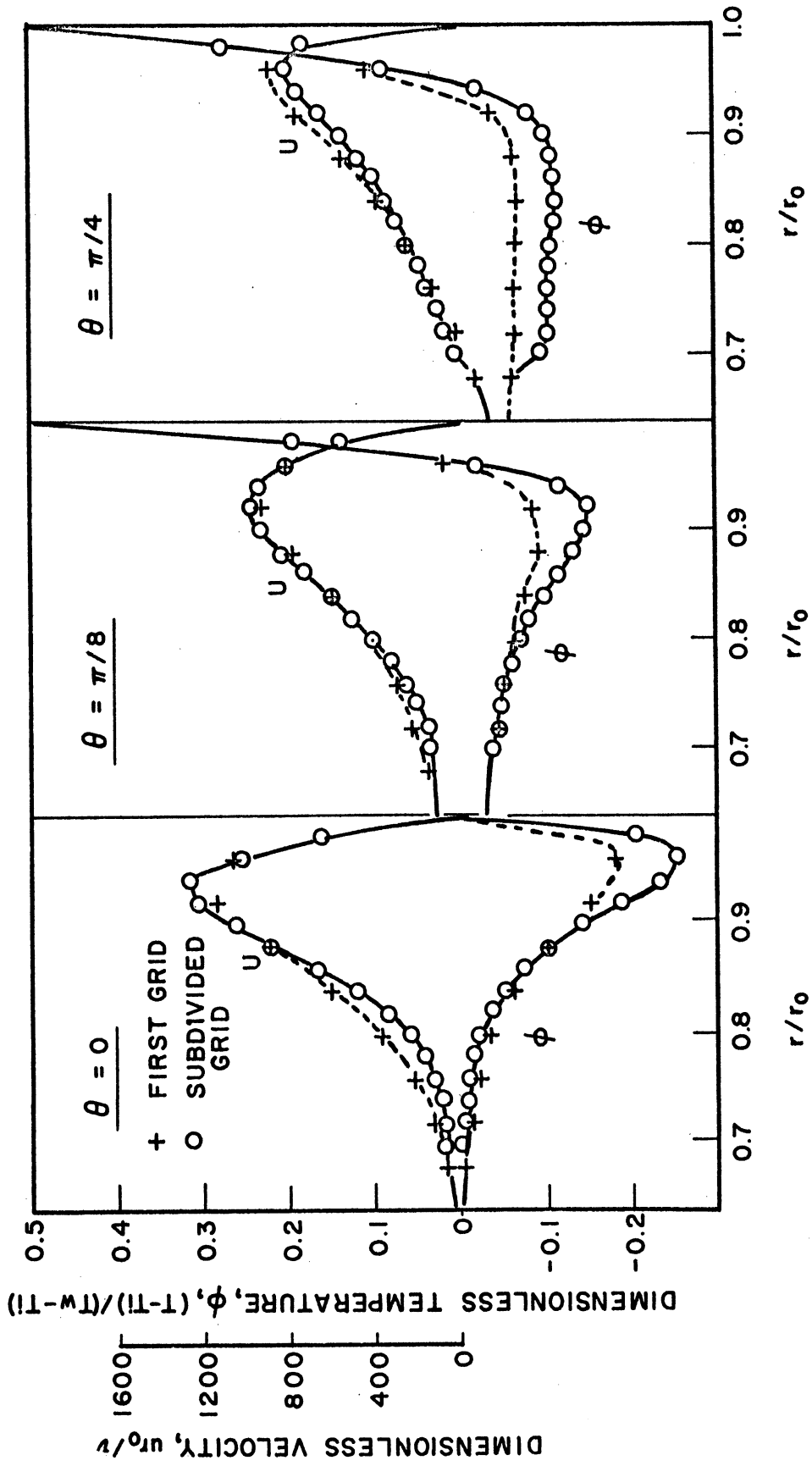


Figure 17. Effect of Subdivision on Velocity and Temperature Profiles for Solution 3 ($Gr = 10^7$).

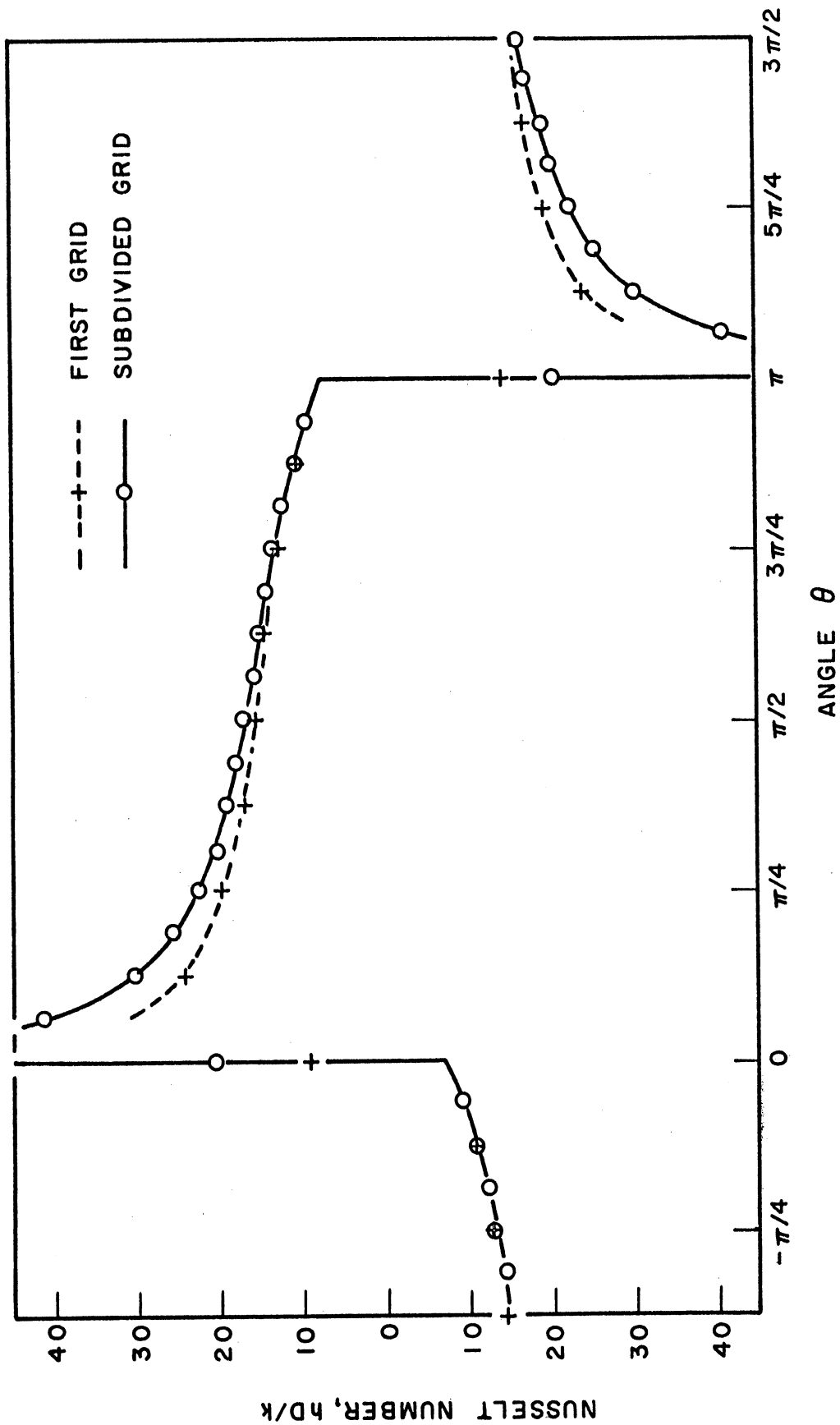


Figure 18. Effect of Subdivision on Nusselt Number for Solution 3
(Gr = 10⁴).

$\Theta = \pi/8$, the point nearest the discontinuity and common to both grids, the first grid solution gives a Nusselt number 3 per cent lower than that from the subdivided solution. The difference between the two solutions is less and less farther from the discontinuity. At the discontinuity there is a larger difference between the two solutions; but, as indicated earlier, the results here are meaningless or open to interpretation. It is concluded that even in the large Grashof number solution the difference equations and the space grid used give a good approximation to the solution to the differential problem.

4. Direct Comparison with Experiment

In this section the results of the calculations for the case of Grashof number of 6.15×10^5 and Prandtl number of 0.7 will be compared with the measurements of Martini and Churchill (21). The values of the parameters were selected to correspond to Martini and Churchill's experiment number 4 for which experimental results were presented in most detail. Some additional comparisons with the experiments will be given in the next section.

Figure 19 shows calculated velocity profiles in comparison with the measurements. The points are calculated and the curves without points are from Martini and Churchill. The broken parts of the experimental curves are estimated and are uncertain. The overall agreement is good considering the great difficulty encountered in measuring velocities in natural convection in enclosed spaces. The largest deviation near the maximum velocity is about 30%. Martini and Churchill's results are the most certain on the ray $\Theta = 3\pi/2$: in the middle of the cold side. It is satisfying to notice that the measured velocity profile is in the best agreement with the calculations on this ray.

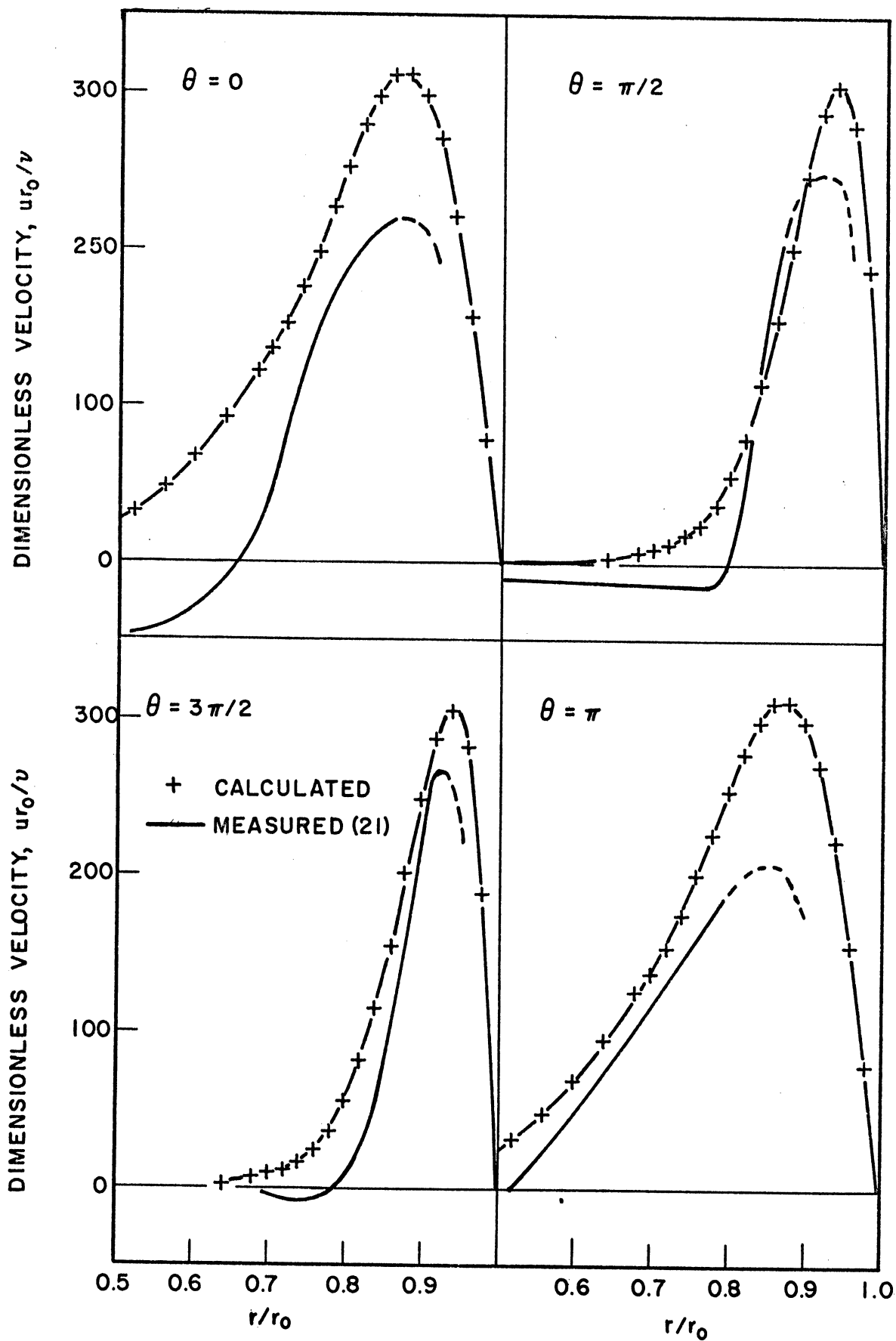


Figure 19. Comparison of Velocities with Measurements.

A comparison of temperature distributions is given in Figure 20. Martini and Churchill measured temperatures along horizontal and vertical lines rather than along radial lines. The calculations were carried out in cylindrical coordinates so it was necessary to interpolate between calculated values to give temperature distributions along horizontal lines as shown in the figure. From Figure 20 it is seen that the agreement is excellent near the boundary where the results are of most interest. The agreement in the central region is not as good as it is near the boundary although the overall agreement is good. The calculations show a more nearly isothermal central region than was measured. The difference is probably due in part to a deficiency in the model which has been mentioned before: the radial velocity is that velocity required to satisfy the continuity equation without regard to radial momentum changes. The radial fluid motion in the central region in the calculations is large which tends to make the central region isothermal.

Figure 21 gives a comparison of the calculated and measured Nusselt numbers. Here the agreement is remarkably good. The only deviations which are not within the accuracy of the measurements occur near the discontinuities in the boundary temperature, and, at these points, the mathematical model was different from the physical situation. In the physical situation the boundary temperature changes continuously at $\phi = 0$ and the Nusselt number is a smooth function of ϕ . Martini and Churchill's measurements for both sides of the cylinder are given on Figure 21 to show that the physical situation is symmetrical in the same way as the mathematical model. As indicated before, only one half of the cylinder need be considered, although more than one half is given in the figure for clarity.

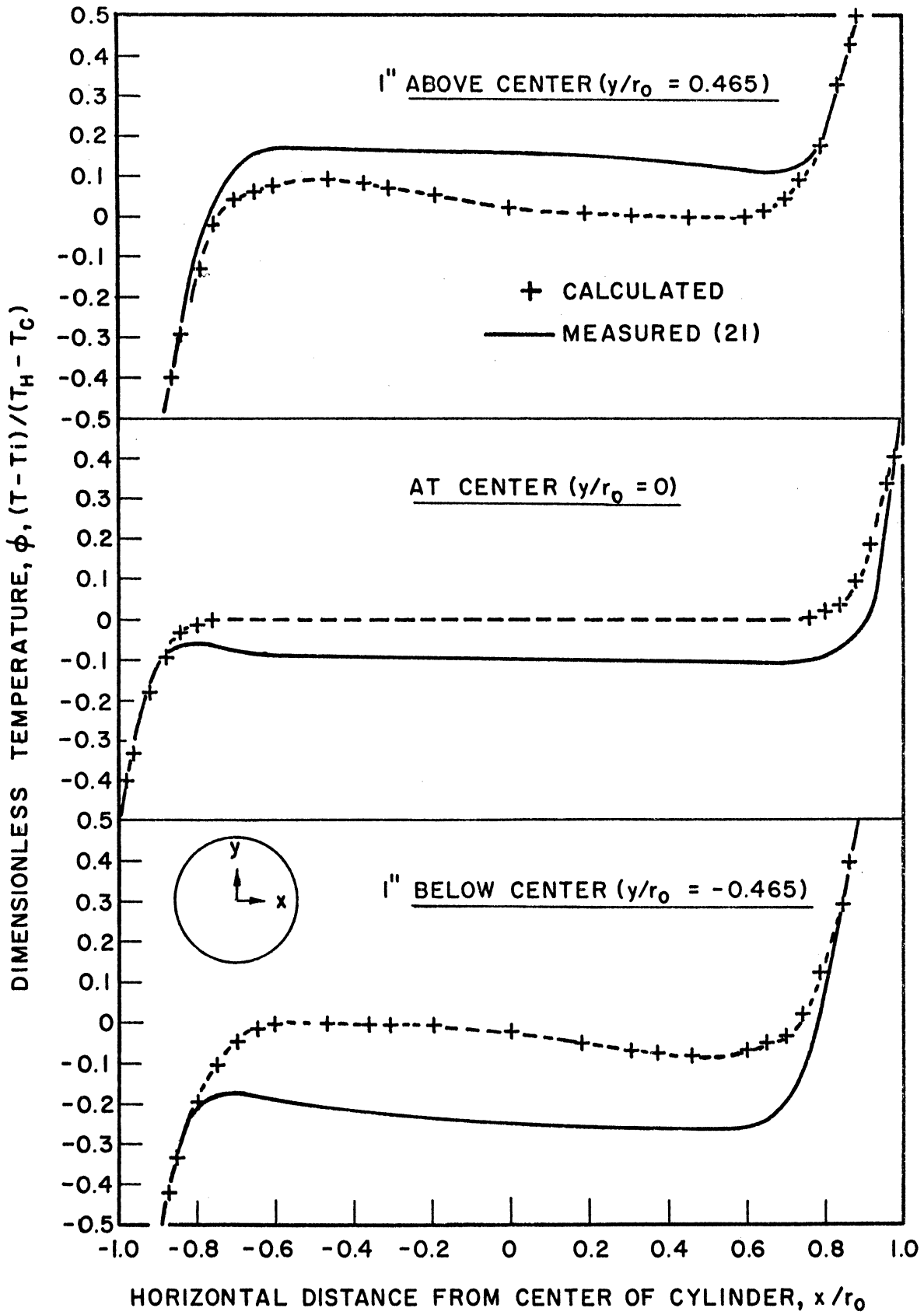


Figure 20. Comparison of Temperature with Measurements.

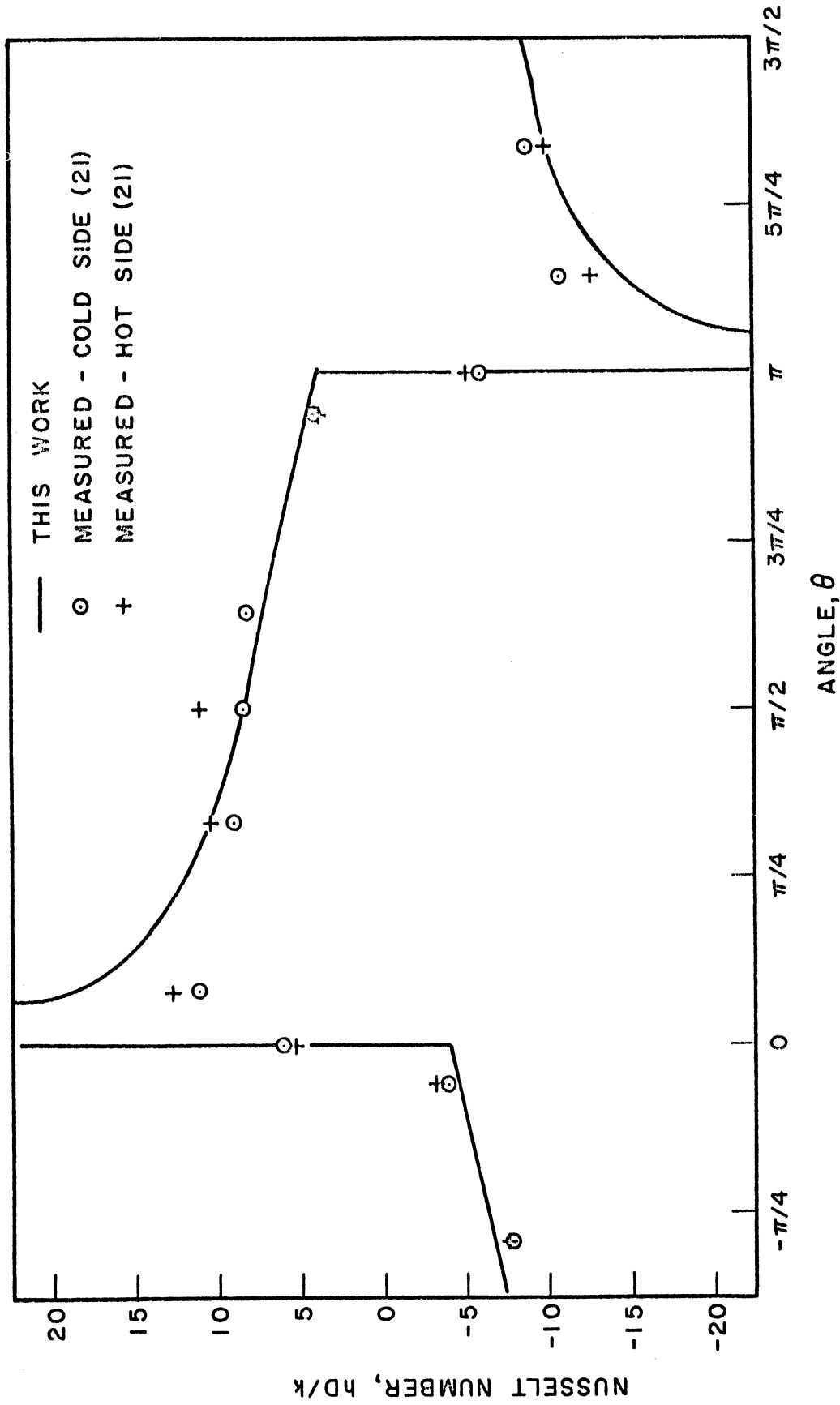


Figure 21. Comparison of Nusselt Numbers with Measurements.

It is concluded that the calculations and the measurements of Martini and Churchill's experiment number 4 are in good agreement.

In the next section it will be shown that the calculations do not agree with all the measurements because the idealizations of the mathematical model are not valid under all conditions.

5. Variation of Parameters and Additional Comparisons with Experiment

The cylinder problem was solved for two additional values of the Grashof number and one additional value of the Prandtl number. The results are sufficient to allow prediction of heat transfer rates in the cylinder over wide ranges of both parameters. In this section most of the results will be presented in terms of the variables from the simple analysis as mentioned before. A summary of the cases solved is given in Table II along with the principal results.

TABLE II
SUMMARY OF SOLUTIONS

	Solution 1	Solution 2	Solution 3	Solution 4
Grashof Number, $g\beta\Delta T r_0^3/\nu^2$	6.15×10^5	4.5×10^4	10^7	6.15×10^5
Prandtl Number, ν/α	0.7	0.7	0.7	10.0
Rayleigh Number, $(g\beta\Delta T r_0^3)/(\nu\alpha)$	4.3050×10^5	3.1500×10^4	7.0000×10^6	6.1500×10^6
$\left(\frac{g\beta\Delta T r_0^3}{\nu\alpha}\right)^{\frac{1}{4}}$	25.615	13.322	51.437	49.799
$h_m D/k$	9.434	4.562	18.338	16.291
$\frac{h_m}{k} \left(\frac{\alpha r_0 \nu}{g\beta\Delta T}\right)^{\frac{1}{4}}$	0.1841	0.1712	0.1782	0.1629

The results of most interest were considered to be those for gases so a wide range of the Grashof group was covered in three solutions for a fixed Prandtl number of 0.7. Then a solution for a Prandtl number of 10 was developed to give an indication of how well the simple analysis predicts the effect of the Prandtl number.

Figures 22 and 23 give velocity and temperature profiles for the four solutions at various positions. Where the points are coincident only the point for Solution 1 is given. It is seen that the profiles for the three solutions of $Pr = 0.7$ are brought together remarkably well by use of the composite variables. Solutions 1 and 3 are very nearly indistinguishable and Solution 2 deviates from the others by no more than 15 per cent near the maximum velocity. The deviation is much less near the boundary. The deviation is undoubtedly due in large part to the fact that Solution 2 was not subdivided whereas all other solutions were.

The solution for $Pr = 10$, Solution 4, deviates considerably from the other solutions especially in the velocity profile. All the velocity profiles show that the fluid accelerates while traversing the hot (or cold) side of the cylinder. Then on passing the top (or bottom) of the cylinder, the fluid decelerates before once again picking up speed. The large Prandtl number fluid is much more prone to accelerate and decelerate than the other fluid. On starting up the hot side the fluid practically stops; yet by the time the fluid has completed a traverse of a side of the cylinder, it has accelerated relatively more than the fluid of $Pr = 0.7$. When the fluid first starts up the hot side (or down the cold side) of the cylinder, the "buoyant force" as well as drag opposes the motion. This opposition must be overcome by the inertia of the fluid if the motion is to continue. Therefore, the behavior of the large Prandtl number fluid is in accordance

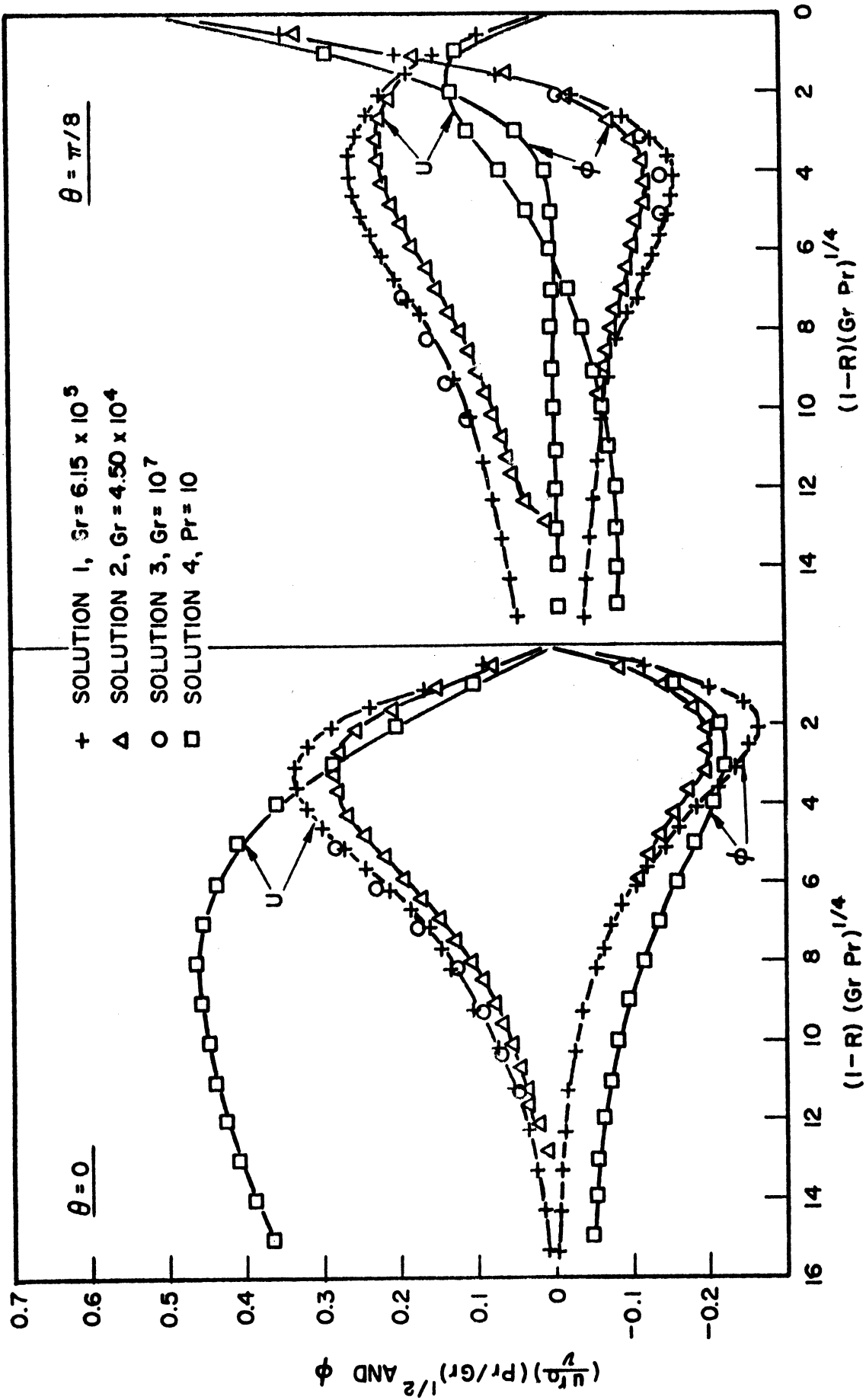


Figure 22. Collected Profiles Near the Discontinuity.

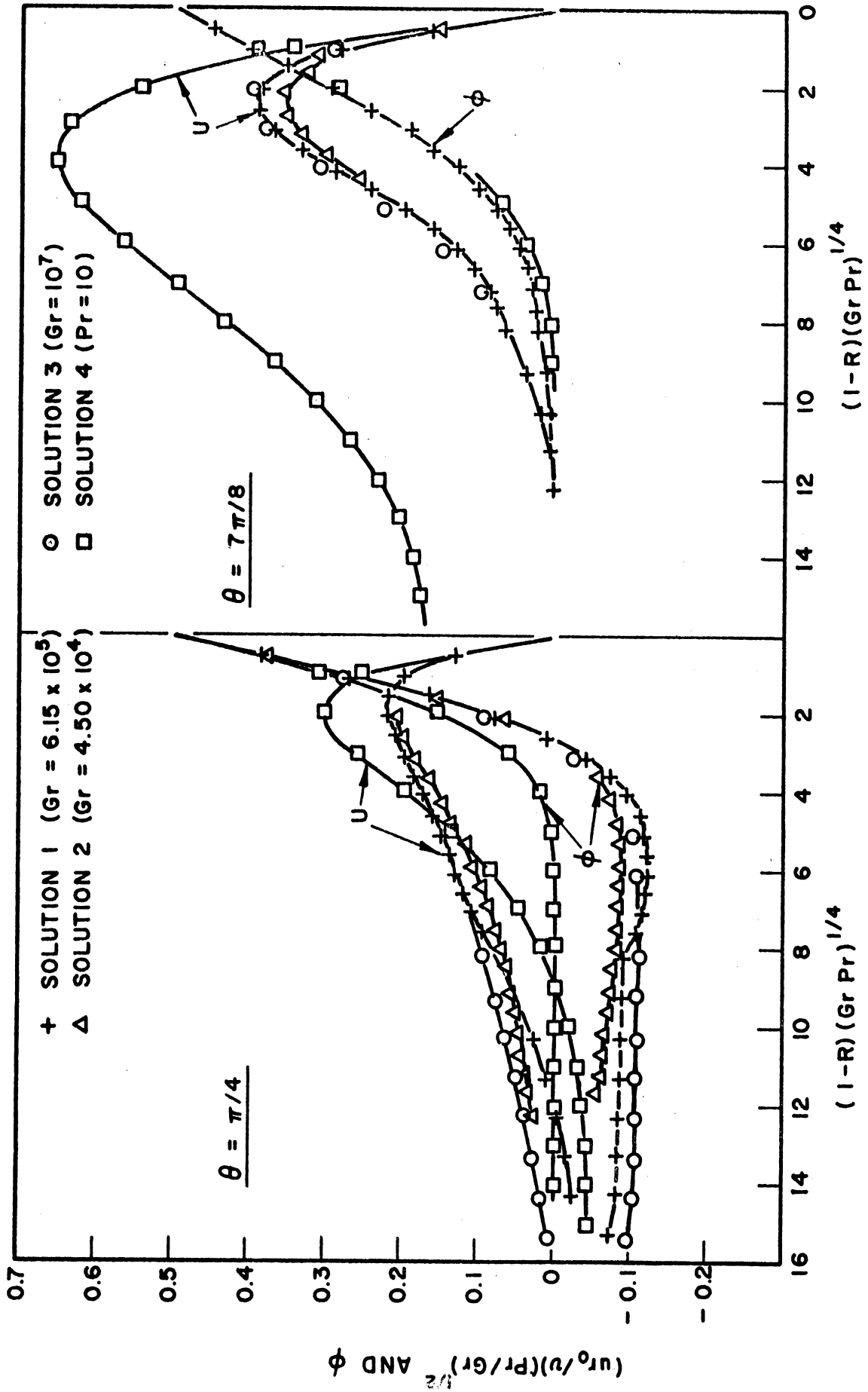


Figure 23. Collected Profiles on the Hot Side of the Cylinder.

with the analysis given earlier (also see Appendix A) which showed that the relative importance of the inertial forces is inversely proportional to the Prandtl number. The large Prandtl number fluid has relatively little inertia or relatively little resistance to acceleration and deceleration in comparison to the viscous and buoyant force terms.

The temperature profiles for the fluids of different Prandtl number are in better agreement than the velocity profiles. Along the ray $\theta = 7\pi/8$ the profiles almost coincide. However, there are appreciable differences close to the bottom of the cylinder.

The heat transfer results for all four solutions are given in Figure 24. Notice that the heat transfer group from the simple analysis serves to bring all the results together. The three solutions for $Pr = 0.7$ are brought together remarkably well, and the solution for a Prandtl number of 10 deviates from the others only near the discontinuity. At $\theta = \pi/16$ the large Prandtl number solution is about 32 per cent below the other solutions.

The results of Solution 4 have an interesting property that has not been mentioned: in contrast to the other solutions, fluctuations occurred in a part of the space grid after the grid was subdivided. The results presented heretofore did not show the fluctuations because the amplitude is practically too small to be distinguished on the graphs except in one small part of the space grid. The calculations were continued much longer than in the other solutions to study the behavior of several cycles of fluctuation. It was established that the fluctuations were decaying and that they were restricted in area and amplitude. The fluctuations were not decaying very rapidly, however, so the calculations were discontinued before steady state was reached.

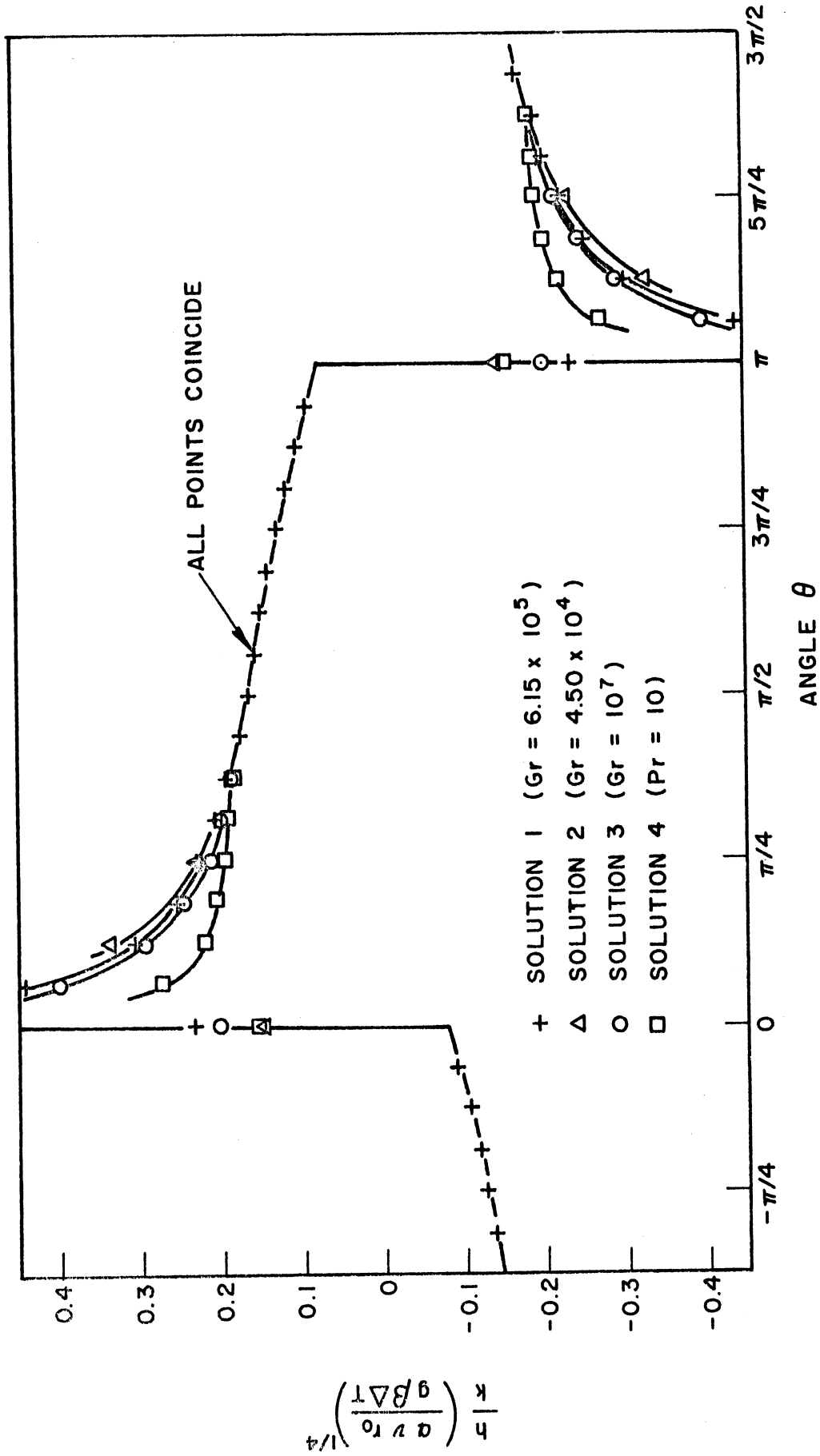


Figure 24. Collected Heat Transfer Results.

Figure 25 gives velocity and temperature profiles near $\Theta = 0$ for Solution 4. The crosses represent the profiles at dimensionless time of 0.068, and the circular points represent the profiles at a dimensionless time of 0.084 where the time is measured starting from the subdivision of the grid. The difference between the profiles represents the maximum amplitude of the last cycle of fluctuations in the calculations. Where only crosses are given on the figure, such as at $\Theta = -\pi/16$, the fluctuations are too small to show on the graph. Notice that the fluctuation in the velocity along the ray $\Theta = \pi/16$ is pronounced, but it does not carry over to adjacent rays to any appreciable degree. The fluctuation in the temperature profile is much less than that of the velocity profile.

The velocity at the point of maximum fluctuation is shown versus time in Figure 26 for the three rays where the fluctuations are the largest. The scale of Figure 26 is enlarged and the maximum and minimum values of the velocity on the ray $\Theta = \pi/16$ are indicated on the figure. The maximum amplitudes of the first three cycles are 87.7, 62.6, and 59.6, respectively. Hence it is clear that the fluctuation is decaying such that steady state would be reached if the calculations were continued. It is equally clear that steady state is being approached only very slowly. The points of Figure 26 represent 1920 time steps which took two hours of computer time. Only one out of forty of the points are shown on the graph.

The influence of the fluctuations on the heat transfer coefficient is indicated in Table III. The heat transfer coefficient fluctuates by as much as ± 2.4 per cent at one point, but the mean fluctuation is only ± 0.8 per cent.

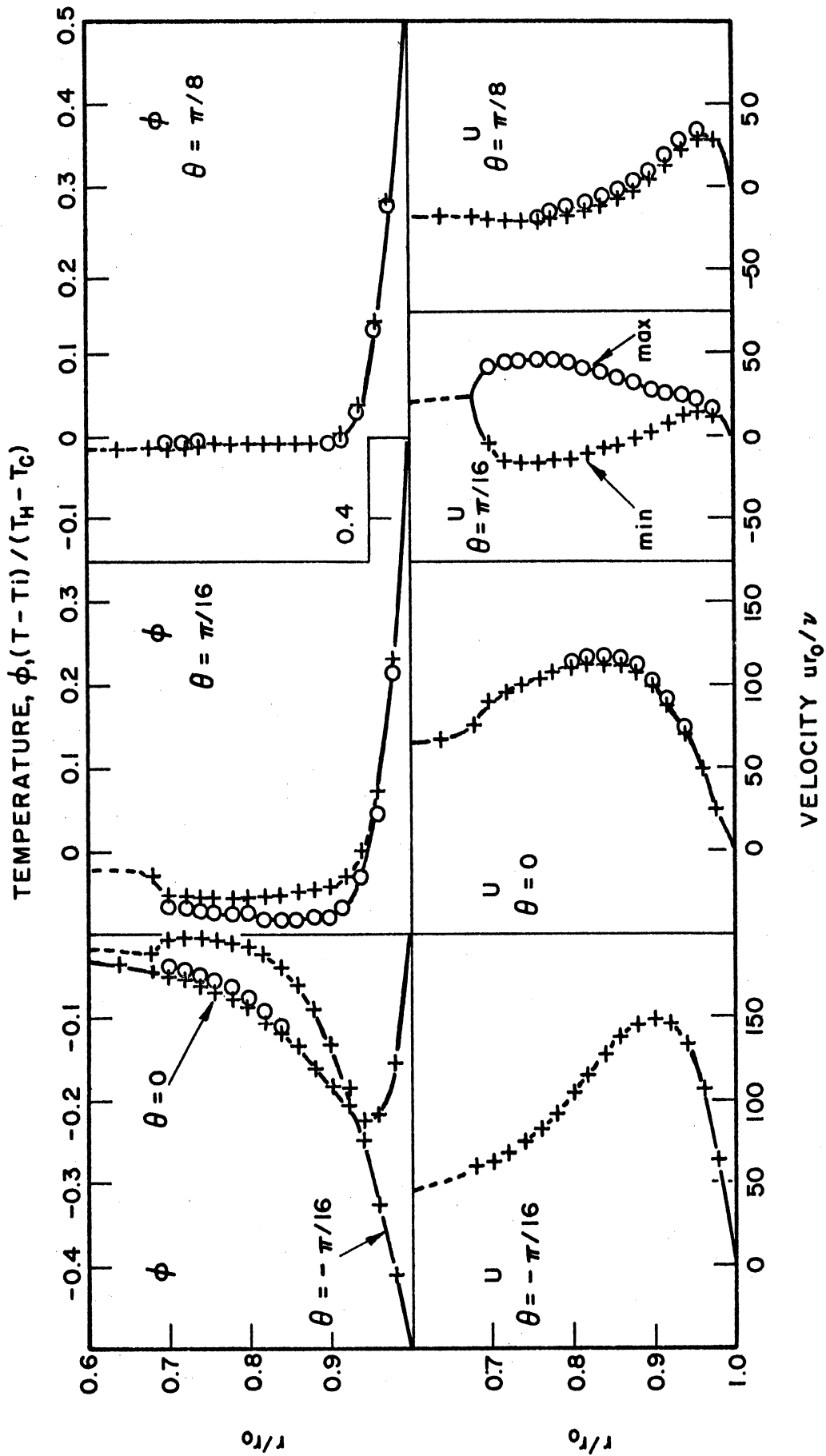


Figure 25. Profiles from Solution 4 (Pr = 10) Showing Fluctuations.

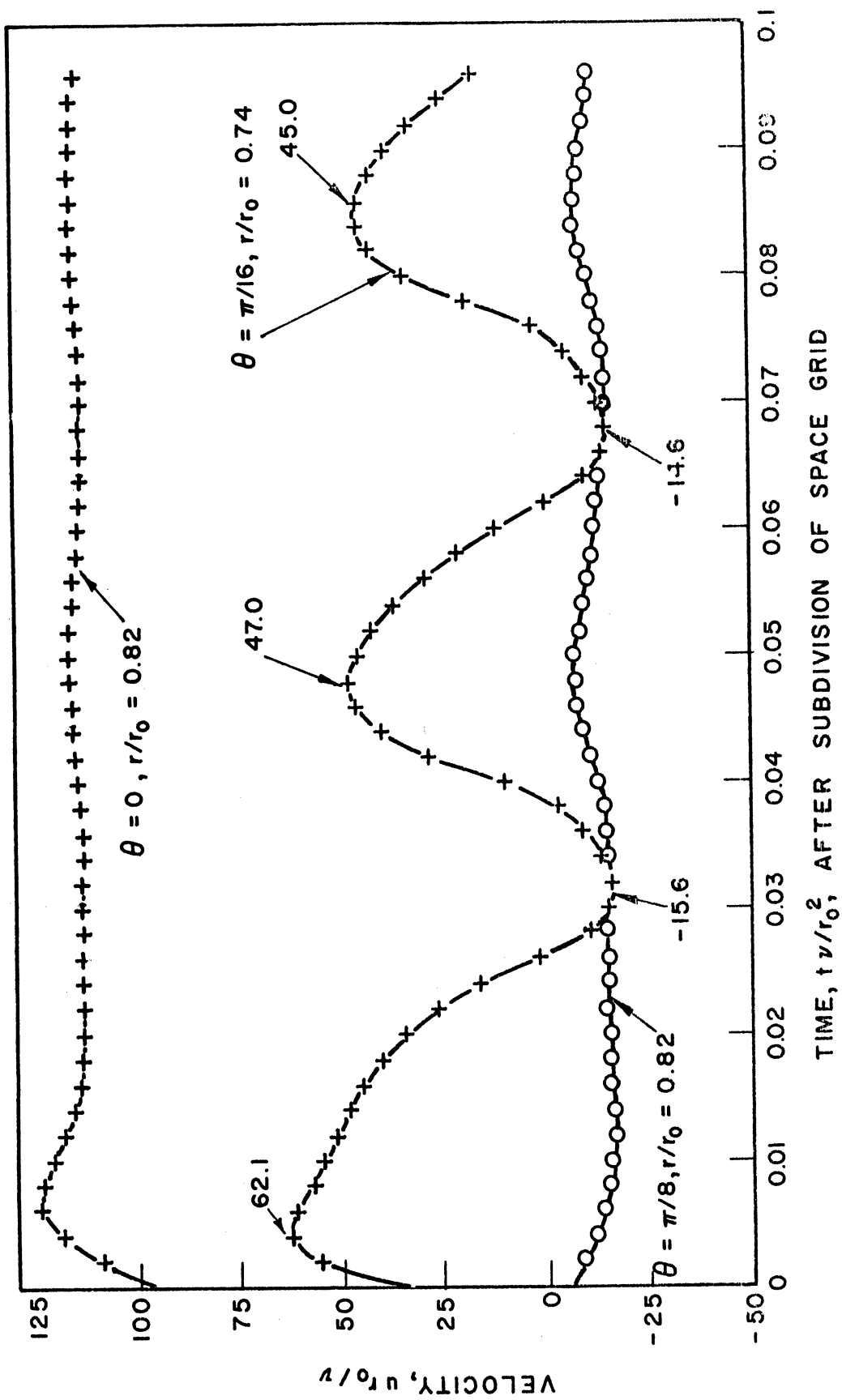


Figure 26. Velocity Fluctuations in Solution 4 (Pr = 10).

TABLE III

FLUCTUATIONS IN THE HEAT TRANSFER RESULTS OF SOLUTION 4

Angle,	$h\bar{D}/k$		
	maximum	minimum	deviation from the mean, %
0	15.728	15.508	0.7
$\pi/16$	28.040	26.736	2.4
$2\pi/16$	22.263	21.555	1.6
$3\pi/16$	20.498	20.019	1.2
$4\pi/16$	19.578	19.229	0.9
$5\pi/16$	18.907	18.643	0.7
$6\pi/16$	18.317	18.113	0.6
$7\pi/16$	17.741	17.581	0.5
$8\pi/16$	17.143	17.017	0.4
$9\pi/16$	16.497	16.398	0.3
$10\pi/16$	15.777	15.700	0.2
$11\pi/16$	14.933	14.874	0.2
$12\pi/16$	13.925	13.880	0.2
$13\pi/16$	12.692	12.662	0.1
$14\pi/16$	11.092	11.073	0.1
$15\pi/16$	8.716	8.694	0.1
$16\pi/16$	-15.727	-15.508	0.7
Overall	16.423	16.158	0.8

It is interesting to consider the cause of the fluctuation. No direct assumption of laminar flow has been made in this work and the time dependent form of the basic differential equations has been preserved. However, the basic equations were simplified to such a degree that it seems highly unlikely that the simplified equations are capable of describing turbulent flow. The fluctuations almost certainly do not correspond to the actual behavior of the fluid, but were induced by the particular method by which the grid was subdivided. This expectation is supported by the fact that no fluctuations occurred prior to subdivision of the grid. The large Prandtl number fluid practically stops near the bottom (and top) of the cylinder as indicated before. In doing so the fluid which was moving relatively rapidly near the boundary is forced out into the central region causing the boundary layer to thicken as shown earlier in Figures 22, 23, and 25. On subdivision of the grid it was assumed that the boundary layer was thin such that the result from the first grid served as an adequate approximation to the solution in the central region. This assumption is less satisfactory for the large Prandtl number solution than for the other solutions. The main difficulty is associated with the fact that the rays added on subdivision do not have a direct connection with the central region of the first grid. The connecting points of the added rays were established by linear interpolation using the values on adjacent rays. This procedure was adequate in all solutions except Solution 4 because the azimuthal gradients were relatively small. In Solution 4 the azimuthal gradients are much larger near $\Theta = 0$ as indicated before and linear interpolation is less accurate. Refer back to Figure 25. The two rays $\Theta = \pm \pi/16$ were added on subdivision. The points are those from the subdivided grid and the dotted lines in the central region were found by linear interpolation.

Notice that the velocity profile at $\theta = \pi/16$ seems to tend to collapse much like the profile at $\theta = \pi/8$. However, the velocity at the connection to the central region is artificially prevented from decreasing and is held constant at the value found by linear interpolation. This artificial restraint on the velocity at $\theta = \pi/16$ probably induced the fluctuation. The error due to this restraint is difficult to assess. It seems likely that the velocity profile at $\theta = \pi/16$ would be considerably different were it not restrained. However, the fluctuation has only a small influence on the temperature profile, and the fluctuation is confined to a small part of the grid. Therefore it seems likely that there is little error in the solution considered as a whole.

It should be mentioned that the fluctuation does not seem to be caused by instability of the difference equations as previously defined. The magnitudes of the independent variables are bounded and they seem to be approaching values independent of time.

It has been shown that the results of all the calculations for a Prandtl number of 0.7 are brought together by a choice of variables from analysis of a simplified model. As a final part of this section the generalized results will be compared with Martini and Churchill's (21) measurements. Martini and Churchill treated the two sides of the cylinder separately. That is, they calculated Nusselt, Grashof, and Prandtl groups based on the overall temperature drop and the fluid properties evaluated at the temperature of the side of the cylinder in question. There is a substantial difference in the Grashof numbers for the two sides of the cylinder in the experiments at large temperature differences. For example, in Martini and Churchill's experiment 15 the Grashof number on the cold

side is 19 times as large as that on the hot side. The model for this work is based on an assumption of a constant Grashof number as well as a small overall temperature drop so that it is expected that the agreement with experiment will decrease with increasing temperature difference. It has been pointed out before that the model is theoretically restricted to large Grashof numbers so agreement with experiment cannot be expected for very small temperature differences. It will be shown that these expectations are confirmed by comparison with the experiments insofar as the velocity profiles are concerned. However, the heat transfer results agree with the experiments more closely than might be expected.

Martini and Churchill's results were recalculated to conform to the model used in this work. The viscosity and the Prandtl number were taken as the average of the values at the hot and cold sides of the cylinder. The heat transfer coefficient was taken to be that reported by Martini and Churchill as the mean value for the hot side. Martini and Churchill found the mean heat transfer coefficient on the cold side to be consistently lower than that from the hot side by two to twenty per cent. This difference must be due to heat losses since from the definition the two mean values must be equal. The recalculated results are given in Table IV. It is interesting to notice that increasing the temperature difference for air does not necessarily produce an increase in the Grashof number as calculated here. For example, compare experiments 6 and 15. The overall temperature drop is increased from 20°C to 200°C yet the Grashof number is practically unchanged because the viscosity of the air and the mean temperature both increase.

A comparison of the calculations with the four experiments for which Martini and Churchill measured velocity profiles with the most

TABLE IV
PARAMETERS FROM THE RESULTS OF MARTINI AND CHURCHILL

Experiment	$\frac{\Delta T}{\text{OK}}$	T_i OK	$\sqrt{X10^4}$ ft ² /sec (avg.)	Gr X10 ⁻⁴	Pr	$(GrPr)^{\frac{1}{4}}$	$\frac{hD}{k}$ (mean-) (hot side)	$\frac{h_m}{k} \left(\frac{\alpha \sqrt{rQ}}{g\beta\Delta T} \right)^{\frac{1}{4}}$
3	24.0	326.7	2.03	33.1	0.701	22.0	7.47	0.1700
4	38.9	317.2	1.93	61.5	0.702	25.6	8.74	0.1705
5	25.7	302.6	1.78	49.7	0.707	24.3	6.83	0.1405
6	20.7	303.1	1.78	40.2	0.706	23.1	6.13	0.1325
7	55.72	293.2	1.67	12.89	0.705	17.34	3.95	0.1140
8	11.93	290.4	1.66	4.50	0.710	13.38	6.85	0.2550
9	51.9	319.7	1.97	78.0	0.699	27.2	7.06	0.1300
10	90.5	344.6	2.37	86.7	0.697	27.9	8.13	0.1455
11	75.2	335.8	2.15	90.0	0.698	28.1	8.41	0.1495
12	110.5	365.3	2.81	71.1	0.693	26.5	7.04	0.1330
13	111.2	364.3	2.80	72.3	0.695	26.6	7.33	0.1375
14	174.1	406.4	3.98	50.3	0.716	24.5	7.26	0.1482
15	203.7	425.5	4.55	43.1	0.720	23.6	7.32	0.1552

confidence is given in Figure 27 and Table V. The comparison is along the ray $\theta = 3\pi/2$ (in the middle of the cold side). On this ray the illumination of Martini and Churchill's dust particles was the most intense so the measurements should be the most accurate. Martini and Churchill made one experiment, experiment 8, at a very small Grashof number. The agreement between this work and that experiment as shown in Figure 27 is poor as expected. It should be mentioned that the measurement of the velocity profile by Martini and Churchill's method should be more accurate for small Grashof numbers than for large Grashof numbers because the boundary layer is thicker and the most important measurements are made at a greater distance from the wall. Glare from reflection of light at the boundary caused difficulty in Martini and Churchill's work. Since this difficulty should be the least pronounced for small Grashof numbers it seems unlikely that the deviation between experiment 8 and this work is due to experimental error. The deviation is due to inadequacy of the model as indicated earlier. The deviations between experiments 4, 9, and 10 (which are at larger Grashof numbers) and this work are much less, and the trend of increasing deviation with increasing temperature difference is followed as expected.

The temperature profiles of Figure 27 are all in good agreement with this work. It should be pointed out, however, that the agreement in the case of experiment 8 on the ray $\theta = 3\pi/2$ is not typical of the other rays. In experiment 8 the overall temperature drop was less than 2°C and Martini and Churchill obtained their heat transfer coefficients by measuring gradients in temperature near the boundary. Since they were measuring such small differences in the case of experiment 8, the data scatter more than in the other experiments, and the results are presumably somewhat less accurate.

TABLE V
COMPARISON WITH THE RESULTS OF MARTINI AND CHURCHILL

	Experiment 4	Experiment 8	Experiment 9	Experiment 10
Grashof Number $\frac{g \beta \Delta T r_0^3}{\nu^2}$	6.15×10^5	4.50×10^4	7.80×10^5	8.67×10^5
Prandtl Number	0.702	0.710	0.699	0.697
Rayleigh Number	4.32×10^5	3.20×10^4	5.45×10^5	6.04×10^5
$\Delta T, ^\circ\text{C}$	38.9	1.93	51.85	90.50
$\Delta T/T_i$	0.123	0.066	0.162	0.262
Agreement with velocity of this work	Excellent	Very Poor	Fair	Poor
The h Group, $\frac{h_m}{k} \left(\frac{\alpha \nu r_0}{g \beta \Delta T} \right)^{\frac{1}{4}}$	0.1705	0.255	0.1300	0.1455
Deviation in the heat transfer group from 0.178	-3%	44%	-26%	-18%

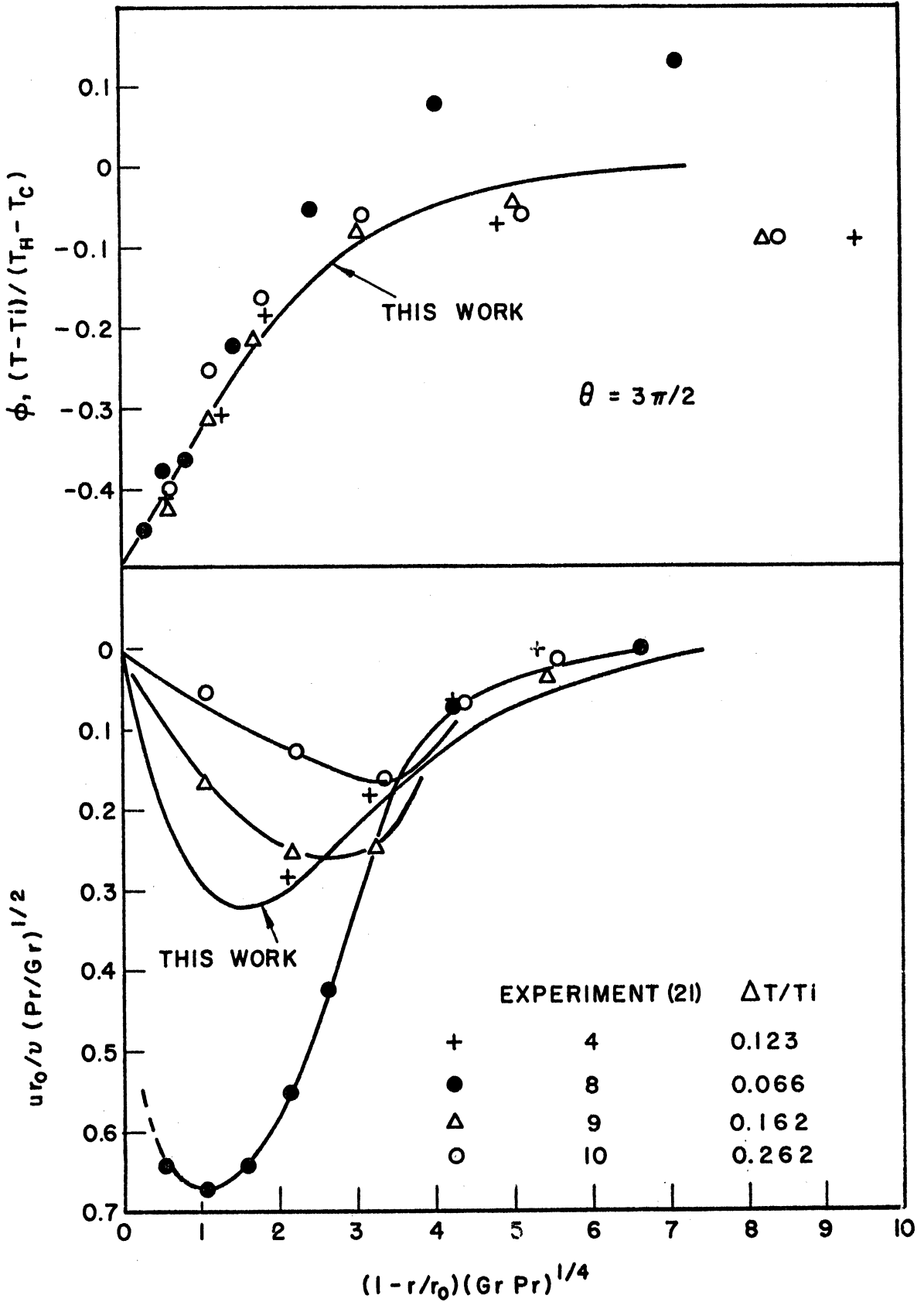


Figure 27. Comparison of Solution with Experiments for Several Grashof Numbers.

The final results of this work in terms of the mean heat transfer coefficient are presented in Figure 28 in comparison with all of Martini and Churchill's results. The mean heat transfer coefficients were calculated using Simpson's rule. Two lines are shown on the figure: the full line representing the results of this work for a Prandtl number of 0.7, and the dotted line representing Martini and Churchill's results. The results of this work for $Pr = 0.7$ can be expressed in a very concise form:

$$\frac{h_m D}{k} = 0.356 \left(\frac{g \beta \Delta T D_o^3}{\nu^2} \frac{c_p \mu}{k} \right)^{1/4}$$

or, the equivalent form:

$$\frac{h_m}{k} \left(\frac{\alpha \nu D_o}{g \beta \Delta T} \right)^{1/4} = 0.178$$

For a Prandtl number of 10 the constant 0.178 should be replaced by 0.163, a change in the constant of only 8.5 per cent.

Martini and Churchill's results seem to be in good agreement with this work although there are insufficient data at low Grashof numbers to establish the trend of their results there with certainty. The dotted line through Martini and Churchill's results falls 16 per cent lower than the results of this work. The physical situation is expected to give lower heat transfer results than the mathematical model. In the physical situation the wall temperature varies continuously between the two extremes. That is to say the discontinuous change in wall temperature of the mathematical model is only approximately realized in the physical situation. As a result the difference between the wall temperatures in the physical situation tends to be somewhat less than that of the mathematical model near the top and bottom of the cylinder.

The results are given in tabular form in Appendix C.

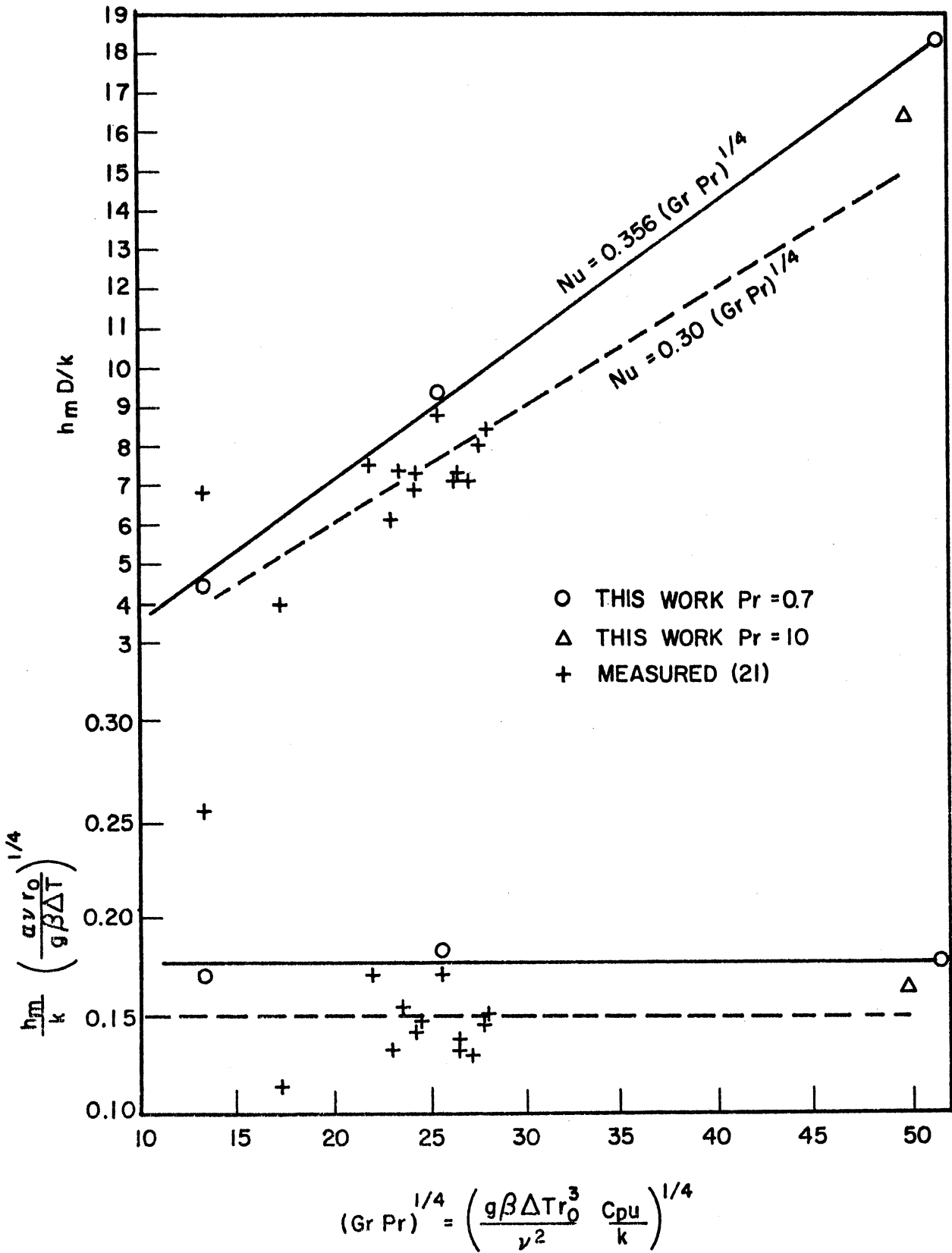


Figure 28. Comparison of Overall Heat Transfer Results.

VI. DISCUSSION OF APPLICATIONS TO RELATED PROBLEMS

The main difficulties in problems of the type considered in this work are associated with stability of the difference equations. It has been shown that difference equations which intuitively appear to be the best choice and which give the lowest truncation error are often useless because of instability. There are many possible choices of difference approximations to a given differential problem and finding a stable choice may be difficult. In seeking a useful system of difference equations the following comments may be helpful.

1. Stability criteria may be additive in a certain sense. In first attacking a complicated problem it is advisable to work with one term (other than the time derivative) at a time. If a stable scheme is found using a single term then other terms can be considered and the stability criteria may be additive in a certain sense. For example, three equations and their stability criteria are given below for differences of the types used in this work:

$$\frac{\partial u}{\partial t} = -a \frac{\partial u}{\partial x} \quad ; \quad \frac{u \Delta t}{\Delta x} \leq 1$$

$$\frac{\partial u}{\partial t} = a \frac{\partial^2 u}{\partial x^2} \quad ; \quad \frac{2a \Delta t}{(\Delta x)^2} \leq 1$$

$$\frac{\partial u}{\partial t} = -a \frac{\partial u}{\partial x} + a \frac{\partial^2 u}{\partial x^2} \quad ; \quad \frac{u \Delta t}{\Delta x} + \frac{2a \Delta t}{(\Delta x)^2} \leq 1$$

There is no assurance in general that the criteria will add as indicated above but this was found to be true in all cases of this work. An analysis of the complete equations should always be made but the simple approach is useful for eliminating differences which lead to unconditional instability.

2. It may be necessary to use different formulas in the approximation according to the sign of the coefficient of the derivative in the non-linear terms. This point was discussed in connection with the approximations used in this work.

3. Implicit schemes are ordinarily more strongly stable than explicit schemes. A partly implicit scheme is not necessarily difficult to solve at each time step. As an example consider the leading terms in the flat plate momentum balance using implicit differences:

$$\frac{u'_{j,l} - u_{j,l}}{\Delta \tau} = -u_{j,l} \frac{(u'_{j,l} - u'_{j-1,l})}{\Delta X} - v_{j,l} \frac{(u'_{j,l+1} - u'_{j,l})}{\Delta Y} + \dots \quad (70)$$

In the explicit scheme of calculation the stability depended on velocity as indicated by the terms $|U|/\Delta \tau/\Delta X$ and $|V|/\Delta \tau/\Delta Y$ in the criterion.

However, if implicit differences such as those of Equation 70 are used, the terms involving velocity no longer appear in the stability criterion.

Equation 70 can be solved directly. At $X = 0$ and $Y = \infty$ there is a

"corner" of the boundary ($Y = \infty$ is actually approximated by $Y = \text{constant}$ in the calculations by finite differences in accordance with the discussion

given earlier). U is always known on the boundary so that $U'_{j,l}$ for the interior point nearest the corner can be computed directly using $U'_{j-1,l}$

and $U'_{j,l+1}$ which are on the boundary. The other values of U then can be calculated in a sequence of decreasing l and increasing j since the U'

values needed will be known. The same remarks apply to the energy equations.

4. The conduction terms of the energy equation probably should be approximated using implicit differences for very low Prandtl number fluids. The conduction terms in the energy equation as treated in the cylinder problem contributed the terms $2\Delta\tau/(\text{Pr})(R\Delta\Theta)^2$ and $2\Delta\tau/(\text{Pr})(\Delta R)^2$ to the stability criterion. For very small Prandtl numbers a correspondingly small time step would be required to assure stability. If the conduction terms are approximated using implicit differences the time step is independent of the Prandtl number. Use of implicit differences here need not cause undue difficulty because methods of direct solution of the equations are highly developed. For example, Douglas and Peaceman (4) give a direct, partly implicit scheme in which the time step limitation is avoided.

5. In applying finite difference methods to the most general problems in fluid mechanics, there may be stability problems associated with the pressure or with the way the momentum and continuity equations are coupled. In this work the pressure distribution was known and assumed to be constant, and only the momentum balance in the direction of principal motion was taken into account. Such idealizations will not be admissible in many problems, and in such problems the momentum balances are coupled through the pressure or the continuity equation.

Consider as an example a fragment of a simple isothermal, one-dimensional problem in which the pressure distribution is variable. A similar example is given by Richtmyer (28). Pressure is replaced by ρRT in the equations where R is a gas law constant.

$$\frac{\partial u}{\partial x} = - \frac{RT}{\rho} \frac{\partial \rho}{\partial x} + \dots \quad (71)$$

$$\frac{\partial \rho}{\partial x} = - \rho \frac{\partial u}{\partial x} + \dots \quad (72)$$

Equations 71 and 72 could be approximated as indicated below

$$\frac{u'_j - u_j}{\Delta t} = \frac{-RT}{\rho \Delta X} (\rho_j - \rho_{j-1}) \quad (73)$$

$$\frac{\rho'_j - \rho_j}{\Delta t} = -\frac{\rho_j}{\Delta X} (u'_{j+1} - u'_j) \quad (74)$$

and the equations will be stable for a sufficiently small time step. This scheme is actually explicit in the procedure of calculation despite the fact that an implicit difference is used in the continuity equation. Equation 73 is used first to get the values of u' used in Equation 74. It does not seem to be possible to construct a stable, wholly explicit system of equations using simple differences involving only two time levels. Equations 73 and 74 are stable if the following inequality is satisfied:

$$\sqrt{RT} \frac{\Delta t}{\Delta X} \leq 1 \quad \text{or} \quad \sqrt{\frac{P}{\rho}} \frac{\Delta t}{\Delta X} \leq 1 \quad (75)$$

An indication of the relative magnitude of the time step can be obtained by considering dimensionless variables of the type used previously: $\tau = tV/L^2$, $U = uL/V$, $X = x/L$ where L is some length such as the radius in the cylinder problem. The maximum time step in terms of the same dimensionless time as was used in the cylinder problem is

$$\Delta \tau = \Delta(X/L) \sqrt{\frac{\rho V^2}{PL^2}}$$

which for the conditions and increment size of the cylinder problem is of the order of 10^{-8} . In the cylinder problem a time step of about 10^{-5} was used. It is concluded that coupling of the continuity and momentum equations through the pressure or density places a severe restriction on the time step if the equations are approximated in the way shown above.

Some additional work on the stability problem is needed before finite difference methods can be applied to the most general problems. It seems likely that to avoid the time step limitation either an implicit scheme or an explicit scheme involving three or more time levels will need be used.

There is a different approach to the more general problems which may be preferred to that discussed heretofore. The pressure can be eliminated between the momentum balance equations giving equations involving the components of the curl of the velocity (the vorticity transport equations). It appears that the stability problems associated with the vorticity equations would be much less difficult than those associated with the basic Navier-Stokes equations. For two-dimensional motion the vorticity has only a single non-zero component.

VII. SUMMARY OF RESULTS

The principal results and conclusions are given below.

1. The system of partial differential equations governing fluid motion and heat transfer were solved by finite difference methods for two physical situations: the classical case of the isothermal vertical flat plate, and the case of the fluid confined by an infinite horizontal cylinder with the vertical halves of the walls at different uniform temperatures. The flat plate problem was solved for a Prandtl number of 0.733 to correspond to prior analytical solutions. The cylinder problem was solved for three different values of the Grashof number with the Prandtl number held constant at 0.7. An additional solution to the cylinder problem was obtained for a Prandtl number of 10. In both problems the most general equations were simplified to correspond to laminar boundary layer flow.

2. The initial value (time dependent) approach to the problems was used thereby obtaining both the transient and steady state solutions in one operation. This approach seems to be preferable to methods in which steady state is assumed at the outset.

3. In problems of laminar boundary layer flow explicit difference equations can be developed which will be stable for sufficiently small time increments providing different equations are used in different parts of the space-time grid depending on the sign of the velocity components.

4. The solution of the difference problems required very little computation and very little computer storage capacity by modern standards.

5. The solution of the flat plate problem is in good agreement with the short time analytical solution for conduction alone, and with the steady state solution of Ostrach. The steady state heat transfer results for a Prandtl number of 0.733 are:

$$\frac{h}{k} \left(\frac{\nu^2 \gamma}{g\beta \Delta T} \right)^{1/4} = 0.3653$$

The constant, 0.3653, is only 2 per cent larger than that obtained by Ostrach.

6. The solutions to the cylinder problem are in good agreement with the measurements of Martini and Churchill except at very low Grashof numbers where the idealizations of the mathematical model are inadequate. The heat transfer results for a Prandtl number of 0.7 are:

$$\frac{h_{cm}}{k} \left(\frac{\alpha \nu D_0}{g\beta \Delta T} \right)^{1/4} = 0.178$$

For a Prandtl number of 10 the constant, 0.178, should be replaced by 0.163, a change in the constant of only 8.5 per cent.

7. Finite difference methods apply to a great variety of problems which resist ordinary methods of analysis. The methods are well suited for testing the idealizations often used in fluid mechanics. It seems certain that the most difficult problems in fluid mechanics and heat transfer will eventually be solved by finite difference methods. This work constitutes a step in that direction.

REFERENCES

1. Batchelor, G. K., "Heat Transfer by Free Convection Across a Closed Cavity Between Vertical Boundaries at Different Temperatures," Quart. Appl. Math., 12, 209-33 (1954).
2. Birkhoff, G., "Hydrodynamics," Dover Publications, Inc., New York (1955).
3. de Graaf, J. G. A. and van der Held, E. F. M., "The Relation Between the Heat Transfer and the Convection Phenomena in Enclosed Plane Gas Layers," Appl. Sci. Res., A3, 393 (1954).
4. Douglas J., and Peaceman, D. W., "Numerical Solution of Two Dimensional Heat Flow Problems," Am. Inst. Chem. Engrs. J., 1, 505 (1955).
5. Eckert, E. R. G. and Diaguila, A. J., "Experimental Investigation of Free Convection Heat Transfer in Vertical Tube at Large Grashof Numbers," Natl. Advisory Comm. Aeronaut. Report 1211 (1955).
6. Foster, C. V., "Heat Transfer by Free Convection to Fluids Contained in Vertical Tubes," Ph.D. Thesis, University of Delaware (1953).
7. Fujii, T., "Mathematical Analysis of Transfer from Vertical Flat Plate by Free Convection," Trans. Jap. Soc. Mech. Engrs., 24, 957-72 (1958).
8. Globe S., and Dropkin, D., "Natural Convection Heat Transfer in Liquids Confined by Two Horizontal Plates and Heated from Below," J. Heat Transfer, 81, 24 (1959).
9. Hartnett, J. P. and Welsh, W. E., "Experimental Studies of Free Convection Heat Transfer in a Vertical Tube with Uniform Wall Heat Flux," Am. Soc. Mech. Engrs. Paper 56-A-113 (1956).
10. Hellums, J. D. and Churchill, S. W., "Dimensional Analysis and Natural Convection," Presented at the Joint Am. Inst. Chem. Engrs.-Am. Soc. Mech. Engrs. Heat Trans. Conf., August, 1960.
11. Herman, R., "Heat Transfer by Free Convection from Horizontal Cylinders in Diatomic Gases," V. D. I. Forschungsheft, No. 379 (1936). Translation from the German: Natl. Advisory Comm. Aeronaut. Tech. Memo. 1366 (1954).
12. Herman, R., "Warmeubergang bei freier Konvektion," Physik Zeitschr., 33, 425 (1932).
13. Illingworth, C. R., "Unsteady Laminar Flow of Gas Near an Infinite Flat Plate," Proc. Cambridge Phil. Soc., 46, 603 (1950).
14. Jakob, M., "Heat Transfer," Volume 1, John Wiley and Sons, New York, pp. 443-450 (1949).

15. Jodlbauer, K., "The Temperature and Velocity Fields in the Vicinity of a Tube Under Free Convection Conditions," Forschung auf dem Gebiete des Ingenieurwesens, 4, 157 (1933).
16. John, Fritz, "On the Integration of Parabolic Equations by Difference Methods," Comm. Pure and Appl. Math., 5, 155 (1952).
17. Klei, H. E., "A Study of Unsteady State Natural Convection for a Vertical Plate," B. S. Thesis, MIT, June, 1957.
18. Lighthill, M. J., "Theoretical Considerations on Free Convection in Tubes," Quart. J. Mechanics Appl. Math., 6, 398-439 (1953).
19. Lorenz, L., "The Conductivity of Metals for Heat and Electricity," Annalen d. Physik, u. Chemie, 13, 582 (1881).
20. Martin, B. W., "Free Convection in an Open Thermosyphon, with Special Reference to Turbulent Flow," Proc. Royal Soc. (London) A231 502 (1955).
21. Martini, W. R. and S. W. Churchill, "Natural Convection inside a Horizontal Cylinder," Am. Inst. Chem. Engrs. J., 6, 251 (1960).
22. Merk, H. J. and Prins, J. A., "Thermal Convection in Laminar Boundary Layers," Appl. Sci. Research, A4, 11-24 195-224, 207-221 (1954).
23. Morgan, G. E. and Warner, W. H., "On Heat Transfer in Laminar Boundary Layers at High Prandtl Numbers," J. Aero. Sciences, 23, 937 (1956).
24. Mull, W. and Reiher, J., as reported in Reference 14, pp. 535-539.
25. Ostroumov, G. A., "Free Convection Under the Conditions of the Internal Problem," State Publishing House, Technico-Theoretical Literature, Moscow-Leningrad (1952). Translation from the Russian: Natl. Advisory Comm. Aeronaut. Tech. Memo. 1407 (1958).
26. Ostrach, S., "An Analysis of Laminar Free-Convection Flow and Heat Transfer About a Flat Plate Parallel to the Direction of the Generation Body Force," Natl. Advisory Comm. Aeronaut. Tech. Report 1111 (1953).
27. Poots, G., "Laminar Free Convection in Enclosed Plane Gas Layers," Quart. J. Mech. and Appl. Math., 11, 257 (1958).
28. Richtmyer, R. D., "Difference Methods for Initial-Value Problems," Interscience Publishers, Inc., New York (1957).
29. Schlichting, H., "Boundary Layer Theory," Pergamon Press, New York, 278-279 (1955).
30. Schuh, H., "Temperaturgrenzschichten," Gottinger Monographien B 6 (1946). (See Reference 29).
31. Schmidt, E. and Beckmann, W., "Das Temperature-und Geschwindigkeitsfeld vor einer Warme abgeben senkrechter Platte bei natuerlicher Konvektion," Techn. Mech. u. Thermodynamik, 1, 341, 391 (1930).

32. Schmidt, I. E. and Silveston, P. L., "Natural Convection in Horizontal Liquid Layers," Preprint 24 of paper presented at Am. Inst. Chem. Engrs.-Am. Soc. Mech. Engrs. Heat Transfer Conference (1958).
33. Siegel, R., "Analysis of Laminar and Turbulent Free Convection from a Smooth Vertical Plate with Uniform Heat Dissipation per Unit Surface Area," G. E. Report R546L89, 1954.
34. Siegel, Robert, "Transient Free Convection from a Vertical Flat Plate," Trans. Am. Soc. Mech. Eng., 80, 347 (1958).
35. Sparrow, E. M., "Free Convection with Variable Properties and Variable Wall Temperature," Ph.D. Thesis, 1956, Harvard University, Cambridge, Mass.
36. Sparrow, E. M. and Gregg, J. L., "Details of Exact Low Prandtl Number Boundary-Layer Solutions for Forced and for Free Convection, Nat'l. Advisory Comm. Aeronaut. Memo 2-27-59E (1959).
37. Sparrow, E. M. and Gregg, J. L., "Laminar Free Convection from a Vertical Plate with Uniform Surface Heat Flux," Trans. Am. Soc. Mech. Engrs., 78, 435-440 (1956).
38. Sparrow, E. M. and Gregg, J. L., "Similar Solutions for Free Convection from a Nonisothermal Vertical Plate," Trans. Am. Soc. Mech. Engrs., 80, 379 (1958).
39. Sparrow, E. M. and Gregg, J. L., "The Variable Fluid-Property Problem in Free Convection," Trans. Am. Soc. Mech. Engrs., 80, 879 (1958).
40. Sugawara, S. and Michiyoshi, I., "Effects of Prandtl Number of Heat Transfer by Natural Convection," Proc. Third Japan Nat. Cong. Appl. Mech., 315 (1953).
41. Sugawara, S. and Michiyoshi, I., "The Heat Transfer by Natural Convection in the Unsteady State on a Vertical Flat Wall," Proc. Third Japan Nat. Cong. Appl. Mech., 501 (1951).
42. Zhukhovitskii, E. M., "Free Stationary Convection in an Infinite Horizontal Tube," Zhur. Tech. Fiz., 22, pp. 832-835 (1952). (See Reference 25).

APPENDIX A

ANALYSIS FOR THE CYLINDER

Equations 25a, 25c, and 25d as given previously are

$$\begin{aligned} \frac{\partial U}{\partial \tau} + \frac{U}{R} \frac{\partial U}{\partial \Theta} + V \frac{\partial U}{\partial R} &= G_{\pi} \phi \sin \Theta - \frac{1}{R} \frac{\partial P'}{\partial \Theta} \\ &+ \frac{\partial^2 U}{\partial R^2} + \frac{1}{R} \frac{\partial U}{\partial R} - \frac{U}{R^2} - \frac{VU}{R} + \frac{1}{R^2} \frac{\partial^2 U}{\partial \Theta^2} + \frac{2}{R^2} \frac{\partial V}{\partial \Theta} \end{aligned} \quad (25a)$$

$$\frac{\partial \phi}{\partial \tau} + \frac{U}{R} \frac{\partial \phi}{\partial \Theta} + V \frac{\partial \phi}{\partial R} = \frac{\alpha}{V} \left[\frac{\partial^2 \phi}{\partial R^2} + \frac{1}{R} \frac{\partial \phi}{\partial R} + \frac{1}{R^2} \frac{\partial^2 \phi}{\partial \Theta^2} \right] \quad (25b)$$

$$\frac{\partial(RV)}{\partial R} + \frac{\partial U}{\partial \Theta} = 0 \quad (25d)$$

A new set of variables can be introduced as indicated below

$$\begin{aligned} U' &= U (P_{\pi}/G_{\pi})^{1/2} & ; & & V' &= V (P_{\pi}^3/G_{\pi})^{1/4} \\ Y &= (1-R)(G_{\pi} P_{\pi})^{1/4} & ; & & \tau' &= \tau (G_{\pi}/P_{\pi})^{1/2} \end{aligned}$$

In terms of these variables the equations become:

$$\begin{aligned} \frac{1}{P_{\pi}} \left[\frac{\partial U'}{\partial \tau'} + \frac{(G_{\pi} P_{\pi})^{1/4}}{(G_{\pi} P_{\pi})^{1/4} - Y} U' \frac{\partial U'}{\partial \Theta} - V' \frac{\partial U'}{\partial Y} + \frac{V' U'}{(G_{\pi} P_{\pi})^{1/4} - Y} \right] &= \phi \sin \Theta \\ + \frac{1}{(G_{\pi})^{3/4}} \left[\frac{(P_{\pi})^{1/4}}{(G_{\pi} P_{\pi})^{1/4} - Y} \right] \frac{\partial P'}{\partial \Theta} + \frac{\partial^2 U'}{\partial Y^2} - \frac{1}{(G_{\pi} P_{\pi})^{1/4} - Y} \frac{\partial U'}{\partial Y} \\ - \left[\frac{1}{(G_{\pi} P_{\pi})^{1/4} - Y} \right]^2 \frac{U'}{(Y')^2} + \left[\frac{1}{(G_{\pi} P_{\pi})^{1/4} - Y} \right]^2 \frac{\partial^2 U'}{\partial \Theta^2} + \frac{2}{(G_{\pi} P_{\pi})^{1/4}} \left[\frac{1}{(G_{\pi} P_{\pi})^{1/4} - Y} \right]^2 \frac{\partial V'}{\partial \Theta} \end{aligned}$$

$$\frac{\partial \phi}{\partial \zeta} + \frac{(GrPr)^{1/4}}{(GrPr)^{1/4} - \gamma} U' \frac{\partial \phi}{\partial \Theta} - v' \frac{\partial \phi}{\partial \gamma} = \frac{\partial^2 \phi}{\partial \gamma^2}$$

$$-\left[\frac{1}{(GrPr)^{1/4} - \gamma} \right] \frac{\partial \phi}{\partial \gamma} + \left[\frac{1}{(GrPr)^{1/4} - \gamma} \right]^2 \frac{\partial^2 \phi}{\partial \Theta^2}$$

$$-\frac{1}{(GrPr)^{1/4}} \frac{\partial}{\partial \gamma} [v'(GrPr)^{1/4} - v'\gamma] + \frac{\partial U'}{\partial \Theta} = 0$$

From inspection of these equations it is evident that the idealizations made in developing the system of equations used in the calculations are valid only for large Grashof numbers. Suppose that Pr is bounded away from zero which is valid from physical considerations. Then in the asymptotic case as $Gr \rightarrow \infty$, $GrPr \rightarrow \infty$, and the equations can be simplified by dropping the terms corresponding to $\partial P'/\partial \Theta$, VU/R , U/R^2 , $(1/R)\partial U/\partial R$, $(2/R^2)(\partial V/\partial \Theta)$, $(1/R^2)(\partial^2 U/\partial \Theta^2)$, $(1/R)(\partial \phi/\partial R)$ and $(1/R^2)(\partial^2 \phi/\partial \Theta^2)$. Other simplifications follow from the fact that $0 \leq Y \leq 1$ so that Y may be neglected beside $(GrPr)^{1/4}$. It should be mentioned that in this procedure of dropping terms it is assumed that as the coefficient of a term in the differential equation tends to zero, the effect of the term on the solution also tends to zero. This assumption cannot be justified from the mathematical standpoint although it has been used successfully in boundary layer theory for many years. Birkhoff (2) gives a good discussion of this difficulty.

The simplified equations are given below.

$$\frac{1}{Pr} \left[\frac{\partial U'}{\partial Z} + U' \frac{\partial U'}{\partial \Theta} - v' \frac{\partial U'}{\partial Y} \right] = \phi \sin \Theta + \frac{\partial^2 U'}{\partial Y^2}$$

$$\frac{\partial \phi}{\partial Z} + U' \frac{\partial \phi}{\partial \Theta} - v' \frac{\partial \phi}{\partial Y} = \frac{\partial^2 \phi}{\partial Y^2}$$

$$- \frac{\partial v'}{\partial Y} + \frac{\partial U'}{\partial \Theta} = 0$$

The variables in these equations are the same as those used in the analysis of a highly simplified model given in Part IIC. The functional dependence is given below in terms of the original variables of the problem.

$$\frac{u \lambda_0}{V} = (Gr/P_r^2)^{1/2} f_1 \left[\Theta, (1 - \lambda/\lambda_0)(Gr/P_r)^{1/4}, P_r \right]$$

$$\frac{v \lambda_0}{V} = (Gr/P_r^3)^{1/4} f_2 \left[\Theta, (1 - \lambda/\lambda_0)(Gr/P_r)^{1/4}, P_r \right]$$

$$\phi = f_3 \left[\Theta, (1 - \lambda/\lambda_0)(Gr/P_r)^{1/4}, P_r \right]$$

$$\frac{h \lambda_0}{K} = (Gr/P_r)^{1/4} f_4 \left[\Theta, P_r \right]$$

The Grashof number has been taken into account in the analysis. However, the Prandtl number still appears as a parameter in the problem. Notice that the importance of the inertial terms relative to the viscous terms in the momentum balance decreases with increasing Prandtl number. In the limit as $Pr \rightarrow \infty$ the inertial terms may be dropped and the problem is reduced to the form of that of the analysis of a highly simplified model given in Part IIC.

APPENDIX B

RESULTS FOR THE FLAT PLATE

The transient results for the flat plate are given in Table VI in terms of the variables used in the calculations. These results are for the line $X = 100$ for the 40 by 40 grid. To put the results in terms of the composite variables the velocity parallel to the plate as well as the time step number need only be divided by 10. The velocity normal to the plate should be multiplied by $\sqrt{10}$. The composite distance variables corresponding to the values of ℓ are given in Table VII. Where there is a blank space in Table VI (such as all the V values for the first 120 time steps) the variable is less than 10^{-10} .

Table VII gives the steady state solution after the Y coordinate (corresponding to $Y = \infty$) was extended and 240 additional time steps were carried out. Comparison of the steady state values in Table VI with those of Table VII shows the influence of the Y coordinate.

Table VIII gives transient values of the heat transfer group along with Ostrach's result (26).

The symbol E is used in the tables to denote an exponent of 10. For example $22.5E-02$ is the same as 0.225.

TABLE VI. TRANSIENT RESULTS FOR THE FLAT PLATE

$\frac{D}{L} = 2$	$\frac{D}{L} = 3$	$\frac{D}{L} = 4$	$\frac{D}{L} = 5$	$\frac{D}{L} = 6$	$\frac{D}{L} = 7$	$\frac{D}{L} = 8$	$\frac{D}{L} = 9$	$\frac{D}{L} = 12$	$\frac{D}{L} = 16$	$\frac{D}{L} = 20$	$\frac{D}{L} = 24$	$\frac{D}{L} = 28$	$\frac{D}{L} = 32$	$\frac{D}{L} = 32$	$\frac{D}{L} = 32$	$\frac{D}{L} = 32$
1	33.200E-03	19.102E-03	83.083E-04	32.369E-04	11.911E-04	42.380E-05	50.682E-06	15.244E-04	50.378E-07	29.789E-11	38.156E-07	24.599E-09	38.026E-06	19.060E-07		
2	61.396E-03	43.176E-03	22.120E-03	98.925E-04	40.999E-04	16.192E-04	61.885E-05	61.760E-05	59.490E-04	22.674E-05	52.703E-04	53.125E-05	38.026E-06	31.181E-05		
3	87.925E-03	70.173E-03	40.256E-03	98.925E-04	40.999E-04	38.773E-04	15.974E-04	25.974E-04	18.618E-02	37.223E-03	62.911E-03	13.148E-03	23.209E-04	40.419E-04		
4	11.234E-02	98.274E-03	20.144E-03	32.932E-03	16.094E-03	73.900E-04	15.513E-03	42.119E-02	15.710E-01	21.445E-02	23.715E-02	73.908E-03	19.441E-03	19.317E-03		
5	15.659E-02	12.677E-02	84.846E-03	48.527E-03	25.219E-03	73.900E-04	15.513E-03	42.119E-02	15.710E-01	21.445E-02	23.715E-02	73.908E-03	19.441E-03	19.317E-03		
6	17.687E-02	15.525E-02	10.983E-02	66.513E-03	32.080E-02	57.226E-02	15.513E-03	42.119E-02	15.710E-01	21.445E-02	23.715E-02	73.908E-03	19.441E-03	19.317E-03		
7	19.614E-02	18.349E-02	13.593E-02	86.790E-02	73.079E-02	57.226E-02	15.513E-03	42.119E-02	15.710E-01	21.445E-02	23.715E-02	73.908E-03	19.441E-03	19.317E-03		
8	21.455E-02	21.136E-02	11.535E-02	86.790E-02	73.079E-02	57.226E-02	15.513E-03	42.119E-02	15.710E-01	21.445E-02	23.715E-02	73.908E-03	19.441E-03	19.317E-03		
9	26.724E-02	16.194E-02	11.535E-02	86.790E-02	73.079E-02	57.226E-02	15.513E-03	42.119E-02	15.710E-01	21.445E-02	23.715E-02	73.908E-03	19.441E-03	19.317E-03		
10	30.760E-02	17.793E-01	21.637E-01	27.329E-01	28.172E-01	18.755E-01	21.637E-01	27.329E-01	28.172E-01	18.755E-01	21.637E-01	27.329E-01	28.172E-01	18.755E-01		
120	11.503E-01	19.522E-01	30.552E-01	34.888E-01	37.078E-01	41.522E-01	45.210E-01	47.522E-01	50.367E-01	53.111E-01	55.616E-01	58.108E-01	60.622E-01	63.155E-01		
160	15.041E-01	27.235E-01	40.403E-01	47.522E-01	50.367E-01	53.111E-01	55.616E-01	58.108E-01	60.622E-01	63.155E-01	65.669E-01	68.161E-01	70.653E-01	73.145E-01		
200	17.042E-01	30.376E-01	44.403E-01	51.592E-01	54.422E-01	57.256E-01	60.189E-01	63.122E-01	66.055E-01	69.008E-01	71.971E-01	74.934E-01	77.897E-01	80.860E-01		
280	17.573E-01	31.341E-01	45.729E-01	53.157E-01	56.090E-01	59.023E-01	62.008E-01	65.041E-01	68.126E-01	71.261E-01	74.446E-01	77.681E-01	80.966E-01	84.301E-01		
320	17.273E-01	30.726E-01	44.705E-01	52.157E-01	55.157E-01	58.157E-01	61.157E-01	64.157E-01	67.157E-01	70.157E-01	73.157E-01	76.157E-01	79.157E-01	82.157E-01		
360	17.169E-01	30.538E-01	44.422E-01	51.592E-01	54.422E-01	57.256E-01	60.189E-01	63.122E-01	66.055E-01	69.008E-01	71.971E-01	74.934E-01	77.897E-01	80.860E-01		
400	17.154E-01	30.509E-01	44.422E-01	51.592E-01	54.422E-01	57.256E-01	60.189E-01	63.122E-01	66.055E-01	69.008E-01	71.971E-01	74.934E-01	77.897E-01	80.860E-01		
480	17.137E-01	30.476E-01	44.377E-01	51.547E-01	54.377E-01	57.211E-01	60.144E-01	63.067E-01	66.000E-01	68.923E-01	71.846E-01	74.769E-01	77.692E-01	80.615E-01		
560	17.130E-01	30.463E-01	44.363E-01	51.540E-01	54.363E-01	57.204E-01	60.137E-01	63.060E-01	66.000E-01	68.923E-01	71.846E-01	74.769E-01	77.692E-01	80.615E-01		
600	17.127E-01	30.457E-01	44.356E-01	51.536E-01	54.356E-01	57.198E-01	60.131E-01	63.054E-01	66.000E-01	68.923E-01	71.846E-01	74.769E-01	77.692E-01	80.615E-01		
160	18.447E-07	69.513E-07	18.015E-06	38.817E-06	73.567E-06	12.570E-05	19.732E-05	28.783E-05	46.841E-05	78.783E-05	125.825E-05	203.132E-05	311.699E-05	471.780E-05		
200	71.477E-05	23.427E-04	51.859E-04	95.988E-04	15.868E-03	24.181E-03	34.565E-03	46.841E-03	66.841E-03	92.841E-03	125.825E-03	171.010E-03	232.808E-03	311.699E-03		
280	37.232E-04	11.863E-03	23.660E-03	39.352E-03	58.446E-03	89.645E-03	131.118E-03	197.510E-03	292.808E-03	425.808E-03	625.808E-03	900.808E-03	1275.808E-03	1775.808E-03		
320	32.667E-04	97.308E-04	19.254E-03	31.602E-03	46.169E-03	63.477E-03	82.198E-03	102.217E-03	125.825E-03	153.867E-03	186.418E-03	224.970E-03	268.522E-03	317.074E-03		
400	32.360E-04	97.501E-04	19.110E-03	31.402E-03	46.027E-03	63.215E-03	81.942E-03	101.952E-03	124.356E-03	151.369E-03	183.382E-03	220.395E-03	262.408E-03	309.421E-03		
480	32.119E-04	95.785E-04	18.969E-03	31.173E-03	45.891E-03	62.767E-03	81.669E-03	101.679E-03	123.083E-03	149.096E-03	180.109E-03	215.122E-03	250.135E-03	295.148E-03		
560	31.998E-04	95.431E-04	18.901E-03	31.063E-03	45.736E-03	62.554E-03	81.561E-03	101.571E-03	122.887E-03	148.900E-03	179.913E-03	214.926E-03	249.939E-03	294.952E-03		
600	31.932E-04	95.238E-04	18.863E-03	31.002E-03	45.647E-03	62.435E-03	81.468E-03	101.478E-03	122.700E-03	148.812E-03	179.825E-03	214.838E-03	249.851E-03	294.864E-03		
160	18.447E-07	69.513E-07	18.015E-06	38.817E-06	73.567E-06	12.570E-05	19.732E-05	28.783E-05	46.841E-05	78.783E-05	125.825E-05	203.132E-05	311.699E-05	471.780E-05		
200	71.477E-05	23.427E-04	51.859E-04	95.988E-04	15.868E-03	24.181E-03	34.565E-03	46.841E-03	66.841E-03	92.841E-03	125.825E-03	171.010E-03	232.808E-03	311.699E-03		
280	37.232E-04	11.863E-03	23.660E-03	39.352E-03	58.446E-03	89.645E-03	131.118E-03	197.510E-03	292.808E-03	425.808E-03	625.808E-03	900.808E-03	1275.808E-03	1775.808E-03		
320	32.667E-04	97.308E-04	19.254E-03	31.602E-03	46.169E-03	63.477E-03	82.198E-03	102.217E-03	125.825E-03	153.867E-03	186.418E-03	224.970E-03	268.522E-03	317.074E-03		
400	32.360E-04	97.501E-04	19.110E-03	31.402E-03	46.027E-03	63.215E-03	81.942E-03	101.952E-03	124.356E-03	151.369E-03	183.382E-03	220.395E-03	262.408E-03	309.421E-03		
480	32.119E-04	95.785E-04	18.969E-03	31.173E-03	45.891E-03	62.767E-03	81.669E-03	101.679E-03	123.083E-03	149.096E-03	180.109E-03	215.122E-03	250.135E-03	295.148E-03		
560	31.998E-04	95.431E-04	18.901E-03	31.063E-03	45.736E-03	62.554E-03	81.561E-03	101.571E-03	122.887E-03	148.900E-03	179.913E-03	214.926E-03	249.939E-03	294.952E-03		
600	31.932E-04	95.238E-04	18.863E-03	31.002E-03	45.647E-03	62.435E-03	81.468E-03	101.478E-03	122.700E-03	148.812E-03	179.825E-03	214.838E-03	249.851E-03	294.864E-03		
160	18.447E-07	69.513E-07	18.015E-06	38.817E-06	73.567E-06	12.570E-05	19.732E-05	28.783E-05	46.841E-05	78.783E-05	125.825E-05	203.132E-05	311.699E-05	471.780E-05		
200	71.477E-05	23.427E-04	51.859E-04	95.988E-04	15.868E-03	24.181E-03	34.565E-03	46.841E-03	66.841E-03	92.841E-03	125.825E-03	171.010E-03	232.808E-03	311.699E-03		
280	37.232E-04	11.863E-03	23.660E-03	39.352E-03	58.446E-03	89.645E-03	131.118E-03	197.510E-03	292.808E-03	425.808E-03	625.808E-03	900.808E-03	1275.808E-03	1775.808E-03		
320	32.667E-04	97.308E-04	19.254E-03	31.602E-03	46.169E-03	63.477E-03	82.198E-03	102.217E-03	125.825E-03	153.867E-03	186.418E-03	224.970E-03	268.522E-03	317.074E-03		
400	32.360E-04	97.501E-04	19.110E-03	31.402E-03	46.027E-03	63.215E-03	81.942E-03	101.952E-03	124.356E-03	151.369E-03	183.382E-03	220.395E-03	262.408E-03	309.421E-03		
480	32.119E-04	95.785E-04	18.969E-03	31.173E-03	45.891E-03	62.767E-03	81.669E-03	101.679E-03	123.083E-03	149.096E-03	180.109E-03	215.122E-03	250.135E-03	295.148E-03		
560	31.998E-04	95.431E-04	18.901E-03	31.063E-03	45.736E-03	62.554E-03	81.561E-03	101.571E-03	122.887E-03	148.900E-03	179.913E-03	214.926E-03	249.939E-03	294.952E-03		
600	31.932E-04	95.238E-04	18.863E-03	31.002E-03	45.647E-03	62.435E-03	81.468E-03	101.478E-03	122.700E-03	148.812E-03	179.825E-03	214.838E-03	249.851E-03	294.864E-03		
160	18.447E-07	69.513E-07	18.015E-06	38.817E-06	73.567E-06	12.570E-05	19.732E-05	28.783E-05	46.841E-05	78.783E-05	125.825E-05	203.132E-05	311.699E-05	471.780E-05		
200	71.477E-05	23.427E-04	51.859E-04	95.988E-04	15.868E-03	24.181E-03	34.565E-03	46.841E-03	66.841E-03	92.841E-03	125.825E-03	171.010E-03	232.808E-03	311.699E-03		
280	37.232E-04	11.863E-03	23.660E-03	39.352E-03	58.446E-03	89.645E-03	131.118E-03	197.510E-03	292.808E-03	425.808E-03	625.808E-03	900.808E-03	1275.808E-03	1775.808E-03		
320																

TABLE VII
 THE STEADY STATE FLAT PLATE SOLUTION AFTER
 EXTENSION OF THE Y COORDINATE

l	$y \left(\frac{g\beta\Delta T}{\nu^2 x} \right)^{1/4}$	$\frac{u}{(xg\beta\Delta T)^{1/2}}$	$v \left(\frac{x}{\nu^2 g\beta\Delta T} \right)^{1/4}$	$(T - T_i) / (T_w - T_i)$
2	20.271E-02	17.127E-02	-10.094E-03	92.594E-02
3	40.542E-02	30.457E-02	-30.107E-03	85.210E-02
4	60.813E-02	40.349E-02	-59.633E-03	77.895E-02
5	81.084E-02	47.199E-02	-98.009E-03	70.714E-02
6	10.135E-01	51.427E-02	-14.431E-02	63.742E-02
7	12.162E-01	53.460E-02	-19.739E-02	57.054E-02
8	14.189E-01	53.713E-02	-25.591E-02	50.719E-02
9	16.216E-01	52.579E-02	-31.847E-02	44.794E-02
10	18.243E-01	50.412E-02	-38.361E-02	39.319E-02
11	20.271E-01	47.521E-02	-44.995E-02	34.319E-02
12	22.298E-01	44.166E-02	-51.624E-02	29.799E-02
13	24.325E-01	40.559E-02	-58.137E-02	25.754E-02
14	26.352E-01	36.867E-02	-64.442E-02	22.166E-02
15	28.379E-01	33.214E-02	-70.468E-02	19.007E-02
16	30.406E-01	29.692E-02	-76.160E-02	16.245E-02
17	32.433E-01	26.363E-02	-81.481E-02	13.844E-02
18	34.460E-01	23.264E-02	-86.410E-02	11.768E-02
19	36.487E-01	20.418E-02	-90.938E-02	99.818E-03
20	38.514E-01	17.830E-02	-95.064E-02	84.495E-03
21	40.542E-01	15.500E-02	-98.800E-02	71.397E-03
22	42.569E-01	13.416E-02	-10.216E-01	60.231E-03
23	44.596E-01	11.566E-02	-10.516E-01	50.737E-03
24	46.623E-01	99.338E-03	-10.783E-01	42.679E-03
25	48.650E-01	85.000E-03	-11.019E-01	35.852E-03
26	50.677E-01	72.471E-03	-11.226E-01	30.077E-03
27	52.704E-01	61.571E-03	-11.408E-01	25.198E-03
28	54.731E-01	52.126E-03	-11.566E-01	21.081E-03
29	56.758E-01	43.976E-03	-11.703E-01	17.611E-03
30	58.785E-01	36.967E-03	-11.822E-01	14.689E-03
31	60.813E-01	30.962E-03	-11.923E-01	12.232E-03
32	62.840E-01	25.836E-03	-12.010E-01	10.167E-03
33	64.867E-01	21.474E-03	-12.084E-01	84.331E-04
34	66.894E-01	17.775E-03	-12.146E-01	69.78 E-04
35	68.921E-01	14.649E-03	-12.199E-01	57.601E-04
36	70.948E-01	12.015E-03	-12.243E-01	47.400E-04
37	72.975E-01	98.052E-04	-12.279E-01	38.868E-04
38	75.002E-01	79.550E-04	-12.310E-01	31.740E-04
39	77.029E-01	64.117E-04	-12.334E-01	25.790E-04
40	79.056E-01	51.281E-04	-12.355E-01	20.826E-04

TABLE VIII

TRANSIENT HEAT TRANSFER GROUP FOR THE FLAT PLATE

$\lambda \left(\frac{g \beta \Delta T}{x} \right)^{\frac{1}{2}}$	$\frac{h}{k} \left(\frac{V^2 x}{g \beta \Delta T} \right)^{\frac{1}{4}}$
0.02	2.7450
0.1	1.4483
0.2	1.0509
0.4	0.7532
0.8	0.5362
1.2	0.4389
1.6	0.3805
2.0	0.3405
2.4	0.3171
2.8	0.3045
3.2	0.2964
3.6	0.2917
4.0	0.2882
4.4	0.2854
4.8	0.2832
5.2	0.2815
5.6	0.2802
6.0	0.2793
6.4	0.2787
6.8	0.2783
Ostrach's result (26)	0.359

APPENDIX C

RESULTS FOR THE CYLINDER

The results of the calculations on the cylinder problem are given in Tables IX, X, XI, XII, and XIII.

Table IX gives the transient Nusselt numbers in the cylinder for Solution 1 using the first grid. The integers j in the table denote angular position in increments of $\pi/8$. The angle θ is $(j-2)(\pi/8)$.

Tables X and XI give the steady state results for the cylinder. In these tables the integers j denote angular position in increments of $\pi/16$. The angle θ is $(j-2)(\pi/16)$.

The variable Y is $(1-r/r_0)(GrPr)^{\frac{1}{4}}$. The odd numbered rays in the central region of the cylinder are blank in Table X because the rays added on subdivision do not extend into the central region. The results in Table X denoted as Solutions 4a and 4b are actually the same solution, that previously called Solution 4, but are at different times to show the maximum amplitude of the velocity fluctuation. Solution 4a is at a dimensionless time of 0.048 and Solution 4b is at a dimensionless time of 0.072. Similarly, Solutions 4c and 4d of Table XI are at different times to show the maximum amplitude of the fluctuations in the heat transfer results. Solution 4c is at a dimensionless time of 0.072 and Solution 4d is at a dimensionless time of 0.096. The fluctuations in the heat transfer rate are out of phase with the velocity fluctuations. The dimensionless time mentioned here is measured from the start of the subdivision of the grid as before.

Tables XII and XIII give the part of Martini's velocity and temperature data used in the figures and the dimensionless variables calculated from the data.

TABLE IX

TRANSIENT NUSSELT NUMBERS FOR THE CYLINDER

Time								
$\frac{tV}{r_0^2} \times 10^3$	j=2	3	4	5	6	7	8	9
0.40	0	15.699	15.699	15.699	15.699	15.699	15.699	15.699
0.80	0.2460	13.181	13.181	13.181	13.181	13.181	13.181	13.181
1.72	0.180	10.859	10.105	9.967	9.837	9.707	9.593	9.583
2.55	0.172	10.299	8.984	8.680	8.412	8.109	7.821	7.668
3.50	0.170	10.197	8.429	7.909	7.505	6.996	6.438	6.003
4.63	0.185	10.328	8.272	7.565	7.036	6.367	5.498	4.574
6.07	0.252	10.523	8.342	7.531	6.943	6.238	5.189	3.678
6.97	0.347	10.617	8.411	7.580	6.989	6.312	5.277	3.594
7.71	0.483	10.687	8.463	7.623	7.035	6.384	5.341	3.644
8.41	0.685	10.755	8.504	7.659	7.074	6.442	5.492	3.741
9.11	0.990	10.838	8.543	7.690	7.105	6.487	5.572	3.835
9.83	1.442	10.956	8.585	7.717	7.130	6.519	5.630	3.924
10.58	2.100	11.140	8.640	7.743	7.152	6.543	5.673	4.009
11.42	3.027	11.451	8.729	7.778	7.171	6.561	5.705	4.100
12.41	4.250	12.011	8.904	7.839	7.198	6.578	5.732	4.216
13.40	5.386	12.786	9.193	7.947	7.240	6.597	5.754	4.327
14.42	6.293	13.722	9.631	8.135	7.320	6.631	5.781	4.439
15.61	6.984	14.765	10.279	8.478	7.490	6.711	5.828	4.555
17.01	7.400	15.639	11.024	8.988	7.800	6.887	5.927	4.675
18.54	7.574	16.138	11.603	9.512	8.201	7.166	6.108	4.819
20.31	7.579	16.331	11.911	9.890	8.572	7.486	6.361	5.014
22.17	7.465	16.330	11.973	10.029	8.763	7.695	6.565	5.196
23.86	7.331	16.255	11.934	10.026	8.796	7.757	6.647	5.287
25.28	7.232	17.171	11.876	9.984	8.777	7.749	6.654	5.306
26.55	7.165	16.080	11.819	9.934	8.730	7.718	6.633	5.293
27.74	7.122	12.028	11.767	9.884	8.684	7.679	6.602	5.265
28.91	7.099	15.973	11.722	9.834	8.635	7.637	6.565	5.232
30.07	7.089	15.930	11.685	9.788	8.588	7.594	6.527	5.197
31.26	7.056	15.899	11.654	9.748	8.544	7.553	6.490	5.164
34.09	7.122	15.870	11.617	9.693	8.478	7.484	6.424	5.101
36.58	7.160	15.882	11.617	9.684	8.463	7.464	6.401	5.076
39.12	7.190	15.908	11.631	9.695	8.470	7.468	6.402	5.075
41.72	7.205	15.933	11.647	9.713	8.488	7.482	6.413	5.086
44.36	7.208	15.948	11.660	9.730	8.505	7.498	6.428	5.099
47.05	7.204	15.954	11.666	9.739	8.516	7.509	6.438	5.108

TABLE X. CONTINUED

r/ro 1/2 3 4 5 6 7 8 9 10 11 12 13 14 15 16 17 18

Values of 2F Solution 3

Table with 18 columns (r/ro 1/2 to 18) and multiple rows of numerical data. The data is organized into two main sections: 'Values of 2F Solution 3' and 'Values of v for Solution 3'.

Values of v for Solution 3

Table with 18 columns (r/ro 1/2 to 18) and multiple rows of numerical data, continuing from the previous table.

TABLE X. CONTINUED

r/σ 3 4 5 6 7 8 9 10 11 12 13 14 15 16 17 18

Values of U for Solution Ia

Table with 18 columns (r/σ) and multiple rows of numerical data. Values range from approximately -10.0000 to 10.0000.

Values of V for Solution Ia

Table with 18 columns (r/σ) and multiple rows of numerical data. Values range from approximately -10.0000 to 10.0000.

X Y Z 4 5 6 7 8 9 10 11 12 13 14 15 16 17 18

Values of U(Pr/Gr) for Solution Ia

Table with 18 columns (X-Y-Z) and multiple rows of numerical data. The values range from approximately -42.462E-05 to 97.693E-04.

Values of V(Pr3/Gr) for Solution Ia

Table with 18 columns (X-Y-Z) and multiple rows of numerical data. The values range from approximately -15.958E-01 to 97.693E-04.

Values of U(Pr/Gr) for Solution Ib

Table with 18 columns (X-Y-Z) and multiple rows of numerical data. The values range from approximately -16.472E-04 to 97.693E-04.

Values of V(Pr3/Gr) for Solution Ib

Table with 18 columns (X-Y-Z) and multiple rows of numerical data. The values range from approximately -16.472E-04 to 97.693E-04.

TABLE X. CONTINUED

r/r₀ j=2 3 4 5 6 7 8 9 10 11 12 13 14 15 16 17 18

Values of (T₁-T₀)/(T_H-T₀) for Solution 1

Table with 18 columns (j=2 to 18) and multiple rows of numerical data. Values range from 0.00000 to 1.00000.

Values of (T₁-T₀)/(T_H-T₀) for Solution 3

Table with 18 columns (j=2 to 18) and multiple rows of numerical data. Values range from 0.00000 to 1.00000.

Values of $(T-T_1)/(T_H-T_0)$ for Solution 4a

Table with 19 columns labeled 0, 1, 2, 3, 4, 5, 6, 7, 8, 9, 10, 11, 12, 13, 14, 15, 16, 17, 18. Rows contain numerical values for various parameters.

Values of $(T-T_1)/(T_H-T_0)$ for Solution 4b

Table with 19 columns labeled 0, 1, 2, 3, 4, 5, 6, 7, 8, 9, 10, 11, 12, 13, 14, 15, 16, 17, 18. Rows contain numerical values for various parameters.

TABLE XI

STEADY STATE HEAT TRANSFER RESULTS
FOR THE CYLINDER

j	Solution 1		Solution 2		Solution 3	
	Nu	$\text{Nu}/(\text{GrPr})^{\frac{1}{4}}$	Nu	$\text{Nu}/(\text{GrPr})^{\frac{1}{4}}$	Nu	$\text{Nu}/(\text{GrPr})^{\frac{1}{4}}$
2	11.980	0.4677	3.954	0.2968	20.787	0.4022
3	22.524	0.8793	--	--	41.131	0.7996
4	15.689	0.6125	8.890	0.6673	30.335	0.5897
5	13.094	0.5112	--	--	25.385	0.4935
6	11.639	0.4544	6.131	0.4602	22.551	0.4384
7	10.635	0.4152	--	--	20.601	0.4005
8	9.830	0.3838	5.068	0.3804	19.065	0.3707
9	9.143	0.3569	--	--	17.796	0.3460
10	8.541	0.3334	4.387	0.3293	16.723	0.3251
11	8.002	0.3124	--	--	15.785	0.3069
12	7.498	0.2927	3.813	0.2862	14.928	0.2902
13	6.998	0.2732	--	--	14.081	0.2738
14	6.473	0.2527	3.206	0.2407	13.160	0.2558
15	5.897	0.2302	--	--	12.107	0.2354
16	5.232	0.2043	2.740	0.2057	10.855	0.2110
17	4.462	0.1742	--	--	9.356	0.1819
18	-11.980	-0.4677	-3.953	-0.2968	-20.687	-0.4022

TABLE XI (cont.)

j	Solution 4c		Solution 4d	
	Nu	$\text{Nu}/(\text{GrPr})^{\frac{1}{4}}$	Nu	$\text{Nu}/(\text{GrPr})^{\frac{1}{4}}$
2	15.508	0.3114	15.728	0.3158
3	26.736	0.5369	28.040	0.5631
4	21.555	0.4328	22.263	0.4471
5	20.019	0.4020	20.498	0.4116
6	19.229	0.3861	19.578	0.3931
7	18.643	0.3744	18.907	0.3797
8	18.113	0.3637	18.317	0.3678
9	17.581	0.3530	17.741	0.3563
10	17.017	0.3417	17.143	0.3442
11	16.398	0.3293	16.497	0.3313
12	15.700	0.3153	15.777	0.3168
13	14.874	0.2987	14.933	0.2999
14	13.880	0.2787	13.925	0.2796
15	12.662	0.2543	12.692	0.2549
16	11.073	0.2224	11.092	0.2227
17	8.694	0.1746	8.716	0.1750
18	-15.508	-0.3114	-15.728	-0.3158

TABLE XII

VELOCITIES FROM MARTINI AND CHURCHILL (21)

<u>Experiment 4</u>							
$(1-r/r_0)(GrPr)^{\frac{1}{4}}$	5.31	4.25	3.19	2.13			
u, in./sec.	0	0.75	2.21	3.40			
$(ur_0/\nu)(Pr/Gr)^{\frac{1}{2}}$	0	0.063	0.183	0.282			
<u>Experiment 8</u>							
$(1-r/r_0)(GrPr)^{\frac{1}{4}}$	6.65	4.22	2.67	2.14	1.61	1.07	0.54
u, in./sec	0	0.50	1.20	1.55	1.80	1.90	1.80
$(ur_0/\nu)(Pr/Gr)^{\frac{1}{2}}$	0	0.178	0.428	0.555	0.642	0.678	0.642
<u>Experiment 9</u>							
$(1-r/r_0)(GrPr)^{\frac{1}{4}}$	5.45	4.35	3.26	2.18	1.09		
u, in./sec.	0.45	1.02	3.44	3.58	2.32		
$(ur_0/\nu)(Pr/Gr)^{\frac{1}{2}}$	0.032	0.074	0.247	0.257	0.167		
<u>Experiment 10</u>							
$(1-r/r_0)(GrPr)^{\frac{1}{4}}$	5.58	4.46	3.34	2.23	1.12		
u, in./sec.	0.20	1.38	2.87	2.22	0.88		
$(ur_0/\nu)(Pr/Gr)^{\frac{1}{2}}$	0.012	0.078	0.162	0.125	0.050		

TABLE XIII

TEMPERATURES FROM MARTINI AND CHURCHILL (21)

	<u>Experiment 4</u>							
$(1-r/r_0)(GrPr)^{\frac{1}{4}}$	0	0.60	1.31	1.91	4.88	9.47		
T, °C	28.5	31.8	35.5	40.1	44.3	43.6		
$(T-T_i)/(T_H-T_C)$	-0.500	-0.411	-0.311	-0.187	-0.073	-0.092		

	<u>Experiment 8</u>								
$(1-r/r_0)(GrPr)^{\frac{1}{4}}$	0.0	0.310	0.56	0.87	1.49	2.49	4.05	7.16	
T, °C	15.97	16.07	16.23	16.26	16.58	16.95	17.25	17.37	
$(T-T_i)/(T_H-T_C)$	-0.500	-0.453	-0.381	-0.368	-0.224	-0.058	0.076	0.130	

	<u>Experiment 9</u>								
$(1-r/r_0)(GrPr)^{\frac{1}{4}}$	0	0.63	1.14	1.77	3.04	5.06	8.22	14.55	
T, °C	26.5	29.5	34.6	38.8	44.5	46.0	44.0	44.0	
$(T-T_i)/(T_H-T_C)$	-0.500	-0.430	-0.312	-0.215	-0.082	-0.048	-0.094	-0.094	

	<u>Experiment 10</u>							
$(1-r/r_0)(GrPr)^{\frac{1}{4}}$	0	0.65	1.17	1.82	3.11	5.19	8.43	
T, °C	37.2	44.5	55.0	61.6	69.0	69.0	66.8	
$(T-T_i)/(T_H-T_C)$	-0.500	-0.400	-0.255	-0.165	-0.063	-0.063	-0.093	

APPENDIX D
COMPUTER PROGRAM

The computer program used for the calculations on the unsubdivided grid is given on the following pages. The symbols U and V in the program are the same as in the text. The meaning of the principal symbols which are not defined in the program are given below.

P	dimensionless temperature, $(T-T_i)/(T_H-T_C)$
T1,T2	temporary locations
XNU	local Nusselt number
S	sine of the angle
DT	time increment
DR	radial increment
DTH	angular increment
I	integer denoting time step
IEND	maximum number of time steps
G	Grashof number
PR	Prandtl number
PS	either the Prandtl number or 1, whichever is smaller
ANG	angle
L,Y	integer denoting radial position
J	integer denoting angular position
R	dimensionless radius, r/r_0

```

1 DIMENSION U(18,26),V(18,26),P(18,26),T1(26),T2(26),XNU(18),S(10)
2 DT=1.0E-6
3 DR=1./25.
4 DTH= 3.1415927/8.
  READ INPUT TAPE 7,5,IEND,G,PR
5 FORMAT(15,2P2E14.5)
  IF(1.0-PR) 501,501,502
501 PS=1.0
  GO TO 503
502 PS=PR
503 CONTINUE
601 TIME=0.
602 I=0
  ANG=0.
  DO 603 J=3,9
  ANG=ANG+DTH
603 S(J)=SIN(ANG)
  S(2)=0.
  S(10)=0.
  12 DO 13 J=3,9
  13 P(J,26)=0.5
  14 READ INPUT TAPE 7,106,
  C((U(J,L),L=2,25),J=2,10),
  C((V(J,L),L=2,25),J=2,10),
  C((P(J,L),L=2,25),J=2,10)
  GO TO 82
  7 A= DT/(DR*DR)
  AS=A/PS
  8 AP= A/PR
  9 B= DT/DTH
  10 C= DT/DR
  11 GDT = G*DT
  D=DT/(DTH*DTH)
  65 DO 69 L=2,25
651 V(1,L)=V(9,L)
652 V(11,L)=V(3,L)
  66 U(1,L)=U(9,L)
  67 U(11,L)=U(3,L)
  68 P(1,L)=-P(9,L)
  69 P(11,L)=-P(3,L)
185 I=I+1
186 TIME=TIME+DT
  DO 19 J=2,10
  19 T2(J)=P(J,26)
  Y=26.
  R=1.
  L=26
  20 L=L-1
  R=R-DR
  Y=Y-1.
  DEL=D/(R*R*PR)
  IF(L-2) 52,22,22
  22 DO 48 J=2,10
  BET=ABSF(U(J,L))*B/R
  GAMS=V(J,L)*C
  GAM=ABSF(GAMS)
  C1=1.-BET-GAM-2.*AP+AP/(Y-1.)-2.*DEL
  30 IF(U(J,L)) 34,32,32
  32 C2=DEL+BET

```

```

C5=DEL
GO TO 36
34 C2=DEL
C5=DEL+BET
36 IF(V(J,L)) 40,38,38
38 C3=AP-AP/(Y-1.) + GAM
C4=AP
GO TO 42
40 C3=AP-AP/(Y-1.)
C4=AP+GAM
42 T1(J)=C1*P(J,L)+C2*P(J-1,L)+C3*P(J,L-1)+C4*P(J,L+1)+C5*P(J+1,L)
XA=ABSF(T1(J))
IF(XA-1.0E-10) 44,44,46
44 T1(J)=0.
46 P(J,L+1)=T2(J)
T2(J)=T1(J)
48 CONTINUE
50 GO TO 20
52 DO 54 J=2,10
54 P(J,2)=T2(J)
70 DO 76 J=2,10
71 L=26
72 L=L-1
73 Y=L-1
74 V(J,L) = ((U(J+1,L) - U(J-1,L) + U(J+1,L+1) - U(J-1,L+1))
C / (4.*DTH) + (Y+1.)*V(J,L+1))/Y
75 IF(L-3) 76,76,72
76 CONTINUE
DO 160 J=2,10
160 T2(J)=0.
Y=26.
R=1.
L=26
162 L=L-1
R=R-DR
Y=Y-1.
DEL=D/(R*R)
U(11,L+1)=T2(3)
IF(L-2) 194,164,164
164 J=11
166 J=J-1
IF(J-2) 162,168,168
168 BET=ABSF(U(J,L))*B/R
GAMS=V(J,L)*C
GAM=ABSF(GAMS)
C1=1.-BET-GAM-2.*DEL-A*R*(1./(R+0.5*DR) + 1./(R-0.5*DR))
IF(U(J,L)) 172,170,170
170 C2=BET+DEL
C5=DEL
GO TO 174
172 C2=DEL
C5=BET+DEL
174 IF(V(J,L)) 178,176,176
176 C3=GAM+ A*(R-DR)/(R-0.5*DR)
C4= A*(R+DR)/(R+0.5*DR)
GO TO 180
178 C3= A*(R-DR)/(R-0.5*DR)
C4= GAM+ A*(R+DR)/(R+0.5*DR)

```

```

180 CONTINUE
184 T1(J)=(C1*U(J,L)+C2*U(J-1,L)+C3*U(J,L-1)+C4*U(J,L+1)+C5*U(J+1,L)
      C+GDT*P(J,L)*S(J))
      XA=ABSF(T1(J))
      IF(XA-1.0E-10) 188,188,190
188 T1(J)=0.
190 U(J,L+1)=T2(J)
      T2(J)=T1(J)
      GO TO 166
194 DO 196 J=2,10
196 U(J,2)=T2(J)
198 SC=0.
      Y=0.
      DO 28 L=2,25
      Y=Y+1.
      R=Y*DR
      DEL=(D/PS)/(Y*DR)**2.
      DO 28 J=2,9
      BET=ABSF(U(J,L))*B/R
      GAMS=V(J,L)*C
      GAM=ABSF(GAMS)
      X=BET+GAM+2.*DEL+2.*AS
26 IF(X-SC) 28,28,27
27 SC=X
28 CONTINUE
      DT=DT/SC
199 IF(I-3) 82,82,200
200 DO 201 N=1,10
      NN=40*N
      IF(I-NN) 201,82,201
201 CONTINUE
      IF(I-IEND+1) 7,82,105
82 WRITE OUTPUT TAPE 6,85,I,((U(J,L),J=2,10),L=1,26)
83 WRITE OUTPUT TAPE 6,85,I,((V(J,L),J=2,10),L=1,26)
84 WRITE OUTPUT TAPE 6,85,I,((P(J,L),J=2,10),L=1,26)
841 WRITE OUTPUT TAPE 6,842, TIME,DT
842 FORMAT (6H TIME 2P2E14.5)
85 FORMAT(5H6 I=I5/(2P9E13.4))
      DO 851 J=2,10
851 XNU(J)=50.*(P(J,26)-P(J,25))
      WRITE OUTPUT TAPE 6,852,(J,XNU(J),J=2,10)
852 FORMAT(14H6 J AND NU(J)/(I5,2PIE14.5))
      X=0.
      DO 853 NN=2,10
853 X=X + XNU(NN)
      DO 854 NN=3,9
854 X=X + XNU(NN)
      DO 855 NN=3,9,2
855 X=X+2.*XNU(NN)
      X=X/24.
      WRITE OUTPUT TAPE 6,856,X
856 FORMAT(18H6MEAN NU ONE SIDE 2PE14.5)
      IF(I-IEND) 7,105,105
105 PUNCH 106,
      C((U(J,L),L=2,25),J=2,10),
      C((V(J,L),L=2,25),J=2,10),
      C((P(J,L),L=2,25),J=2,10)
106 FORMAT(5E14.7)

```